Role of cellular trafficking on Dpp morphogen gradient formation and signaling

Inauguraldissertation

zur

Erlangung der Würde eines Doktors der Philosophie

vorgelegt der

Philosophisch-Naturwissenschaftlichen Fakultät

der Universität Basel

von

Sheida Hadji Rasouliha

Basel, 2024

Genehmigt von der Philosophisch-Naturwissenschaftlichen Fakultät auf Antrag von

Erstbetreuer: Prof. Dr. Markus Affolter

zusätzlicher Erstbetreuer: Dr. Shinya Matsuda

Zweitbetreuerin: Prof. Dr. Fiona Doetsch

Externer Experte: Dr. Giorgos Pyrowolakis

Basel, 28.03.2023

Prof. Dr. Marcel Mayor, Dekan

Abstract

Dpp/BMP is a well-studied morphogen that controls patterning and growth in the *Drosophila* wing disc. However, how the Dpp morphogen gradient is established and is interpreted by endocytic trafficking remains largely unknown. By utilizing the endogenously tagged *dpp* alleles with the monomeric proteins mGreenLantern and mScarlet, I investigated the role of different trafficking factors in shaping the intra- and the extracellular Dpp gradient. Using these alleles, I showed that dynamin is a major regulator of the Dpp gradient and blocking dynamin-dependent endocytosis expanded the extracellular Dpp gradient and impaired Dpp signaling. I also found that blocking the early endosomal trafficking by knocking down Rab5 not only expanded the extracellular Dpp gradient, but also increased the range of Dpp signaling possibly due to an impaired termination of its receptor Tkv. I also demonstrated that blocking multivesicular body (MVB) formation, but not the endo-lysosomal fusion, expanded the internalized Dpp distribution and signaling range without affecting the extracellular Dpp gradient. By investigating the role of recycling endosomes, I also showed that while the slow recycling endosomes slightly affected the intracellular Dpp distribution, the fast recycling endosomes minimally affected the extracellular Dpp gradient and neither of these factors influenced the Dpp signaling activity. My findings indicated that the early endocytic factors act as a sink for the extracellular Dpp gradient and are required to activate Dpp signaling, while the late endocytic factors terminate Dpp signaling activity by sorting the activated receptors into the intraluminal vesicles (ILVs). Taken together, our results suggest that extracellular Dpp morphogen gradient is shaped and interpreted by distinct endocytic trafficking pathways.

List of abbreviations

A/P	Anterior/Posterior
Aa	Amino acid
Ap	Apterous
Ap-2	Adaptor protein-2
BMP	Bone morphogenetic protein
BMP/LBPA	bis(monoacylglycero)phosphate/lysobisphoshatidic acid
Brk	Brinker
Cav	Caveolin
CCV	Clathrin-coated vesicle
Ci	Cubitus interruptus
CIE	Clathrin-independent endocytosis
CME	Clathrin-mediated endocytosis
Co-Smad	Common-mediator Smad
CORVET	Class C core vacuole/endosome tethering factor
D/V	Dorsal/Ventral
Dad	Daughters against Dpp
Dally	Division abnormally delayed
DARPin	Design Ankyrin Repeat Protein
DFz	DFrizzled
Disp	Dispatched
Dll	Distalless
Dlp	Dally-like protein
Dpp	Decapentaplegic
DUB	de-ubiquitinating enzyme
EE	Early endosome
EEA1	Early endosome antigen 1
EGF	Epidermal growth factor
En	Engrailed
ESCRT	Endosomal sorting complex required for transport
FGF	Fibroblast growth factor

Flp	Flippase
FRT	Flippase recognition site
Fz	Frizzled
GAP	GTPase activating proteins
Gbb	Glass bottom boat
GDF	Growth and differentiation factor
GDI	GDP dissociation inhibitor
GDP	Guanosine diphosphate
GEF	Guanine nucleotide exchange factor
GFP	Green fluorescent protein
GPI	Glycosylphosphatidylinositol
GS	Glysine-Serine
GTP	Guanosine triphosphate
Hh	Hedgehog
HOPS	Homotypic fusion and vacuole protein sorting
Hrs	Hepatocyte growth factor receptor-regulated tyrosine kinase substrate
HSPG	Heparan sulfate Proteoglycan
I-Smad	Inhibitory Smad
ILV	Intraluminal vesicle
LAMP	Lysosomal-associated membrane protein
LE	Late endosome
Mad	Mothers against Dpp
MIM	MIT-interacting motif
MIT	Microtubule-interacting and transport
MVB	Multi-vesicular body
NEM	N-ethylmaleimide
NGS	Normal goat serum
NMJ	Neuromuscular junction
NSF	N-ethylmaleimide-sensitive factor
Omb	Optomotor blind
PB	Protein-binder
PBS	Phosphate Buffered Saline

PCR	Polymerase chain reaction
PFA	Paraformaldehyde
PI3P	Phosphatidylinositol-3-phosphate
PIP2	phosphatidylinositol-4,5-bisphosphate
pMad	Phospho-mothers against Dpp
POI	Protein of interest
Ptc	Patched
Put	Punt
R-Smad	Regulatory Smad
Sal	Spalt
SARA	Smad anchor for receptor activation
Sax	Saxophone
ScFv	Single chain variable Fragment
Scw	Screw
Sens	Sensless
Shh	Sonic hedgehog
Shi	Shibire
Shn	Schnurri
Sna	Snail
SNARE	Soluble N-ethylmaleimide-sensitive factor
TFG	Transforming growth factor
TGN	Trans-Golgi network
Tkv	Thickveins
TS	Temperature-sensitive
UAS	Upstream activation sequence
Vg	Vestigial
Vn	Vein
Wg	Wingless
Wit	Wishful Thinking
Wnt	Wingless-related integration site
Wt	Wildtype
YFP	Yellow fluorescent protein

List of figures

Content

Table of Contents

Acknowledgements

I would like to thank my supervisor Shinya Matsuda for giving me the opportunity to work on this exciting project, for always asking the critical questions, and for supporting me all the way until the end of this project. Thank you for your encouragement and for choosing me to be one of the first PhD students that you supervised.

I would also like to thank Markus Affolter for giving me the opportunity to work in his lab for the past 4 years, and for supporting me throughout this PhD, for always being enthusiastic about the projects in the lab, and for your humor, making the Affolter lab one of the best labs in the Biozenturm.

I thank the members of my PhD committee, Prof. Fiona Doetsch, for your time and scientific input. You always kept our meetings very balanced, and it was always a pleasure to speak with you. I would also like to thank Dr. Giorgos Pyrowolakis, for your time, for your scientific input, and for sharing some of your fly stocks with us, without which this project would have taken a much longer time to finish.

I would like to give a big thank you to the Imaging Core Facility (IMCF) at the Biozentrum. Thank you, Oliver, for believing in me (and my Drosophila under the Lightsheet) to be a part of the small IMCF family. Thank you, Sara, for always being so approachable and friendly, for helping me through a rough patch and for being a great mentor. Thank you, Kai, for always being ready to help, regardless of the microscope system or the image analysis project. Thank you, Alexia, for all of your much needed microscopy wisdom. I am now an expert in colocalization analysis because of you. Thank you, Laurent, Niko and Sébastien for your image analysis input, and for holding the fort together. At last, thank you, little Sophia for making it possible for me to join the IMCF family.

A big thank you to the Affolter lab members who made me look forward to go to the lab every day. Thank you, Gustavo, for your amazing ideas and for being my unofficial supervisor. This project would not have been possible without your help. Thank you, Niklas, for always bringing humor to every situation, and for all of the snacks and the sweets to keep us going strong. Thank you, Cindy, for helping me with the last push, and for being my right hand in the lab when I needed you the most. Thank you, Maria, for always encouraging me, and for the

amazing conversations. Thank you, Kasia and Ludo, for making the lab a fun place to be in, and thank you, Milena and Daniel for your friendship. Thank you, Martin for holding the lab together, and Helen, for all of your help. A big thank you to the whole Affolter lab for making everyone feel like a part of a family, and for the fun times eating cake and having coffee together. Also, a special thank you to the Biozentrum media kitchen for providing the world's best fly food.

I would like to thank my friends, Cova, Elizabeth, Maryam, Ehssan, Christian, Gwen, Camila, and Fatemeh for supporting me through this journey, for reducing my worries and for keeping me sane through insane times.

I truly owe this opportunity to my loving family who sacrificed a lot for me to reach this stage of my life. I am who I am, thanks to my parents, who were a constant support and never doubted me for a second. Thank you for always being there for me, even if there were five thousand kilometers between us. مامان و بابای عزیزم, دست گل هردوتون درد نکنه.

Last, but not least, thank you, Marco, for loving and supporting me and for reminding me that "present" is truly a gift we should be enjoying now. Thank you for bringing many adventurous moments to my life, and for putting a smile on my face every day. I'm truly happy to have you in my life.

1 Introduction

For many generations, developmental biologists have been studying how a single fertilized cell develops into a multicellular organism with distinct cell types and organs. Developmental biology is the science of understanding the processes involved in an organism's growth, shape and structure throughout its lifecycle. In simplest terms, it describes how a single cell can become a completely formed organism through studying properties of individual cells, their organization into tissues, organs and organisms, their homeostasis and regeneration, aging and eventually death (Trainor, 2016). One of the important factors involved in development of the organism and its shape and patterning are morphogens and their gradients (Rogers & Schier, 2011).

The morphogen term was first introduced by Alan Turing in his paper "The chemical basis of morphogenesis", where he speculated on a chemical mechanism for biological pattern formations (Turing, 1952, 1990). In biological research, morphogens are defined as a class of long-range signaling molecules that act directly on cells to produce specific cellular responses and pattern developing tissues in a concentration-dependent manner (Briscoe et al., 2010). The influential "French flag" model (Figure 1.1) was described by Lewis Wolpert in 1969 and illustrated how gradients of signaling molecules could subdivide the developing tissues into differentiated regions (Wolpert, 1969). In most cases, morphogens are produced and secreted from a defined group of cells within the tissue (source cells), and they form a concentration gradient. The graded distribution of morphogens within a tissue exposes the cells to different concentration thresholds of the morphogen, which leads to different cellular responses and cellular fates within each threshold group (Rogers & Schier, 2011).

In the early twentieth century, the idea that gradients may be coordinating cellular fate and development was suggested by Thomas Hunt Morgan (Boveri, 1901; Morgan, 1901). He proposed that a gradual decrease in distribution of "material" in the developing sea urchin could generate patterns within the developing tissue and control gastrulation.

Further studies revealed that certain tissues can have inductive abilities, as most prominently shown by Hans Spemann and Hilde Mangold, when they discovered the so-called Spemann organizer by conducting experiments on salamanders. They observed that a secondary embryonic axis could be induced by transplanting the dorsal pole of a gastrula embryo to the

ventral side of a host embryo (Spemann & Mangold, 1924). This famous experiment is the basis of morphogenesis and the idea that secreted signals from a localized group of cells (organizers) induce differentiation of their neighbors (De Robertis, 2006).

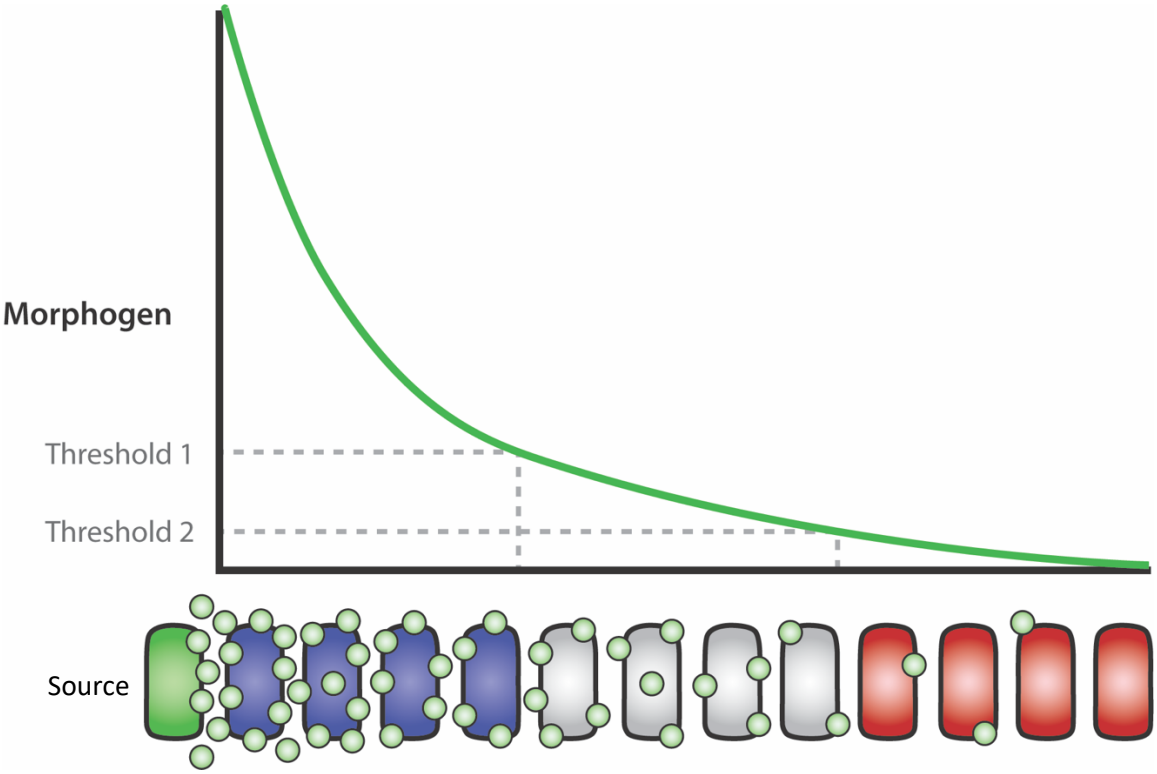

Figure 1.1: The French flag model.
Morphogen is secreted from the source cell (green), and forms a concentration gradient within the tissue. Cells exposed to a certain concentration of the gradient above threshold 1 develop a certain "blue" response. Cells exposed to the intermediate levels of the morphogen (between threshold 1 and 2) develop the "white" response, while cells exposed to concentrations below threshold 2 develop the "red" response. In this way, a single diffusing substance can define different cell types and assigns positional values based on its concentration gradient. Figure adapted from Rogers and Schier (2011).

After the proposal of the French flag model by Wolpert (1969), Francis Crick introduced the "source-sink" model in which the morphogens secreted from the source cells diffuse within a tissue and are destroyed by the local "sink" cells that are at the opposite ends of the tissue (Crick, 1970). A stable morphogen concentration gradient would thereby be generated from the processes of diffusion and degradation, with the highest concentration located near the source, and the lowest near the sink cells (Rogers & Schier, 2011).

Decades of research into how animals from fruit flies to mice develop have revealed some of the common principles of how morphogen gradients regulate development of tissue patterns. The development of the Drosophila wing, the vertebrate limb bud, and the neural tube are classic examples of how morphogens regulate development (Mehlen et al., 2005).

1.1 Morphogen gradients in development

The first clear connection between pattern formation and molecular gradients was provided by Driever and Nüsslein-Volhard (1988) with their investigations into the graded distribution and function of Bicoid in *Drosophila* embryos. Bicoid is a transcription factor expressed in the anterior region of a syncytial blastoderm, the latter being formed by the division of nuclei in the embryo without their segregation into individual cells by a membrane during the developmental stage. Bicoid forms an anterior to posterior concentration gradient, where higher concentrations are required for expression of anterior genes, and lower levels for the expression of posterior genes (Driever & Nüsslein-Volhard, 1988; Struhl et al., 1989). Shortly after the discovery of Bicoid and its anterior-posterior gradient, the transcriptional regulator Dorsal was discovered and was found to be required for dorsal-ventral patterning in *Drosophila* (Rogers & Schier, 2011; Roth et al., 1989; Rushlow et al., 1989; Steward, 1989). Accordingly, Bicoid and Dorsal were among the first transcription regulator gradients that were found to control embryonic patterning.

One of the first extracellular morphogens that was identified and validated was Decapentaplegic (Dpp), a member of the transforming growth factor β (TGF-β) family of secreted signaling molecules. Dpp is the *Drosophila* homolog of the Bone morphogenetic Protein (BMP) 2/4, and was found to be essential for patterning of multiple tissues via its long-range activity, including the dorsal-ventral axis of the embryo and the anterior-posterior axis of the wing imaginal discs in the larvae via its long-range activity (Ferguson & Anderson, 1992; Lecuit et al., 1996; Nellen et al., 1996). Following the discovery and characterization of Dpp, further extracellular morphogen ligands were discovered, including Wingless (Wg)-related integration site (Wnt), Hedgehog (Hh), Fibroblast growth factor (FGF) and Epidermal growth factor (EGF) (Rogers & Schier, 2011). These raised the questions of how morphogen gradients are formed, how morphogen signals are transduced, and how the graded signal is interpreted by receiving cells in the field of developmental biology.

1.2 The TGF-β superfamily

The TGF-β superfamily of secreted factors comprises of more than 30 members in mammals, with multiple members also identified in fish, frogs, flies and worms. In general, the TFG-β superfamily members can be further subclassified into TGF-βs, Bone Morphogenetic Proteins (BMPs), Activins, Nodals, Growth and Differentiation Factors (GDFs), as well as the anti-Müllerian hormone proteins (Lee et al., 2006). The TGF-β superfamily members regulate fundamental cellular processes throughout the development of the multicellular organisms, including proliferation, cytoskeletal organization, differentiation, adhesion, migration and death (Weiss & Attisano, 2013). Aberrant TGF-β superfamily signaling can lead to a wide range of human diseases such as autoimmune, cardiovascular and fibrotic diseases, as well as cancer (Gough et al., 2021).

1.3 Drosophila melanogaster as a model organism

Drosophila melanogaster, also more commonly known as the fruit fly, is a widely used model organism, especially in the field of developmental biology. It is impressive to know that over 65% of genes associated with human diseases have a homolog in *D. melanogaster* (Ugur et al., 2016). Drosophila has a rapid generation time, low maintenance costs, a small genome consisting of 4 chromosomes and 14,000 genes, and researchers have built over the last 100 years an extensive genetic toolbox that makes the fruit fly one of the easiest and most powerful multicellular animals to work with. To name a few of these tools: 1) balancer chromosomes, which make it possible to easily maintain fly stocks with lethal mutations alive, 2) visible markers allowing the tracking of the inheritance of any linked gene, and 3) the UAS-Gal4 system which allows the expression of transgenes in any tissue of interest at any point of time throughout the life cycle of the fly (Markstein, 2018).

1.3.1 Drosophila melanogaster life cycle

At room temperature (25°C), *Drosophila melanogaster* grows from a fertilized egg into an adult within ten days, and its development is subdivided into main stages, e.g., embryo, larva, pupa and the adult. A female fly can lay about 100 eggs during a day, and the embryonic stage lasts only about 24 hours. The first and the second instar larval stage each takes one day, and the third instar stage takes three days. When the third instar larva is matured, it starts to pupate, during which it goes through a complete body metamorphosis, where most larval tissues are degraded and the adult organs are developed from imaginal discs (Fernández-Moreno et al., 2007). The pupal stage lasts about four days and ends with the adult fly hatching from the pupal case. The adult fly can live approximately 60-80 days, depending on its environmental conditions (Fernández-Moreno et al., 2007) (Figure 1.2).

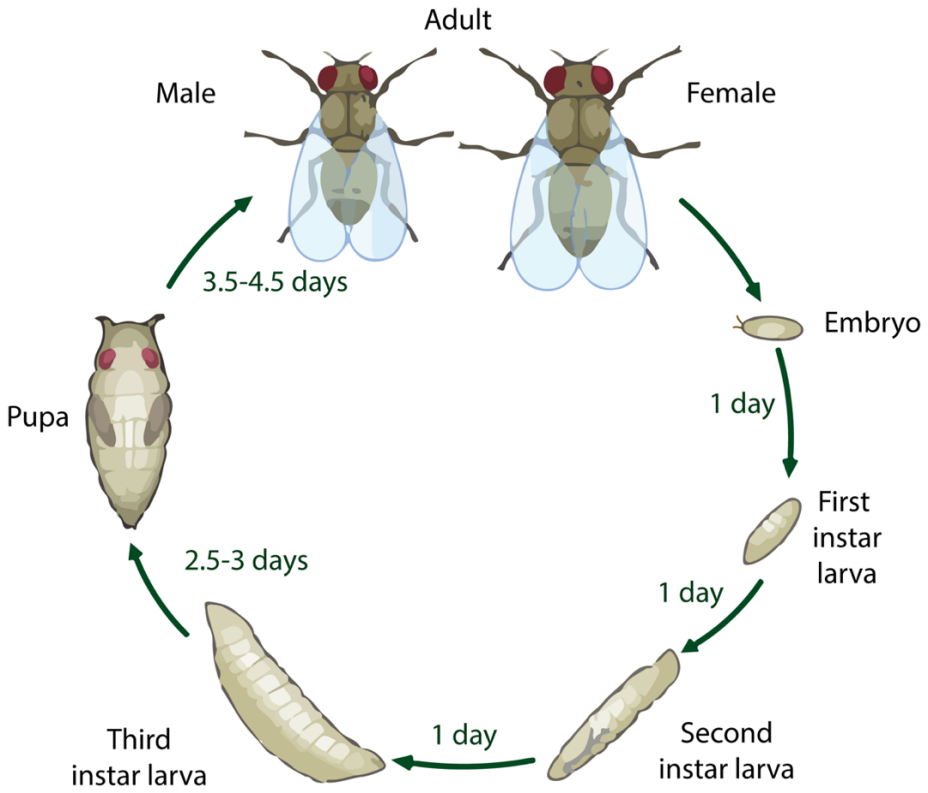

Figure 1.2: Drosophila melanogaster life cycle from an embryo to the adult fly.
Image adapted from Ong et al. (2015).

Drosophila undergoes substantial morphological changes throughout its life cycle. The well-developed appendages such as eyes, wings, legs, halteres and genitals in the adult fly are formed from their precursor structures called “imaginal” discs that are protected within the larva (Beira & Paro, 2016). These imaginal discs not only grow as the fly develops during larval stages, but are also substantially transformed during metamorphosis. The imaginal structures are not limited to discs which are an epidermal sac-like cluster of cells, but also include histoblasts, which in the adult fly form the abdominal epidermis, and small parts of the gut and salivary glands (Beira & Paro, 2016). *Drosophila* contains 19 imaginal discs, and they are comprised of two different cell layers. The outer layer is the peripodial membrane with squamous cells, providing little contribution to the cuticular structures in the adult, the inner layer is the disc proper which is formed by a single columnar epithelial layer, and gives rise to the body of the adult structures (Beira & Paro, 2016; Haynie & Bryant, 1986). In newly hatched first instar larva (roughly 24 hours after egg laying, AEL), the larger discs, such as wings, legs, and eye-antennal discs, are already made of 20-70 cells each (Mandaravally Madhavan & Schneiderman, 1977). The disc cells resume mitosis and continue to divide and grow exponentially during the second and third instar stages, with cell numbers doubling every ten hours, and each disc contains 10,000 to 50,000 cells prior to pupariation (Johnston et al., 1999; Nöthiger, 1972). Imaginal discs are the Swiss army knife in *Drosophila* research, and help to address a variety of scientific questions in cell and developmental biology. Using these epithelial precursor organs as models, together with a variety of novel genetic tools has enabled functional studies in the context of a developing organism, and has contributed to understanding conserved molecular mechanisms.

1.3.2 Drosophila melanogaster wing imaginal disc

The *Drosophila* wing imaginal disc is the precursor of the adult wing, and is first formed from a cluster of roughly 30 cells during embryogenesis that invaginate to form a sac-like structure (Tripathi & Irvine, 2022). These cells undergo extensive proliferation to reach about 35,000 cells in the mature larval wing disc. During this process, the wing disc develops a complex morphology, and distinct cell fates are assigned to different regions (Tripathi & Irvine, 2022). The relative simplicity and accessibility of the wing imaginal disc, together with the availability of advanced genetic tools in *Drosophila* make it an ideal model tissue to study tissue patterning, morphogenesis, growth control, signal transductions, planar cell polarity and tissue mechanics (Tripathi & Irvine, 2022).

The initial specification of the wing disc already occurs during embryogenesis, from cells in the lateral epidermis of T2 at the embryonic stage 12. This cell differentiation is triggered by the expression of *vestigial* (*vg*) and *snail* (*sna*) (Cohen et al., 1993; Fuse et al., 1996; Tripathi & Irvine, 2022; Williams et al., 1991). The growing wing imaginal disc can be subdivided into distinct cell types.

The dorsal/ventral (D/V) polarity in the early wing discs is established through expression of the EGFR ligand *vein* (*vn*) proximally and *wingless* (*wg*) distally. In the second instar larva, the EGFR pathway triggers the expression of the selector gene *apterous* (*ap*) in the prospective dorsal compartment of the wing disc (Milán & Cohen, 2000). Apterous is expressed in all dorsal (D) cells and specifies dorsal identity, and also defines the signaling boundary of Notch. Signaling across the D/V boundary is mediated by the Notch pathway, which is activated along both sides of the boundary. Notch signals bidirectionally between dorsal and ventral cells via the two Notch ligands Serrate and Delta (de Celis et al., 1996; Diaz-Benjumea & Cohen, 1995; Doherty et al., 1996). Activation of Notch drives the expression of *vesitigial* (*vg*), which specifies the wing pouch and gives rise to the adult wing blade (Zecca & Struhl, 2007). Also, Notch drives transcription of *wg* at the D/V boundary in the wing pouch, which acts as a long-range organizing molecule and controls growth and patterning along the dorsoventral axis (Dahmann & Basler, 1999; Neumann & Cohen, 1997). Besides the formation of the actual wing, the wing imaginal disc also gives rise to all dorsal metathoracic structures such as notum, scutellum, wing hinge and pleura (Tripathi & Irvine, 2022) (Figure 1.3).

The anterior/posterior (A/P) compartmentalization is established during embryogenesis. Expression of segment-polarity genes such as *engrailed* (*en*) at the posterior side of each segment defines the posterior fate of the cells (Kornberg, 1981; Morata & Lawrence, 1975). The group of cells giving rise to the wing imaginal discs have their compartment boundaries defined by posterior cells which express En, and anterior cells which lack En expression. En positively regulates *hedgehog* (*hh*) and represses expression of *cubitus interruptus* (*ci*) in the posterior compartment (Eaton & Kornberg, 1990; Zecca et al., 1995). Hh is unable to activate nuclear signaling in the posterior compartment due to lack of Ci. However, Hh also spreads into the anterior compartment, where it directly activates expression of the TGF-β superfamily member *dpp* (Tanimoto et al., 2000).

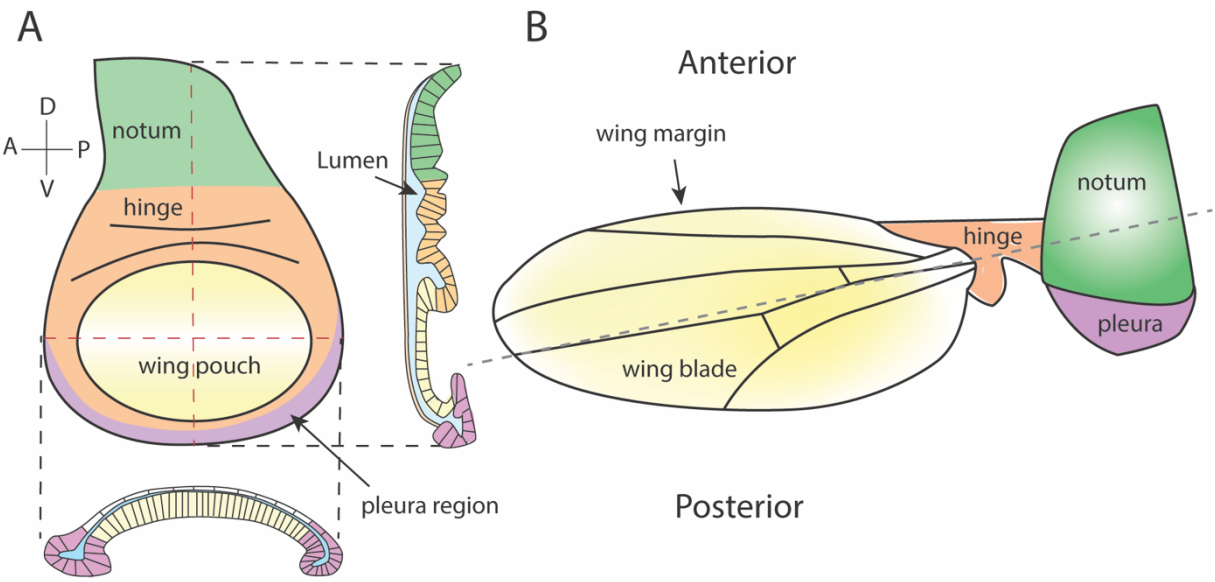

Figure 1.3: The wing imaginal disc and adult wing architecture of Drosophila melanogaster.
(A) Schematic view of a third instar larval wing imaginal disc. The wing pouch (yellow) gives rise to the adult wing blade. The orthogonal views of the wing imaginal disc are depicted below and to the right. Dorsal (D), ventral (V), anterior (A) and posterior (P) orientations are indicated. (B) Top view of the adult wing. The wing is connected to the body via the hinge to the notum. Figure adapted from Tripathi and Irvine (2022).

1.4 BMPs

Bone Morphogenetic Proteins (BMPs) are a group of signaling molecules belonging to the TGF-β superfamily of proteins. They were initially discovered in 1960s and were identified to be involved in inducing bone formation, but are now known for their crucial roles in all organ systems (Urist, 1965). Many processes in early development including cell growth, apoptosis and differentiation are dependent on BMP signaling (Hemmati-Brivanlou & Thomsen, 1995; Kobayashi et al., 2005; Stewart et al., 2010; Wang et al., 2014; Zou & Niswander, 1996). BMPs

have an important role in development and deficiencies in BMP production or functionality can lead to prominent defects or pathologies, such as cancer, as well as vascular and metabolic diseases (Kim & Choe, 2011).

BMP family members are classified into several sub groups based on their sequences and structural homology, including the BMP2/4 group, BMP5/6/7/8 group, BMP9/10 group and BMP12/13/14 groups (Katagiri & Watabe, 2016). All BMPs are initially produced as precursor proteins, and they all contain seven cysteins, six of which build a cysteine knot, and the seventh is used for dimerization with another monomer during dimerization (Xiao et al., 2007). Prior to secretion, all BMPs consist of a signal peptide (proprotein), consisting of a pro-domain and a mature peptide. Once the signal peptide is cleaved, the precursor protein is glycosylated and dimerized (Xiao et al., 2007). After dimerization, the pro-domain is cleaved and the mature domain is released as a dimer. The pro-domain is thought to be important for coordination of proper folding of the mature domain (Sieber et al., 2009) . The mature BMP is derived by proteolytic cleavage from the carboxyterminal region by a proprotein convertase such as furin, and is secreted either as homodimers or heterodimers (Anderson & Wharton, 2017; Xiao et al., 2007).

BMP signaling is initiated when BMPs bind to two distinct type I and type II serine/threonine kinase receptors (Ashique et al., 2002). There are three type II receptors that bind to BMPs: type II BMP receptor (BMPR-II) and activin receptors type II and IIB (ActR-II and ActR-IIB). In addition, there are three type I receptors: BMP receptors type IA and IB (BMPIA and BMPIB) and activin receptor type IA (ActRIA) (Attisano et al., 1993; Xiao et al., 2007). The serine/threonine kinase domains of type II receptors are constitutively active, and upon ligand binding, phosphorylate Gly-Ser (GS) domains in the type I receptors and activate type-I receptor kinases (Xiao et al., 2007). The activated receptor type I recruits the receptor-regulated Smads (R-Smads, Smads 1, 5 or 8). The R-Smads become phosphorylated by the receptor type I, are released and recruit the common mediator Smad (Co-Smad, Smad4) into the complex. The R-Smad/Co-Smad complex migrates into the nucleus where it activates the transcription of specific target genes (Heldin et al., 1997; Xiao et al., 2007). BMP signaling is also modulated by several negative feedback loops. Secretion of BMP antagonists such as Noggin and Chordin, antagonize BMP signaling and the initiation of the signaling cascade by binding with a very high affinity (picomolar) to BMPs and preventing receptor activation

(Kawabata et al., 1998; Piccolo et al., 1996; Zimmerman et al., 1996). Oligomerization of the receptors themselves can determine the specificity of signaling activation. Furthermore, once the signal is transduced intracellularly, it can be modulated by activation of inhibitory Smads (I-Smad, Smad 6,7), or be negatively regulated by Smurf 1, which is a ubiquitin ligase targeting BMP receptors and downstream signaling molecule Smad1/5 (Ebisawa et al., 2001; Murakami et al., 2003; Zhu et al., 1999) . Also, in the nucleus, a number of co-activators are needed for the activation of specific target genes and their transcription can be inhibited by corepressors (Kawabata et al., 1998; Xiao et al., 2007).

BMPs are also present in invertebrates such as Decapentaplegic (Dpp), Glass Bottom Boat (Gbb) and Screw (Scw) in *Drosophila*, and DAF-7 in *Caenorhabditis elegans*. The biological activities of BMPs are highly conserved among species, as it has been shown that *Drosophila* Dpp and Gbb, which are structurally similar to BMP-2/-4 and BMP-6/-7 respectively, can induce ectopic bone formation in rats, and human BMP-4 can rescue the Dpp mutant phenotype in *Drosophila* (Katagiri & Watabe, 2016; Padgett et al., 1993; Sampath et al., 1993).

1.4.1 BMPs in Drosophila

BMPs and their role in development have been studied extensively in the model organism *Drosophila melanogaster.* BMPs in *Drosophila* include Dpp, Gbb and Scw. Dpp, the homologue of the vertebrate BMP2/4, as the first validated secreted morphogen, was first described in 1982, and was named after its distinct mutant phenotype including duplications and pattern deficiencies in 15 out of 19 imaginal discs in the fruit fly (Padgett et al., 1987; Padgett et al., 1993; Spencer et al., 1982). Dpp was validated to be a secreted morphogen in an experiment where Dpp-producing clones were able to induce expression of target genes non-cell-autonomously in a concentration-dependent manner in the surrounding cells. In contrast, clones of cells expressing a constitutively active form of the type I receptor Thickveins (Tkv^{QD}) were able to activate Dpp signaling and expression of target genes only cell autonomously, and did not induce ectopic expression of target genes in the neighboring cells (Affolter & Basler, 2007; Lecuit et al., 1996; Nellen et al., 1996). These results show that Dpp acts directly at a distance and exclude the relay mechanism where Dpp induces other secreted factors to induce target gene expression.

Dpp has been widely studied in flies as it has numerous important biological roles. Dpp is involved in patterning of the embryo and the imaginal discs (Affolter & Basler, 2007; Ashe, 2005; Ferguson & Anderson, 1992; Hamaratoglu et al., 2014; Matsuda et al., 2016; O'Connor et al., 2006; Raftery & Umulis, 2012; Ramel & Hill, 2012), stem cell function and regulation including maintaining self-renewal of germ line stem cell niche (Xie & Spradling, 1998), hematopoesis (Dey et al., 2016), control of number of stem cells in the adult midgut (Z. Li et al., 2013), and in regenerating stem cells in the gastrointestinal tract of the adult fly (H. Li et al., 2013).

The second BMP ligand in *Drosophila* is Gbb, the homologue of BMP5/6/7/8. Gbb is expressed highly expressed during gastrulation of the embryo and to a lower extent in the larval and adult tissues (Wharton et al., 1991). Gbb function is required for midgut formation in embryonic development, and for imaginal disc and fat body morphogenesis during larval development (Bangi & Wharton, 2006a; Khalsa et al., 1998; Wharton et al., 1999). Gbb is also required for synapse growth of *Drosophila* neuromuscular junctions (NMJs) and for synaptic homeostasis (Goold & Davis, 2007; McCabe et al., 2003). In contrast, Scw, another homologue of BMP5/6/7/8 only functions in early blastoderm embryos and has little role later in development. Scw is expressed ubiquitously and together with Dpp as a heterodimer determines the D/V polarity in the embryo (Arora et al., 1994; Shimmi et al., 2005).

The BMP ligands bind to type I receptors Thickveins (Tkv) and Saxophone (Sax), which in turn are activates and phosphorylated via the recruitment of the type II receptors Punt (Put) and Wishful Thinking (Wit). Tkv is involved in the control of growth and patterning in a variety of tissues, while Sax is rather responsible for fine-tuning the BMP signaling (Bangi & Wharton, 2006b; Ruberte et al., 1995; Tanimoto et al., 2000). Tkv is involved in signal transduction via all three Drosophila BMP ligand signal transduction and it binds to Dpp with a high affinity, while Gbb and Scw preferentially bind to Sax (Haerry, 2010; Haerry et al., 1998; Penton et al., 1994; Schwank et al., 2011). Dpp/Gbb and Dpp/Scw heterodimers have been proposed to interact with Tkv and Sax heteromeric receptor complexes, while the homodimers preferentially interact with homomeric Tkv or Sax receptor complexes (Bangi & Wharton, 2006b; Haerry, 2010; Neul & Ferguson, 1998; Nguyen et al., 1998). Type II receptor Put is mostly involved in Dpp signaling, as *put* mutants share high similarities to *dpp* mutant phenotype (Burke & Basler, 1996; Letsou et al., 1995; Ruberte et al., 1995; Simin et al., 1998).

The type II receptor Wit is mainly involved in Dpp signaling for *Drosophila* neuronal development (Aberle et al., 2002; Marqués et al., 2002).

1.4.2 Dpp signaling pathway

Dpp signaling is initiated when Dpp dimers are recognized by the receptors and assemble receptor complexes at the plasma membrane (Hamaratoglu et al., 2014). Depending on the developmental context and the tissue, Dpp, Gbb and Scw form homo- or heterodimers, and bind to the type I receptors Thickveins (Tkv) and Saxophone (Sax). It has recently been discovered that in the developing wing imaginal discs, Dpp is mainly only found as heterodimers together with Gbb, and neither Dpp nor Gbb are present as a homodimers in endogenous physiological conditions (Bauer et al., 2022). Similar to vertebrate BMP signaling, the type I receptor Tkv binds the Dpp ligand and, together with the type II receptor Put, forms a heteromeric complex. The constitutively active kinase of Put then phosphorylates Tkv at the type I receptor-specific juxtamembrane GS domain and activates its associated type I kinase. The activated Tkv in turn phosphorylates a homologue of Smad1, the transcription factor Mothers against Dpp (Mad) (Affolter et al., 2001). In TGF-β signaling, Smad2 and Smad3 are found to be recruited to the receptor complex by an anchor protein containing a FYVE domain called SARA (Smad anchor for receptor activation) (Tsukazaki et al., 1998). What is known about SARA in Dpp signaling in *Drosophila* is that SARA is localized apically in the wing discs, together with the early endosomes, and that SARA is required for symmetric inheritance of Dpp signaling during mitosis via its association with the spindle machinery (Bökel et al., 2006). In absence of SARA, Mad phosphorylation and expression of Dpp target genes are not affected (Bökel et al., 2006). Upon phosphorylation of Mad, two phosphorylated Mad (pMad) proteins form a trimeric complex with the Smad4 homologue Medea, the pMad-Medea complex is then translocated to the nucleus, where it binds to GC-rich regulatory regions of different genes. Together with other transcription factors, this complex regulates transcription of these genes, and can act either as a transcriptional activator or as a repressor (Figure 1.4) (Affolter & Basler, 2007; Affolter et al., 2001; Hamaratoglu et al., 2014).

The pMad-Medea complex binds to the GC-rich regulatory regions of genes such as *spalt* (*sal*) and *daughters against dpp* (*dad*), which encodes for the only known inhibitory Smad (I-Smad)

in *Drosophila,* to activate their transcription. Dad competes with Mad for receptor binding, and inhibits phosphorylation of Mad by acting as a negative feedback regulator (Tsuneizumi et al., 1997; Weiss et al., 2010). In contrast, the pMad-Medea complex recruits Schnurri (Shn), a large zinc-finger protein that acts as a Dpp-mediated transcriptional repressor to repress the expression of *brinker* (*brk*) (Marty et al., 2000; Müller et al., 2003; Pyrowolakis et al., 2004). Brinker is a nuclear protein and preferentially binds to the GC-rich sequence (T)GGCGCC (Sivasankaran et al., 2000; Zhang et al., 2001). *brk* is repressed in cells exposed to Dpp signaling, and this repression is required for activation of most of Dpp target genes. Brinker acts as an antagonist of the Dpp signaling pathway, and is able to repress the genes that are upregulated by Dpp in the embryo and larval tissues (Campbell & Tomlinson, 1999; Jaźwińska, Kirov, et al., 1999; Jaźwińska, Rushlow, et al., 1999; Minami et al., 1999). Following the discovery of Brinker, it was found that genes that were believed to be a direct target of Dpp, such as *omb*, were actually derepressed by Dpp via the removal of Brinker. The genes *sal* and *omb* play a crucial role in patterning the longitudinal vein 2 (L2) and 5 (L5) in the adult wing (Cook et al., 2004). The border of *sal* expression determines the position of L2 in the anterior compartment, while the position of L5 is specified by cells in the posterior compartment that express *omb* but lack *sal* (Cook et al., 2004).

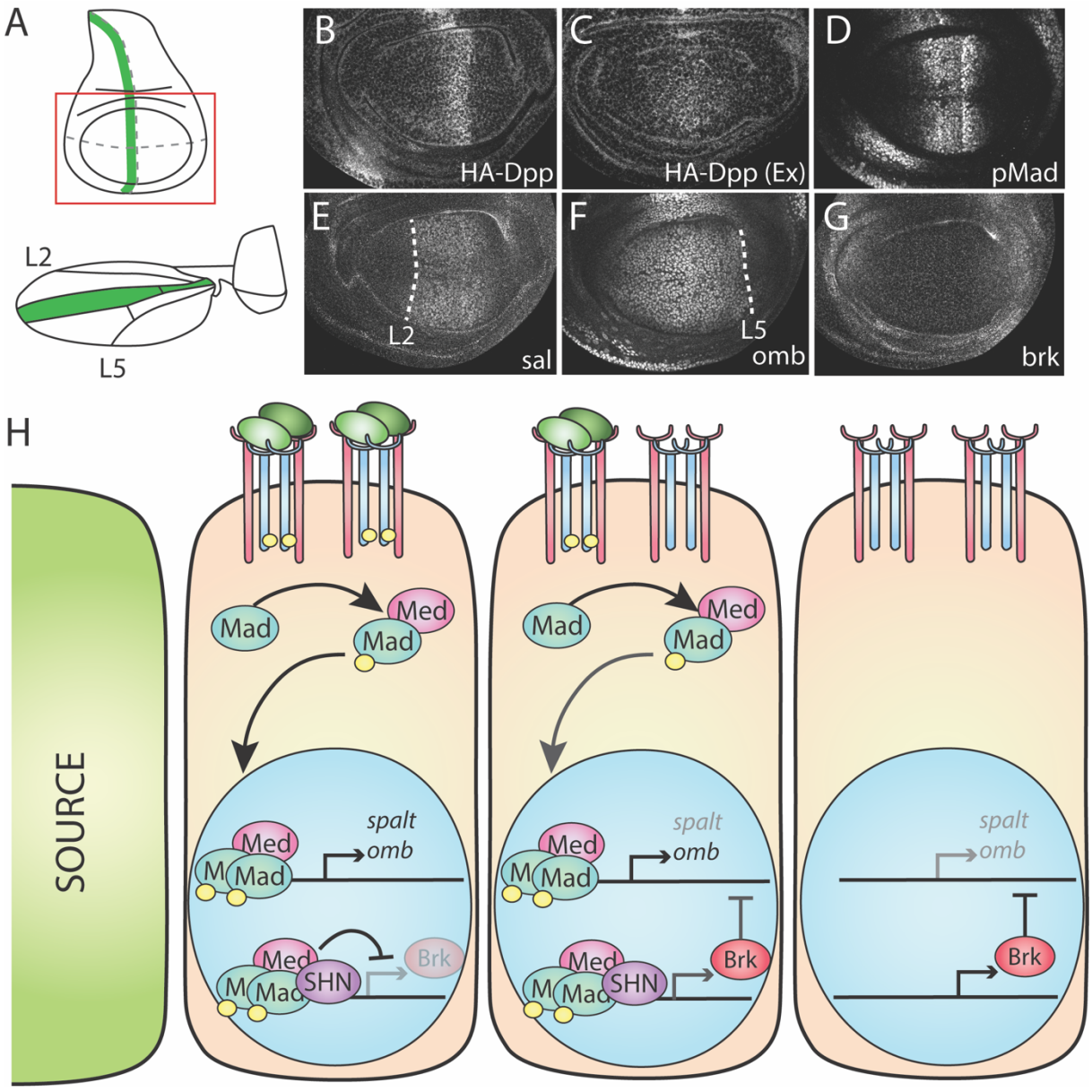

Figure 1.4: Dpp signaling components and pathway in Drosophila melanogaster wing imaginal disc.
(A) Dpp is expressed in a stripe of cells along the A/P boundary in the imaginal disc. Dpp (that is endogenously tagged with HA) can be visualized by a conventional anti-HA antibody staining. (B) Antibody staining showing localization of total HA-Dpp in the wing disc. (C) Extracellular anti-HA staining and visualizing localization of extracellular Dpp in the wing disc. (D) Visualization of Dpp signaling activity through an antibody staining against phosphorylated Mad (pMad). (E-G) Antibody staining against Dpp target genes Sal and Omb, and the transcriptional repressor Brk. Brk forms a gradient inverse in shape to Dpp signaling activity, and the border of Sal in the anterior compartment, and Omb in the posterior compartment determine position of the adult wing vein L2 and L5 respectively. (H) Schematic of Dpp signaling activity. The graded distribution of Dpp leads to different activation levels of the ligand/receptor complex, with high activation levels close to the source, and lower levels in the periphery, leading to a graded pMad gradient. Once Mad is phosphorylated by Tkv upon ligand recognition, pMad together with the co-Smad Medea translocate to the nucleus where it initiated transcription of Dpp target genes spalt and omb. The pMad-Med complex together with Schnurri (Shn) also repress expression of brk close to the Dpp source, leading to a gradient of Brk inverse to pMad. Brk in turn represses transcription of genes sal and omb, restricting Sal and Omb expression closer to Dpp source. In the peripheral region of the wing disc, Dpp signaling activity is absent and Brk levels are high, leading to suppression of sal and omb. Figure adapted form Restrepo et al. (2014).

1.4.3 The Dpp morphogen gradient in the wing disc

In *Drosophila* wing imaginal discs, Dpp is expressed in a narrow stripe of cells in the anterior compartment, along the anterior/posterior compartment boundary (Blackman et al., 1991; Masucci et al., 1990). The secreted Dpp forms a concentration gradient and is dispersed into the anterior and the posterior compartment, and activates Dpp signaling in the receiving cells (Lecuit et al., 1996; Nellen et al., 1996). Due to absence of a reliable antibody against Dpp, visualization of the extracellular gradient of Dpp was impossible until a GFP-Dpp fusion protein was generated (Entchev et al., 2000; Teleman & Cohen, 2000). Overexpression of GFP-Dpp in the *dpp*-producing source cells using the UAS-Gal4 system (*dpp-Gal4>UAS-GFP-dpp*) resulted in a long-range gradient of GFP-Dpp, and partially rescued the *dpp* mutant phenotype by partially restoring growth and patterning of the wing imaginal disc and the formation of an adult wing. Recently, in order to be able to visualize the endogenous Dpp gradient, novel tools were used to tag Dpp with smaller tags, such as HA and Ollas (Bauer et al., 2022; Bosch et al., 2017; Matsuda et al., 2021). These tagged forms of Dpp do not interfere with the function of Dpp and show no aberrant phenotype (Matsuda et al., 2021). Recently, the use of protein binders to tether HA-Dpp to the membrane of the source cells was used to investigate the requirement of Dpp dispersal for the growth and patterning of the wing imaginal disc. While the absence of Dpp dispersal did not highly affect the growth and patterning of the anterior compartment, the growth and patterning of the posterior compartment was strongly affected (Matsuda et al., 2021). To date, how Dpp moves from the producing cells to establish this gradient remains controversial. Different mechanisms of transport have been proposed over the years, which include receptor-mediated transcytosis (Entchev et al., 2000), free diffusion (Lander et al., 2002; Zhou et al., 2012), facilitated transport (Belenkaya et al., 2004) and cytoneme-mediated transport (Hsiung et al., 2005; Roy et al., 2014), which will be further discussed in chapter 1.6.4.3.

1.6 Endocytosis

Cells communicate with their environment through the surface of the outer leaflet of their plasma membrane, and in order to do so, its compositions need to be tightly regulated. Endocytosis is the de novo production of internal membranes from the plasma membrane, in which lipids, integral proteins, and the extracellular fluids become internalized into the cell, and it allows the cell and its interaction with its environment to be precisely regulated (Doherty & McMahon, 2009). For example, endocytosis of a transmembrane receptor can regulate the sensitivity of the cell towards a specific ligand. Endocytosis also plays a role in nutrient uptake, membrane remodeling, neurotransmission, pathogen entry and modulating cellular signaling responses (Doherty & McMahon, 2009). There are several modes of endocytic uptake into cells.

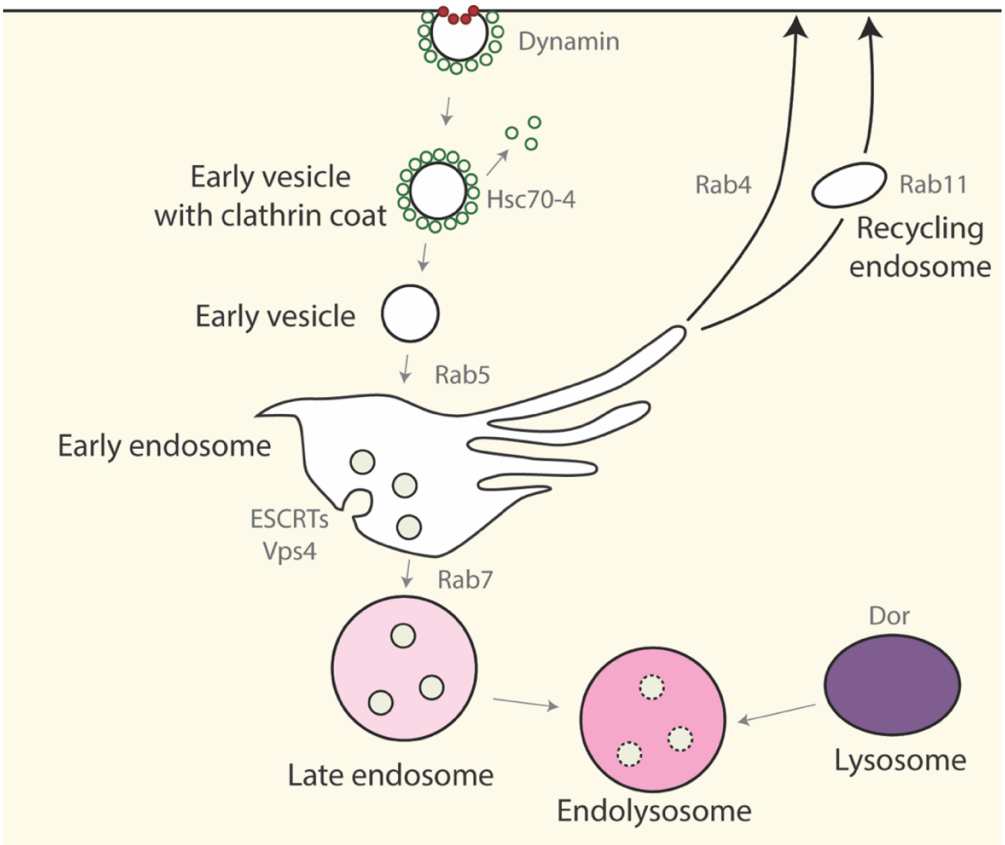

Figure 1.5: Endosome maturation scheme.
Newly formed endocytic vesicles are separated from the plasma membrane by Dynamin, and the coat of clathrin from the early vesicles is removed and recycled. The uncoated vesicles fuse with the early endosome via the function of Rab5. The cargo destined for recycling is sorted into tubular domains and sent directly back to the plasma membrane via fast (mediated by Rab4) or slow (mediated by Rab11) recycling pathways. Ubiquitinated membrane cargo is internalized into intraluminal vesicles via the function of ESCRTs and Vps4, giving the late endosome (marked by Rab7) its characteristic multivesicular body (MVB) appearance. The late endosome fuses with the lysosome to form an endo-lysosome, and to degrade and digest the internalized cargo. Figure adapted from Podinovskaia and Spang (2018).

1.6.1 Clathrin-dependent endocytosis

Clathrin-mediated endocytosis (CME) is an important vesicle biogenesis pathway, where cargo gets packaged into clathrin-coated vesicles (CCV) that are surrounded by a coat predominantly made of clathrin and adaptor protein complexes (Schmid & McMahon, 2007). CME is by far the most studied and best understood endocytic pathway as it is highly relevant in human health and disease, and it can easily be visualized by electron and fluorescent microscopy, and the multiple interactions between its protein partners can be dissected and manipulated (Mettlen et al., 2018). Clathrin forms a triskelion composed of three heavy and three light chains, and polymerizes around the cytoplasmic side of the membrane as a vesicle is budding (Edeling et al., 2006). Formation and initiation of the clathrin complex requires the membrane to have an appropriate lipid environment, which is brought about through an accumulation of adaptor proteins, such as adaptor protein-2 (AP-2), bound to phosphatidylinositol-4,5-bisphosphate (PIP2) on the plasma membrane, and becomes stabilized by accessory proteins that bind to Ap-2 and recruit clathrin (Mousavi et al., 2004; Schmid & McMahon, 2007). Once clathrin is polymerized, Ap-2 is no longer required and clathrin drives the formation of the vesicle. Once the vesicle is fully formed, it is detached from the membrane through the activity of the GTPase dynamin, and the clathrin coat is recycled back to the cytoplasm for reuse in another cycle of endocytosis (McMahon & Boucrot, 2011).

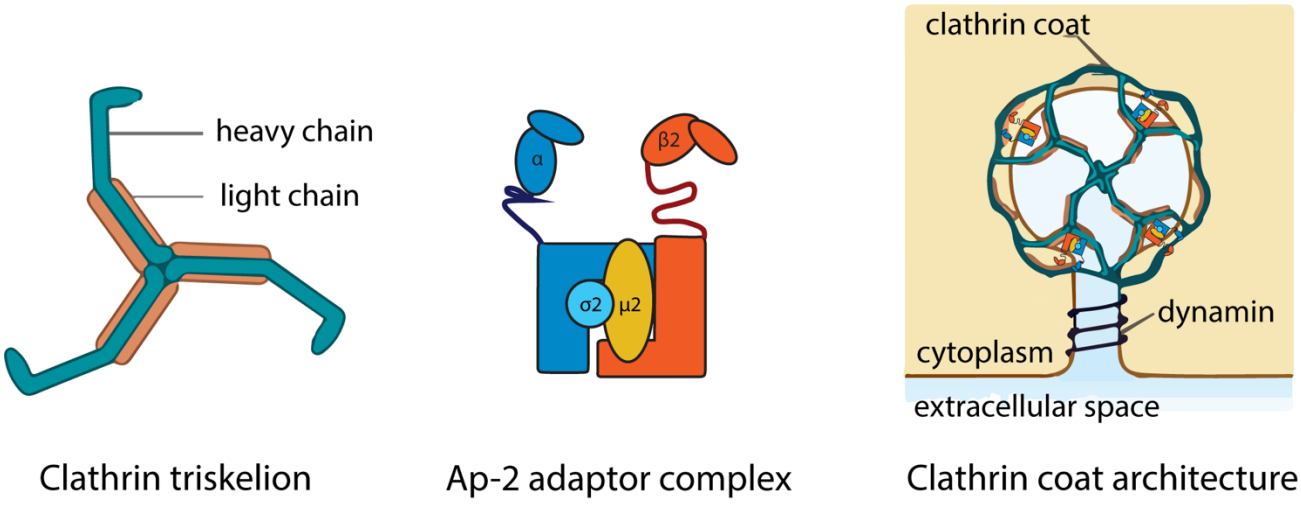

Figure 1.6: Clathrin triskelion, Adaptor-2 complex and their assortment to coat a vesicle.
Figure adapted from MRC-lmb and MBInfo, licensed under CC BY-NC 4.0.

1.6.2 Clathrin-independent endocytosis

CME has been extensively studied and is well characterized. However, several pathways that lead to the internalization of material inside the cells and work independently of clathrin and its molecular machinery have also been characterized and collectively referred to as clathrin-independent endocytosis (CIE) (Mayor et al., 2014). These pathways can either be at the large micrometer-scale, such as macropinocytosis and phagocytosis, or at much smaller scale (<200nm; see Fig. 1.7).

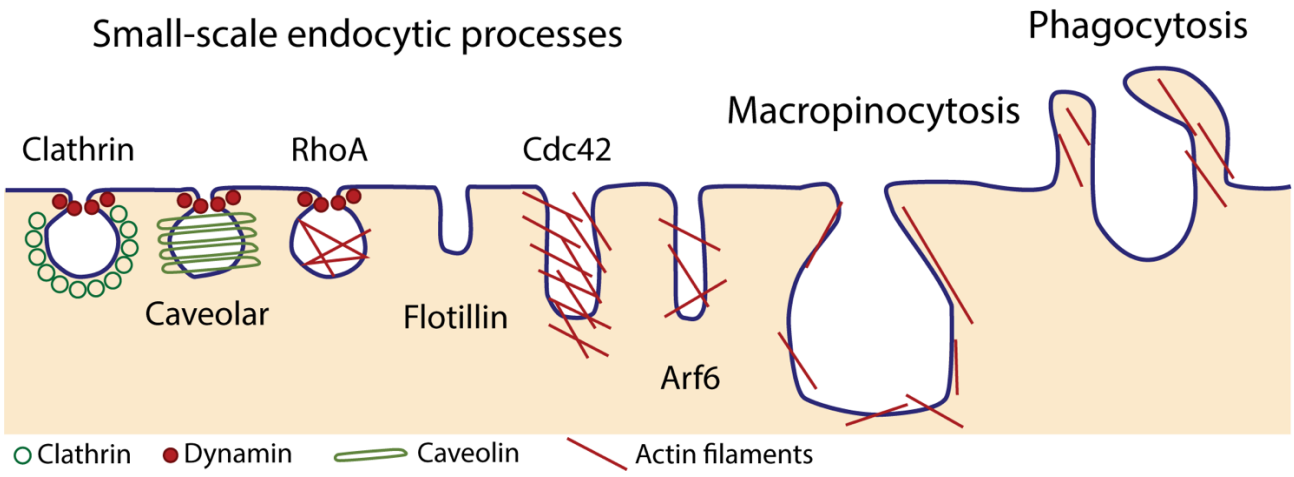

Figure 1.7: Pathways for entry into the cells.
Figure adapted from Mayor et al. (2014).

One mode of internalization that is independent of clathrin is caveolar endocytosis. Caveolae are an abundant feature of mammalian cells, and their formation is dependent on the expression of caveolin-1 (Cav1) in non-muscle cells and caveolin-3 (Cav3) in muscle cells (Galbiati et al., 2001). Cav1 is a membrane protein with a unique topology and is believed to insert its intramembrane domain into the plasma membrane to form a hairpin loop with both C and N terminal regions located towards the cytoplasm (Dupree et al., 1993). Cav1 interacts with cholesterol directly and depletion of cholesterol in the plasma membrane can flatten the caveolae (Rothberg et al., 1990). Caveolar endocytosis is dependent on dynamin, which can be recruited in response to a particular signal, or is localized constitutively to the neck of caveolae in endothelial cells (Oh et al., 1998; Pelkmans et al., 2002).

A second dynamin-dependent CIE pathway is RhoA-mediated internalization. RhoA is a small GTPase and is a key regulator of actin cytoskeleton dynamics, and this could possibly be regulating endocytosis via recruiting the actin machinery (Mayor et al., 2014).

Flotillin-associated endocytosis is a process that is independent of both dynamin and clathrin (Glebov et al., 2006). Flotillin is localized to the plasma membrane to specific microdomains or lipid rafts, and is regulated by the Src family tyrosine kinase Fyn (Riento et al., 2009). Flotillins interact with the cortical cytoskeleton via association with myosin IIA, and can control the formation of protrusions at the plasma membrane at the rear end of motile leukocytes (Meister & Tikkanen, 2014). Examples of cargo that are endocytosed via this route include GPI-anchored protein CD59, and cholera toxinB subunit (Glebov et al., 2006; Saslowsky et al., 2010).

Cdc42-associated endocytosis is another dynamin-independent and CIE, which is regulated by the small GTPase and Rho family member Cdc42. This Cdc42-associated pathway is the main mechanism of fluid-phase internalization in many cell types, and are mostly devoid of cargo from CME (Kirkham et al., 2005; Sabharanjak et al., 2002). This pathway is sensitive to inhibitors of actin polymerization and to cholesterol levels in the plasma membrane (Chadda et al., 2007).

Another mode of CIE that is also independent of dynamin is the Arf6-associated pathway. Arf6 is a member of the ADP ribosylation factor family of GTP-binding proteins and is present on the cell surface. The Arf6-associated pathway works independently of clathrin and dynamin, but it is dependent on cholesterol (Mayor et al., 2014). Some cell surface proteins that enter the cell via this pathway are involved in nutrient transport, in matrix interaction, and in immune function; others are anchored to the membrane by GPI (Eyster et al., 2009).

Larger particles, such as bacteria or debris, are internalized into the cells via macropinocytosis or phagocytosis. Macropinocytosis internalizes large molecules into the cell via invagination of the plasma membrane, and phagocytosis is the process by which the plasma membrane of the cell is extended to form a phagosome and engulf large particles such as pathogens and apoptotic cells (Rosales & Uribe-Querol, 2017).

1.6.3 Overview of endosomal maturation

Upon ingestion of the extracellular material via different endocytic pathways, the newly formed vesicles move away from the cell surface and fuse to the early endosome (EE) (Podinovskaia & Spang, 2018). At a certain point, the EE stops accepting fusion of new vesicles, and becomes a sorting endosome with tubular regions, which allows for the majority of the membrane to be recycled back to the cell surface (Podinovskaia & Spang, 2018). Recycling can either proceed directly to the plasma membrane, indirectly through a recycling endosome, or through the *trans*-Golgi network (TGN) retrograde pathways (Lakadamyali et al., 2006). The internalized membrane cargo that is destined for degradation becomes ubiquitinated and internalized into intraluminal vesicles (ILVs), giving the endosomes their distinct multivesicular body (MVB) morphology (Podinovskaia & Spang, 2018).

To prepare the endosome for degradation of the internalized cargo, the EE needs to mature and acquire properties of the late endosome (LE) to prepare its fusion with the highly acidic lysosomes. The endosomal maturation involves the replacement of Rab5 with Rab7, which in turn allows for fusion with other compartments, PIP conversion and acidification (Podinovskaia & Spang, 2018). Once all ubiquitinated cargo are internalized into ILVs and all the sorting receptors are recycled, the content of the LE is transferred to the lysosome, either via direct fusion of the LE with the lysosome, or via a “kiss-and-run” mechanism (Podinovskaia & Spang, 2018). The cargo is broken down by the hydrolytic environment of the lysosome and transferred outside into the cytoplasm by specific transporters and channels to allow for the lysosome to be regenerated and reused (Guerra & Bucci, 2016) (Refer to Fig.1.5).

1.6.3.1 Rab GTPase Control

Rab proteins are known to be markers of membrane identity and are responsible for regulating intracellular vesicular transport (Wandinger-Ness & Zerial, 2014). They are GTPases belonging to the Ras superfamily, and are highly conserved in eukaryotic cells. They switch between the inactive (GDP-bound) and active (GTP-bound) form, and they associate with membranes via their C-terminal isoprenoid moieties (Goody et al., 2017). Normally, prenylated Rabs are delivered to the membrane, and through the function of guanine nucleotide exchange factors (GEFs), GDP is transformed into GTP, allowing the Rabs to interact with their effectors (Goody et al., 2017). After the vesicles are produced, activated Rabs interact with different motor proteins and tethering factors to transport and bring the vesicle in close proximity of the target membrane. Once membrane fusion occurs, GTP hydrolysis catalyzed by GTPase activating proteins (GAPs) inactivates the Rabs, and the GDP-bound form of Rabs are extracted from the membrane by GDP dissociation inhibitor (GDI) (Hutagalung & Novick, 2011).

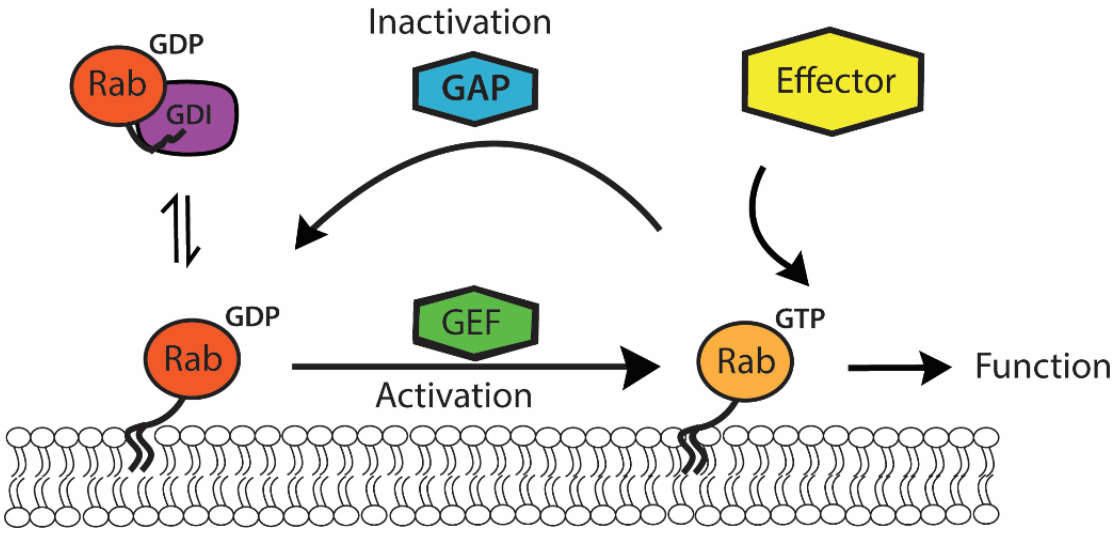

Figure 1.8: General model of Rab delivery, activation, inactivation and turnover on membranes.
GDI delivers prenylated Rabs to the membrane, and if they come across their GEF on the surface of the membrane, they get activated via GDP to GTP exchange. Rabs recruit effector proteins to the membrane in their activated GTP-bound form. GTPase activating protein (GAP) inactivated the Rab by GTP hydrolysis. Figure adapted from Langemeyer et al. (2018).

1.6.3.2 Regulation and function of Rab5

Following endocytosis, Rabex5, the Rab5-specific GEF, binds to internalized and ubiquitinated cargo and activates Rab5 on the endocytic vesicles (Lee et al., 2006). Rab5-GTP then recruits its effectors such as early endosome antigen 1 (EEA1) on the endosomal membrane. EEA1 is a tethering protein that is required for fusion of the early endocytic vesicles with the early endosome (Christoforidis et al., 1999). Rab5 also recruits and activates Vps34, a PI-3-kinase that promotes the synthesis of an organelle-specific lipid, phosphatidylinositol-3-phosphate (PI3P), on the early endosome, which in turn allows specific domains, such as FYVE domain, to be able to be associated with the membrane (Lawe et al., 2002). Thus, activation of Rab5 is needed to recruit specific proteins and synthesize specific lipids on the endosome to provide its early endosome identity (Langemeyer et al., 2018).

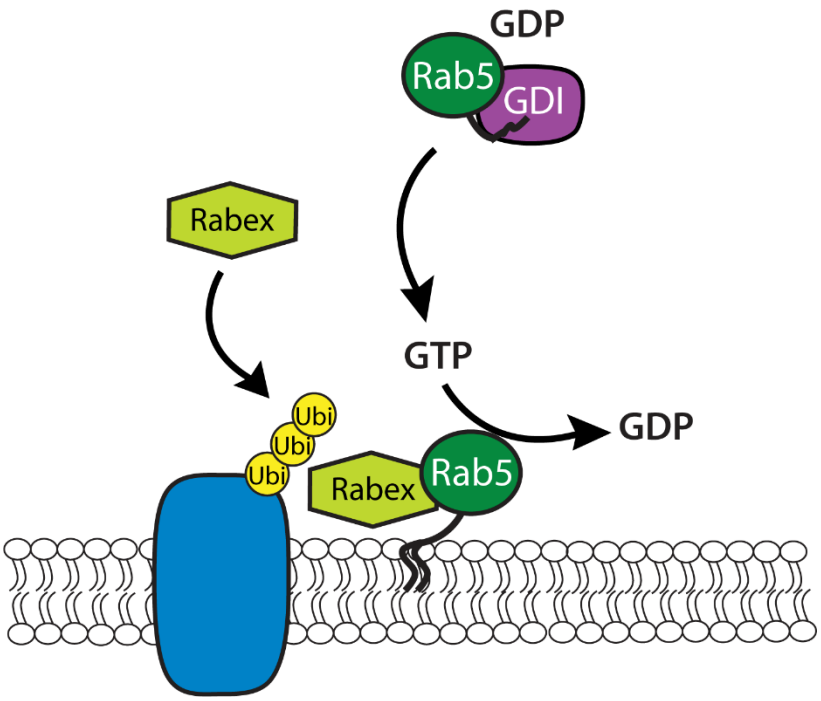

Figure 1.9: The model of recruitment of Rab5 to the early endosome and endocytic vesicles.
The ubiquitinated cargo on the membrane is recognized by Rabex5, the guanine nucleotide exchange factor (GEF of Rab5), and Rabex5 subsequently activates Rab5. Figure adapted from Langemeyer et al. (2018).

1.6.3.3 Endosomal maturation and activation of Rab7

Following rounds of Rab5 activation, additional fusion events lead to enlargement of the membrane content. At a certain point, Rab5-GTP recruits the Mon1-Ccz1 complex, which is a Rab7 GEF and triggers GTP loading of Rab7, and the complex binds to PI3P on the endosomal membrane (Poteryaev et al., 2010). The switch from Rab5 to Rab7 on the endosome occurs together with the release of the Rab5 GEF Rabex5, which prevents further activation of Rab5 (Poteryaev et al., 2010). Furthermore, the Rab5 GAP is recruited to the membrane and inactivates the remaining Rab5 (Haas et al., 2005). The Rab5 to Rab7 displacement has been described as a cut-out switch, which ensures that the progression of the endosomal maturation is unidirectional (Podinovskaia & Spang, 2018).

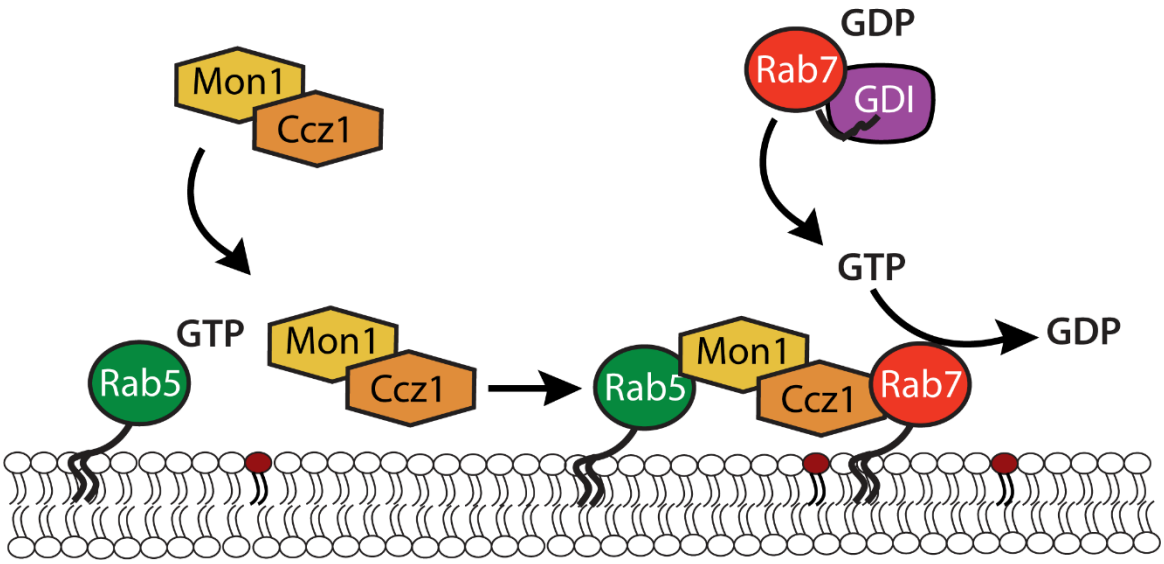

Figure 1.10: Model of Rab7 activation on the late endosome.
The Mon1-Ccz1 GEF binds to the active form of Rab5 and the lipids on membranes (such as PI3P, shown in red), and activates Rab7, which associates with the membrane once it is released from its chaperone GDI. Figure adapted from Langemeyer et al. (2018).

1.6.3.4 Intraluminal vesicles and formation of multivesicular bodies

Multivesicular bodies (MVBs) are organelles that are characterized by accumulation of vesicles in their lumen, and function as intermediates between early and late endosomes. The cargo taken up from the plasma membrane, which is destined for degradation, is internalized into intraluminal vesicles (ILVs) that are formed on the maturing endosome, giving the endosome its distinct MVB characteristic, and the cargo later reaches the lysosomes for degradation (Bucci & Stasi, 2016). There are several reasons for formation of ILVs: one is that, by inclusion of the endocytosed cargo into ILVs, signaling receptors are inactivated as they are deprived of their contact with the cytosol (Huotari & Helenius, 2011). Also, the membrane proteins and lipids can later be delivered to the lysosome in a form that is more easily accessible to the hydrolases, as the ILV membranes are devoid of a protective glycosylated layer. They also contain a phospholipid bis(monoacylglycero)phosphate/lysobisphoshatidic acid (BMP/LBPA), that can promote lipid hydrolysis (Kobayashi et al., 1998).

ILVs are formed on the maturing endosome, and the mechanism that guides their formation is regulated by the sequential action of an endosomal sorting complex required for transport (ESCRT) machineries. The membrane cargos that are destined for degradation are mono-ubiquitinated, and the Ubiquitin is recognized by ESCRT-0, constituting of the hepatocyte growth factor receptor-regulated tyrosine kinase substrate (Hrs) (Urbé et al., 2003). Hrs recruits the downstream ESCRTs by directly interacting with ESCRT-I component TSG101 and subsequently with ESCRT-II components Vps22, Vps25 and Vps36 (Babst et al., 2002; Clague & Urbé, 2003). ESCRT-I and ESCRT-II form a super-complex that can adopt different shapes, generating the initial phase of membrane budding (Wollert & Hurley, 2010). At the same time, ESCRT-II recruits ESCRT-III components, which can adopt a variety of shapes, including rings, filaments and spirals (Ghazi-Tabatabai et al., 2008). ESCRT-III consists of four core subunits of Vps20, Snf7, Vps24, and Vps2. Upon binding of Vps24 and Vps2 to Snf7 polymers, the architecture of ESCRT-III changes from flat spirals into 3D helices, and initiates recruitment of Vps4 (Alonso et al., 2016). Vps4 is an AAA-ATPase and is largely present as a monomer in the cytoplasm (Migliano & Teis, 2018). Vps4 is thought to form a double-ring structure of 10-12 subunits, similar to other AAA ATPases, and it contains a microtubule-interacting and transport (MIT) domain in the N-terminal, which is crucial for its interaction with the MIT-interacting motif (MIM) at the C-terminal of Vps2 (Scott et al., 2005). Binding of Vps4 with the ESCRT-III components drives neck construction at the formed vesicle, as Vps4 constricts

ESCRT-III filaments by pulling individual subunits through the central pore of the Vps4 hexamer (Ghazi-Tabatabai et al., 2008). This process leads to a disassembly of ESCRT network by partially unfolding the subunits, and ultimately to membrane scission and separation of the internal vesicle (Williams & Urbé, 2007).

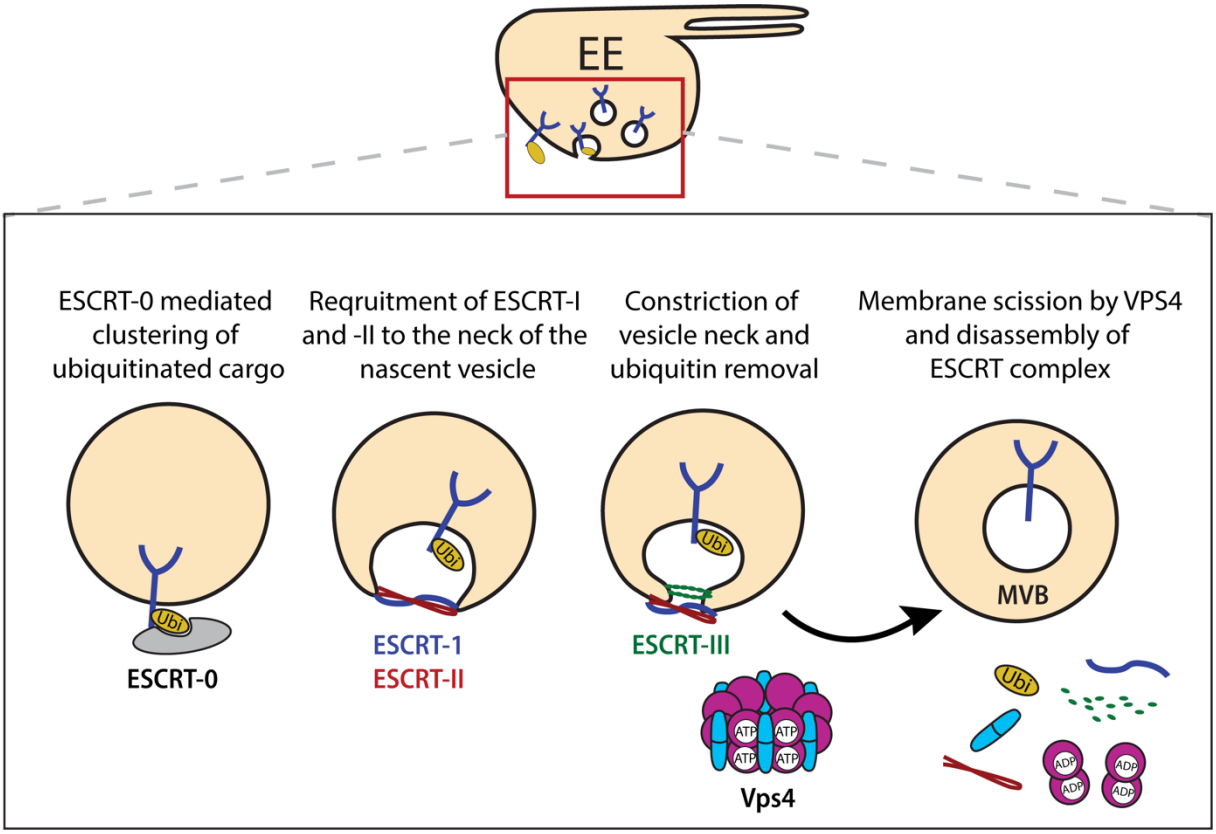

Figure 1.11: Formation of multivesicular bodies and internalization of ubiquitinated membrane proteins into intraluminal vesicles.
The membrane protein destined for degradation is ubiquitinated, and the Ubiquitin is recognized by the cytoplasmic ESCRT-0 component Hrs. ESCRT-0 subsequently recruits ESCRT-I and ESCRT-II components, which help with initiation of the membrane budding. ESCRT-III is also recruited to the complex, developing the structure of the intraluminal vesicles. Lastly, Vps4 is recruited which drives neck constriction at the formed vesicle, leading to membrane scission and separation of the internal vesicle. The components are then released and recycled in the cytoplasm. Figure adapted from Migliano and Teis (2018).

1.6.3.5 De-ubiquitination of endocytosed cargo

The ubiquitinated and endocytosed membrane protein goes through protein sorting and/or degradation during the maturation of the early endosome into the late endosome and MVB formation. As Ubiquitin is a long-lived protein *in vivo*, it needs to be recovered prior to complete internalization of the cargo into ILVs as MVBs are forming. This process is regulated by de-ubiquitinating enzymes (DUBs) (Amerik & Hochstrasser, 2004). ESCRT-III is known to help recruit DUBs to the maturing endosomes and direct them towards the ubiquitinated

cargo that is meant to be degraded via MVB formation and lysosomal degradation. DUBs then de-ubiquitinate the membrane cargo, and Vps4 disassembles and releases the ESCRT components and the DUBs from the endosome surface (Amerik & Hochstrasser, 2004).

1.6.3.6 Late endosome formation and maturation

When MVBs are formed from EEs, they mature into the late endosomes, form larger bodies and move to the perinuclear region, where they can fuse with the lysosome to degrade the transported cargo (Huotari & Helenius, 2011). The maturation of the endosome includes exchange of components on the membrane, movement to the perinuclear area, formation of ILVs, a shift in fusion partner choices, a drop in luminal pH, acquisition of lysosomal components, as well as a change in morphology (Huotari & Helenius, 2011). Also, as the endosome is maturing, PI(3)P, which is abundant in the early endosomal membrane, is substituted by PI(3,5)P2, and the class C core vacuole/endosome tethering factor (CORVET) is also replaced by the late endosomal/lysosomal homotypic fusion and vacuole protein sorting (HOPS) complex (Solinger & Spang, 2013). Furthermore, the early endosomal SNAREs (soluble NSF (N-ethylmaleimide (NEM)-sensitive factor) attachment protein receptors) that are important for fusion are replaced with the late endosomal SNAREs (Bucci & Stasi, 2016).

The LEs are characterized by the presence of numerous ILVs and they contain lysosomal-associated membrane protein 1 and 2 (LAMP1 and LAMP2), which are glycoproteins also present on the membrane of lysosomes to protect the membrane from degradation (Huotari & Helenius, 2011). Acidification and its regulation in endosomes are also an important part of endosomal maturation, as the luminal pH of endocytic organelles is acidic. EEs have a pH range of 6.8-6.1, LEs are in the range of 6.0-4.8, and in the lysosomes the pH level can drop to around 4.5 (Maxfield & Yamashiro, 1987). The low pH in endosomes provides a better environment for hydrolytic reactions and prepares the LE to fuse with the lysosome to degrade the internalized cargo (Huotari & Helenius, 2011).

1.6.4 Role of cellular trafficking in gradient formation and signaling of different morphogens in *Drosophila*

Since the concentration of a morphogen is important for determination of cell fate in a given tissue, endocytic trafficking of the ligand and its receptor play an important role in attenuating the cell-cell signaling during development. Endocytosis and cellular trafficking of different developmental signals to the lysosome for degradation has been discovered to have a role in restricting the range of morphogen gradients and inactivating the ligand-receptor complexes (Seto et al., 2002).

1.6.4.1 Trafficking of Hedgehog

Hedgehog (Hh) is secreted both basally and apically. The apically secreted Hh is re-internalized into the producing cells via Dynamin and Rab5, and recycled back to the basolateral domain of the plasma membrane via the recycling endosomes (Callejo et al., 2011). Dispatched (Disp), a multi-span transmembrane protein with a cholesterol-sensing domain is possibly involved in the regulation of vesicular trafficking necessary for basolateral release of Hh (Callejo et al., 2011). It has been shown that the Hh gradient in the *Drosophila* wing imaginal disc is controlled by its receptor Patched (Ptc), which internalizes Hh from the basolateral side of the cells in the wing imaginal disc through the function of dynamin (Torroja et al., 2004). Recent findings suggest that Ptc itself, is internalized from the apical side of the cells via dynamin, trafficked and externalized in the basal side through the function of the ESCRT machinery and MVBs, in order to come into contact with Hh (González-Méndez et al., 2020).

Furthermore, cytonemes have also been found to be required for the establishment of a normal Hh morphogen gradient, as they act as transporters for the membrane-associated Hh to achieve its restricted spatial distribution needed for tissue patterning (Bischoff et al., 2013). The Hh receiving cells in the anterior compartment extend basolateral cytonemes towards the Hh producing cells in the posterior compartment to receive Hh in a contact-dependent process that resembles a synapse, contributing to the formation of the Hh signal gradient. This cytoneme-mediated interplay between the receiving and the producing cells also requires heparan sulfate proteoglycans (González-Méndez et al., 2017).

1.6.4.2 Trafficking of Wingless

The Wnt signaling is a key regulator of cell-cell communication during development, and Wingless (Wg), the Wnt-1 homologue in *Drosophila*, is required for patterning the embryonic epidermis and the larval wing disc. Wg is secreted from a narrow stripe of cells at the dorsoventral (D/V) compartment boundary in the wing imaginal discs, and moves away from its source to form a long-range protein gradient (Rives et al., 2006). Endocytosis of the ligand and targeting it for degradation is required for attenuating the active receptor complex and signaling. In the case of Wg, the ligand is internalized via its receptors Frizzled (Fz), DFrizzled-2 (DFz2), and the co-receptor Arrow, and this complex is trafficked to the lysosome where it is degraded. The function of dynamin is required for internalization of Wg and for normal Wg signaling, observed through its targets Senseless (Sens) and Distalless (Dll) (Seto & Bellen, 2006). Upon knocking down Dynamin, the distribution of extracellular Wg is expanded, while the expression of Sens and Dll are reduced (Seto & Bellen, 2006). Furthermore, overexpression of $Rab5^{DN}$ in the wing pouch leads to an increase in the extent of Wg dispersal, while Wg targets Sens and Dll are completely lost or reduced, respectively (Seto & Bellen, 2006). Also, extracellular Wg was strongly enriched apically and very basally of the epithelium, suggesting that Wg is internalized from apical and basal, but not lateral surfaces, and that internalization limits the spread of the ligand (Marois et al., 2006).

Furthermore, it has been suggested that Godzilla, a member of the RNF family of membrane-anchored E3 ubiquitin ligase, is responsible for trafficking Wg from the early apical endosomes to the basolateral surface (Yamazaki et al., 2016).

Also, in cells mutant for the ESCRT-0 component Hrs, extracellular Wg distribution is not affected, while intracellular Wg and its receptor and co-receptor are accumulated in large puncta inside the cells (Rives et al., 2006). Also, Wg signaling observed through Sens and Dll staining shows enhancement, meaning degradation of Wg signaling is mediated by MVB formation and lysosomal degradation. In embryos, increased lysosomal degradation of Wg appears to shorten its signaling range (Dubois et al., 2001).

In the study done by Marois et al. (2006), knocking down Rab7, the marker of the late endosome, showed no effect in the extracellular Wg distribution, while intracellular Wg-positive endosomes were increased in size and number, further away from the source. Thus, the increase in range of intracellular Wg was not due to an increase in the spread of the

extracellular ligand, but rather to an enhanced perdurance of the internalized Wg protein (Marois et al., 2006). Also, knocking down Rab4 and Rab11, the markers for recycling endosomes, did not alter the range of the extracellular nor the intracellular Wg protein in the wing imaginal discs (Marois et al., 2006).

1.6.4.3 Trafficking of Dpp

It has been previously shown that Dpp, which is expressed in a stripe of cells along the anterior/posterior (A/P) compartment boundary, forms a long-range gradient activity and activates its target genes at different distances from the source (Basler & Struhl, 1994; Lecuit et al., 1996; Nellen et al., 1996). It has been proposed that Dpp in the wing imaginal discs undergoes clathrin-mediated endocytosis, and upon aberrant function of clathrin heavy chain and its adaptor protein α-Adaptin, the range of Dpp signaling is reduced (González-Gaitán & Jäckle, 1999). In order to study the mechanisms and molecular basis of Dpp gradient formation, Entchev et al. (2000) generated a GFP-tagged version of Dpp by integrating a GFP tag into the mature domain of Dpp, expressed under the UAS transcriptional control. They were able to partially rescue *dpp* mutant flies by overexpressing this tagged form of Dpp in the source cells using a *dpp-Gal4* driver. They proposed that the long-range Dpp gradient is formed via receptor-mediated transcytosis, as they overexpressed GFP-Dpp, they observed an accumulation of GFP-Dpp only on cells closer to the source on *tkv* mutant clones, but not behind the clones. They also proposed that dynamin is playing a role in receptor-mediated transcytosis and in its absence, transcytosis cannot take place. They did so by inducing clones that were mutant for *dynamin*, while trying to observe the Dpp gradient behind the clones using GFP-Dpp. However, they were unable to observe any GFP-Dpp signal in a number of wildtype cells right behind the *dynamin* clones, which they termed a “shadow”, and they concluded that Dpp goes through receptor-mediated transcytosis, and Dynamin is required for Dpp dispersal (Entchev et al., 2000).

Furthermore, upon expressing a dominant negative form of Rab5 (which is blocked in the inactive GDP-bound state) in the posterior compartment of the wing imaginal discs, they observed a reduced range of expression of the Dpp target gene *sal*. The restricted *sal* expression in cells close to the Dpp source upon reduced activity of Rab5 indicated that

endocytosis has a role in establishing the Dpp signaling gradient (consistent with the transcytosis model).

In a separate study, and in the context of studying cell competition, which is defined as a fitness control mechanisms, where unhealthy cells are eliminated from the tissue for optimal survival of the host, it was shown that inducing $Rab5^{DN}$ clones in the wing imaginal discs led to an increase in expression of the Dpp transcriptional repressor Brk (Gradeci et al., 2021; Moreno et al., 2002). The authors argued that cells compete for Dpp to prevent apoptosis, which is triggered by Brk upregulation followed by JNK activation, and that in the absence of a functional Rab5, Dpp cannot be endocytosed to initiate Dpp signaling (Moreno et al., 2002).

Entchev et al. (2000) also observed a shortened range of Spalt expression when they overexpressed the constitutively active form of Rab7, suggesting that degradation of Dpp via the late endosome and the lysosome restricts the signaling range of Dpp (Entchev et al., 2000). The authors concluded that the long-range distribution of Dpp is mediated by planar transcytosis initiated by endocytosis. However, several more recent studies argued against the receptor-mediated transcytosis model (Belenkaya et al., 2004; Lander et al., 2002; Schwank et al., 2011). Lander et al. (2002) mathematically provided evidence that blockade of endocytosis alone cannot distinguish between diffusive and non-diffusive modes of morphogen transport, including the receptor-mediated transport model, and proposed that diffusive mechanisms for Dpp transport are more likely than the non-diffusive ones. Also, Belenkaya et al. (2004) showed that dynamin is required for internalization of Dpp and initiation of its signaling activity, but dynamin-mediated endocytosis is not essential for movement of Dpp in the tissue. They rather suggest that Dpp movement is regulated via the heparan sulfate proteoglycan (HSPG) Dally and Dlp, and proposed the restricted extracellular diffusion model, in which Dpp molecules can move across Dynamin-deficient cells but fail to move across the HSPG-deficient cells (Belenkaya et al., 2004).

Later, Schwank et al. (2011) also argued against the receptor-mediated transcytosis model, as they observed Dpp and its signaling activity behind clones of cells that were mutant for its receptor Tkv. They favored the restricted diffusion model, and suggested that the receptor-independent mode of transport has not yet been studied and could be a possible mechanism for Dpp transport. Finally, by overexpressing UAS-GFP-Dpp and visualizing the internalized ligand through a nanobody binding assay, Romanova-Michaelides et al. (2022) proposed that

Dpp is endocytosed without its receptor Tkv, but through Dally and Pentagone. Pentagone is secreted, directly interacts with Dally, its production is restricted to the most lateral cells in the disc, and plays a key role in scaling of the Dpp gradient activity (Hamaratoglu et al., 2011; Norman et al., 2016). Romanova-Michaelides et al. (2022) also proposed that Dpp is recycled and re-exocytosed via the function of Rab4 and Rab11, and this recycling is required for scaling of the Dpp gradient.

1.7 Protein binders

In the past, studying protein functions relied mostly on genetic and RNA interference approaches. Albeit the recent advances in tools such as CRISPR/Cas9, which has made genetic manipulation much easier and faster, these methods are used to study protein function by altering the DNA, prior to protein production. In recent years, development and usage of functionalized protein binders has made it possible to directly target and manipulate the function of proteins of interest *in vivo* (Aguilar, Matsuda, et al., 2019; Aguilar, Vigano, et al., 2019; Bieli et al., 2016; Harmansa & Affolter, 2018). Protein binders are protein-based affinity reagents that selectively recognize and bind to target proteins, and can be "functionalized" by fusing them to well-characterized protein domains to allow for visualizing and regulating the protein of interest in a predictable manner (Aguilar, Vigano, et al., 2019; Harmansa & Affolter, 2018).

Protein binders can be sub-divided into two broad families of immunoglobulin- and non-immunoglobulin-based binders. The immunoglobulin-based binders are derived from antibodies and their derivatives such as single-chain variable fragments (scFvs) and nanobodies, which are derived from the variable domain of camelid heavy-chain antibodies. The non-immunoglobulin-based binders are natural or designed protein scaffolds such as Design Ankyrin Repeat Proteins (DARPins), monobodies, affibodies and others (Harmansa & Affolter, 2018).

The application of protein binders in developmental biology includes but is not limited to protein visualization (Gross et al., 2013; Rothbauer et al., 2006), protein relocalization (Harmansa et al., 2017), membrane trapping of extracellular proteins on the cell surface (Harmansa et al., 2015; Matsuda et al., 2021), protein interference and degradation (Caussinus et al., 2011; Vigano et al., 2021; Wang et al., 2017; Yamaguchi et al., 2019), as well as post-translational modification of proteins (Lepeta et al., 2022; Roubinet et al., 2017).

A nice example of protein relocalization via protein binders and its function in developmental biology is the study of Harmansa and colleagues (Harmansa et al. (2017); Harmansa et al. (2015)) in which they used a collection of nanobody-based GFP-traps (called GrabFP and Morphotrap) that localized along the apical-basal axis to mislocalize transmembrane, cytoplasmic and extracellular GFP fusion proteins and studied the effect of their mislocalization. They used the Morphotrap and the GrabFP system to study the extracellular dispersal of Dpp and showed that the basolateral Dpp pool is important for patterning and growth of the wing imaginal disc, and that spreading of Dpp is needed for medial but not for lateral wing disc growth. Further research on Dpp dispersal using protein binders were undertaken by Matsuda et al. (2021), where an scFv against the HA tag (HA-trap), as well as a DARPin against Dpp (Dpp-trap) were generated and used to manipulate the Dpp morphogen gradient *in vivo*. They were therefore able to demonstrate that Dpp dispersal was only required for patterning and growth of the posterior compartment of the wing imaginal disc.

Two examples of protein degradation via the use of protein binders include deGradFP and deGradHA, which harnesses the Ubiquitin-proteasome pathway to directly target and degrade GFP-tagged and HA-tagged proteins, respectively (Caussinus et al., 2011; Vigano et al., 2021). DeGradFP comprises of a nanobody against GFP (called VhhGFP) fused with an F-box domain contained in the N-terminal domain of Slmb (an F-Box protein in *Drosophila*), and upon recognition of the GFP-tagged protein by VhhGFP, the protein of interest becomes polyubiquitinated and is degraded in a couple of hours by the proteasomes, or in certain cases via lysosomes (Caussinus et al., 2011). DeGradHA was generated by modifying deGradFP and replacing its vhhGFP with the anti-HA-frankenbody-scFvX15F11, and was shown to effectively degrade proteins carrying single HA epitope tags (Vigano et al., 2021).

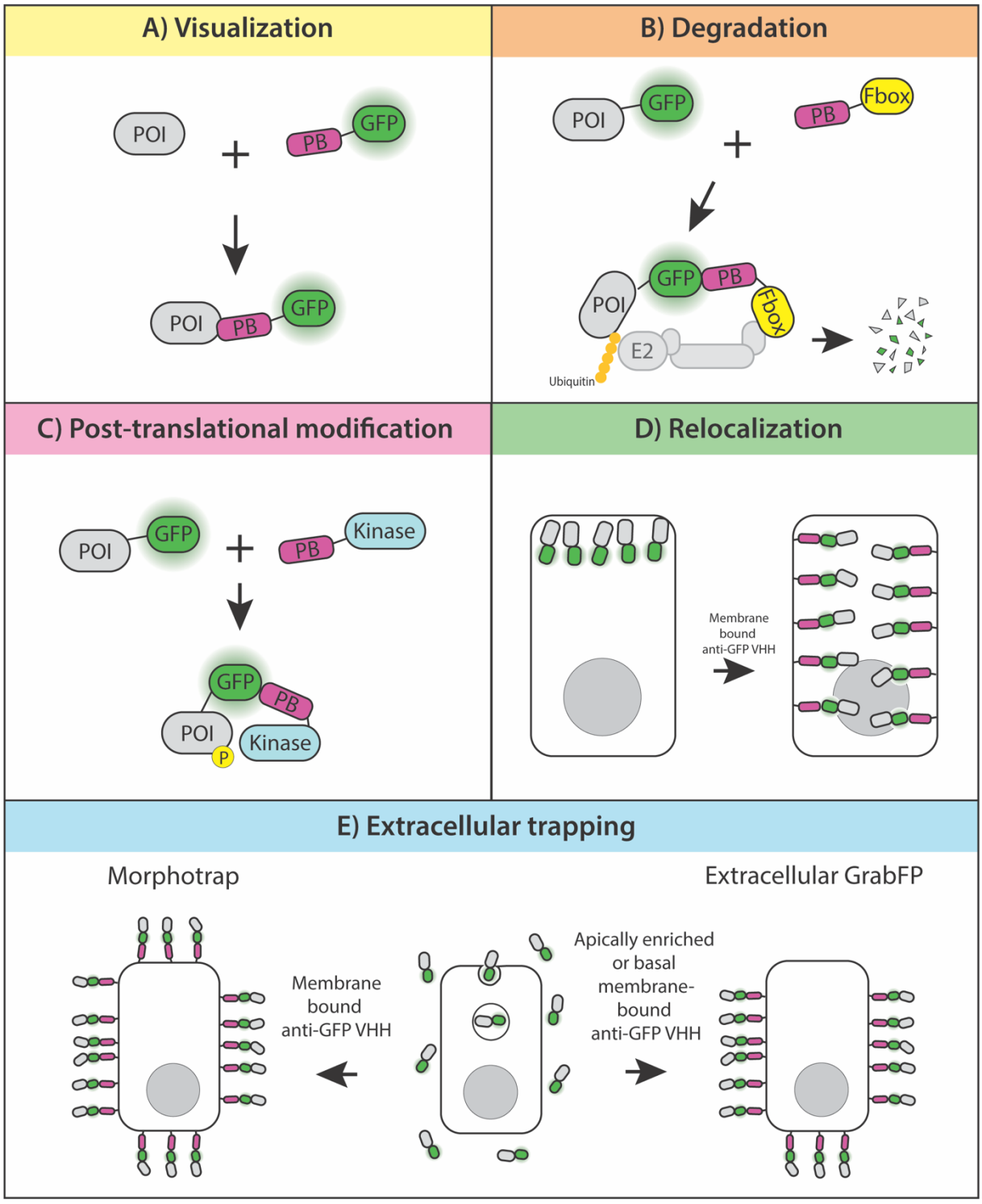

Figure 1.12: Schematic representation of different protein binder (PB)-based methods used in developmental biology.

A) To visualize a protein of interest (POI), the chromobody approach can be use, where upon protein binder fusion with the fluorescent protein, POI can be visualized. B) A protein binder bound to an F-box domain, e.g., deGradFP, targets the GFP-tagged POI for proteasomal degradation. C) GFP nanobodies fused to a kinase minimal domain induced phosphorylation of the GFP-tagged POI. D) GFP nanobodies fused to different plasma membrane scaffolds, e.g., apically enriched, basolateral or homogenously distributed, allow the relocalization of GFP-tagged intracellular proteins to different membrane compartments. E) A GFP nanobody fused to the transmembrane domain of CD8, such as Morphotrap, traps GFP-tagged secreted molecules on the cell surface and restricts their dispersal; or a GFP nanobody fused to different plasma membrane scaffolds, such as extracellular GrabFP, traps sub-populations of the secreted POI. Figure adapted from Aguilar, Vigano, et al. (2019).

A recent fascinating use of protein binders in the field of developmental biology was the engineering of a synthetic morphogen expressed and functioning in *Drosophila* wing primordia (Stapornwongkul et al., 2020). The authors engineered flies to express GFP appended with a secretion targeting signal (SecGFP), along the anterior/posterior axis in the wing imaginal disc. They also added GFP nanobodies to the extracellular domains of the Dpp receptors Tkv and Put, and observed that GFP, in the absence of Dpp, was able to develop patterned wings and partially rescue Dpp signaling activity via activation of the hybrid receptors. Additionally, upon fusing low-affinity GFP nanobodies to GPI-anchored heparan sulfate proteoglycans, they were able to improve Dpp target gene expression and patterning of adult wings further, to a level comparable to the wildtype. The authors utilized synthetic nanobodies to experimentally demonstrate, that a combination of free diffusion GFP ligands and GPI-anchored non-signaling receptor-assisted diffusion is sufficient to imitate the range and activity of a natural morphogen (Stapornwongkul et al., 2020).

2 Methods

2.1 Fly stocks

All fly stocks used for experiments that did not require a temporal knock down of certain factors were kept at 25°C in standard fly vials, containing polenta and a drop of yeast and flipped into new tubes every day. The fly stocks that were used for temporal knocking down of different factors (using tub-Gal80ts) were kept at 18°C and flipped into new tubes every day. The tubes were shifted to 29°C for the required timepoints. In order to distinguish homozygous from heterozygous flies, the balancer chromosomes *CyO,Dfd-YFP* (2nd chromosome) and *TM6B* (3rd chromosome) were used.

The following fly lines were used in this study:

Genotype	Description
ap-Gal4	Gal4 enhancer trap, drives expression in the dorsal compartment of the wing disc; Affolter lab stock.
arm-LacZ, m(2)Z, FRT40	*minute* mutant to induce *rab5*^{2} mutant clones
brk^{XA}	P element insertion located 42 bp upstream of the putative transcription initiation site of t1, disrupting the transcript (Campbell & Tomlinson, 1999).
dally[32]	Amorphic allele of dally, created by P-element insertion in the 5′ region, resulting in deletion of 1.8kb removing the first exon; (Franch-Marro et al., 2005).
dally[attP/B,YFPDally]	Dally tagged with YFP; obtained from Pyrowolakis lab.
dpp-Gal4	Gal4 enhancer trap, drives expression on the anterior/posterior axis.
dpp-LacZ	LacZ reporter line for dpp; Affolter lab stock.
dpp[d12]	hypomorphic allele of dpp; obtained from Pyrowolakis lab.
dpp[d8]	hypomorphic allele of dpp; obtained from Pyrowolakis lab.
FRT82b, Rab7-Gal4-Knock-in	Rab7-Gal4-knock-in used as Rab7 null mutant, recombined with FRT82b cassette to induce clones; (Cherry et al., 2013).
GFP-MadRA	Mad-RA isoform endogenously tagged with sfGFP after the start codon, obtained from McCabe Lab.
HA-dpp	Dpp allele endogenously tagged with HA tag; established by Shinya Matsuda.

HA-tkv	Tkv tagged extracellularly with HA; developed in this study.
hsFlp, tub-Gal80, w, FRT19A; UAS-CD8-GFP	The stock expresses FLP recombinase upon heat shock, as well as ubiquitous Gal80. The induced clones are recognized by expression of GFP, (BDSC, 85134).
hsFlp, UAS-GFP, w ; FRT42D, tub-Gal80/ Cyo; tub-Gal4, FRT82B, tub-Gal80/ Tm6CSbTb	Stock used to induce mosaic analysis with a repressible cell marker (MARCM) clones. The stock expresses Gal4 and Gal80 ubiquitously, and expresses FLP recombinase upon heat shock. The induced clones are recognized by expression of GFP, (BDSC, 86318).
hsFlp; rab5^{2} FRT40	Rab5 null mutant to induce mutant clones
M(vas-int.Dm)zh-2A ; tkv[KO-attP]	Vasa integrase, and attP landing site in tkv locus to insert tagged tkv constructs, obtained from Pyrowolakis lab.
mGL-dpp	Dpp allele endogenously tagged with monomeric Green Lantern fluorescent tag; established by Shinya Matsuda.
mSC-dpp	Dpp allele endogenously tagged with monomeric Scarlet fluorescent tag; established by Shinya Matsuda.
Ollas-dpp	Dpp allele endogenously tagged with HA tag; (Bauer et al., 2022)
rab11-eYFP	Rab11 tagged with eYFP at the N-terminus, (BDSC, 62549); (Dunst et al., 2015).
rab4-eYFP	Rab4 tagged with eYFP at the N-terminus, (BDSC, 62542); (Dunst et al., 2015).
rab5-eYFP	Rab5 tagged with eYFP at the N-terminus, (BDSC, 62543); (Dunst et al., 2015).
rab7-eYFP	Rab7 tagged with eYFP at the N-terminus, (BDSC, 62545); (Dunst et al., 2015).
shibire^{ts1}	A temperature-sensitive dynamin (shibire) allele. Shows adult and larval paralysis at 34 ^{o}C. (BDSC, 7068)
tkv-1xHAeGFP	Tkv tagged with 1xHA and eGFP in the C terminal; (Vigano et al., 2021).
tkv-YFP	Tkv tagged with YFP in the C-terminal; Obtained from Pyrowolakis lab.
tub-GAL80[ts]2	Temperature-sensitive GAL80 expressed under the control of the alphaTub84B promoter.
UAS-Dally RNAi	Expresses dsRNA for RNAi of Dally under UAS control, (VDRC, 14136).
UAS-dor RNAi	Expresses dsRNA for RNAi of dor under UAS control, (BSDC, 54460).
UAS-GrabFP-V5	Intracellular vhhGFP4 fused to transmembrane CD8 protein and V5 tag (extracellular); developed in this study, adapted from Harmansa et al. (2017).
UAS-hsc70-4 RNAi	Expresses dsRNA for RNAi of Hsc70-4 under UAS control, (BDSC, 28709).
UAS-LOT deGradHA	Anti-HA-frankenbody against HA-tagged proteins, modified from deGradFP tool; (Vigano et al., 2021).

UAS-morphotrap.int	vhhGFP4 (intracellular) fused to transmembrane CD8 protein and mCherry tag (extracellular); (Harmansa et al., 2017).
UAS-Rab11 RNAi	Expresses dsRNA for RNAi of Rab11 under UAS control, (VDRC, 22198).
UAS-Rab4 RNAi	Expresses dsRNA for RNAi of Rab4 under UAS control, (VDRC, 24672).
UAS-Rab5 RNAi	Expresses dsRNA for RNAi of Rab5 under UAS control, (BDSC 30518, 34096, 51847; VDRC, 103945).
UAS-Rab5.S43N	Expresses a dominant negative Rab5 protein under UAS control, (BDSC 42703, 42704).
UAS-Rab7 RNAi	Expresses dsRNA for RNAi of Rab7 under UAS control, (BDSC, 27051).
UAS-Shrub RNAi	Expresses dsRNA for RNAi of shrub under UAS control, (BDSC, 38305).
UAS-tkv RNAi	Expresses dsRNA for RNAi of tkv under UAS control, (BDSC, 40937).
UAS-TSG101 RNAi	Expresses dsRNA for RNAi of TSG101 under UAS control, (BDSC, 35710).
UAS-Vps4 RNAi	Expresses dsRNA for RNAi of vps4 under UAS control, (VDRC, 105977).
y w hs-Flp ; tub >CD2> Gal4, UAS-LacZ / CyO ; tub-Gal80TS / Tm6BTb	Flip-out cassette with tubulin promotor to induce clones, Affolter lab stock.

2.2 Immunostaining

2.2.1 Immunostaining procedure for wing imaginal discs

Third instar *Drosophila* larvae were dissected in ice-cold PBS (Gibco™, 20012027) by cutting the larvae in the middle and inverting the anterior half inside out. Fat tissue, gut and the salivary glands were removed while keeping the wing imaginal discs attached to the trachea and the cuticle. The dissected larvae were fixed in 4.0% PFA ((Electron Microscopy Sciences, 15714) diluted in PBS) fixative solution for 25 minutes at room temperature in 1.5 mL Eppendorf tubes on the rotor. The samples were washed three times for ten minutes with ice-cold PBS, and three times with 0.3% PBST (Triton-X diluted in PBS) to permeabilize the tissues. They were then blocked in 5% NGS (Abcam, ab7481) diluted in PBST for 30 minutes, and incubated with the primary antibody diluted in 5% NGS in PBST at four degrees overnight. The next day, the samples were washed three times for ten minutes with PBST and incubated in the dark with the secondary antibody diluted in 5% NGS + PBST for two hours at room

temperature. At last, the samples were washed three times for 15 minutes with PBST, two times with PBS, and then embedded in 5 drops of Vectashield plus antifade mounting medium (Vector Laboratories, H-1900). After incubating in Vectashield for at least one hour, the wing imaginal discs were mounted on microscope slides with the apical side of the discs facing the coverslip (#1.5H). The coverslip was then sealed with nail polish for long-term storage of the samples.

2.2.1.1 Removal of extracellular molecules using acid wash

In order to remove the extracellularly bound molecules prior to immunostaining to focus only on the intracellular molecules, an acid wash was performed. The larvae were dissected in ice-cold Schneider's Drosophila medium (Gibco™, 21720024), and prior to fixing the tissues, the live samples were washed three times for ten seconds with 1 mL of ice-cold Drosophila S2 media with its pH dropped to 3.0 by HCl. To remove the unbound molecules, the samples were washed three times for ten minutes with ice-cold S2 media at the physiological pH of 7.4 and fixed as described above (2.2.1).

2.2.1.2 Extracellular immunostaining of wing imaginal discs

For staining the extracellular molecules, the larvae were dissected in ice-cold Schneider's Drosophila medium. To ensure the primary antibody was able to reach the most apical side of the wing imaginal disc, a small scission was made above and below the wing pouch to disrupt the peripodial membrane and allow access to the antibody. The wing discs were then blocked in 200 µl of blocking solution (5% NGS in Schneider's medium) for ten minutes, and incubated with the primary antibody (diluted with 5% NGS in Schneider's Drosophila medium) for 60-70 minutes on ice. The primary antibody solution was mixed every ten minutes by gently tapping the bottom of the tubes. The samples were then washed ten times with 1 mL of Schneider's Drosophila medium to remove the excess primary antibody, and fixed as described above (2.2.1). All steps were done on ice to preserve the samples and to prevent internalization of the extracellular molecules.

2.2.2 Antibodies

The following primary antibodies were used for immunostaining in the project: Rabbit anti-phospho-Smad 1/5 (Cell signaling 9516S; 1:200), mouse anti-patched (DSHB; 1:40), mouse anti-wingless (4D4, DSHB; 1:120), rabbit anti-GFP (Abcam ab6556; 1:2000 for conventional staining, 1:200 for extracellular staining,), rat anti-HA (Roche 3F10; 1:300 for conventional staining, 1:20 for extracellular staining), rat anti-ollas (Invitrogen MA5-16125; 1:300 for conventional staining, 1:20 for extracellular staining), guinea pig anti-rab5 (provided by Akira Nakamura; 1:1000), rabbit anti-rab11 (provided by Akira Nakamura; 1:8000), mouse anti-rab7 (DSHB; 1:30), mouse anti-ubiquitin (Enzo PW8810-0100; 1:1000), mouse anti- beta galactosidase (Promega Z378825580610; 1:500), rabbit anti-spalt (provided by Rosa Barrio; 1:500), rabbit anti-omb (provided by Gert Pflugfelder; 1:500), guinea pig anti-brk (provided by Gines Morata; 1:1000), mouse anti-V5 (Invitrogen; 1:5000).

The secondary antibodies were mainly used from a selection of Alexa Fluor antibodies. Also, for staining proteins tagged with HA extracellularly, FITC goat anti-rat secondary antibody (Fc specific, Abcam ab97089; 1:250) was used.

2.2.3 Fluorescent microscopy and imaging

The wing imaginal discs were imaged with the 40X oil objective (NA 1.25) on Leica Sp5 and 25X oil objective (NA 0.8) on Zeiss 880 Airyscan inverted microscopes, with a Z-stack size of 0.5 µm, as well as the 60X oil objective (NA 1.5) on Olympus Spinning Disk CSU-W1 microscope, with a Z-stack of 0.21 µm. The images used for the colocalization analysis were taken with the 63x oil objective (NA 1.4) with 1.5x - 2.0x zoom on Zeiss 880 Airyscan inverted microscope with z-stack size of 0.21 µm.

2.2.4 Gradient intensity analysis

To quantify the intensity of pMad and extracellular mGL-dpp gradient in the images, an average intensity of three sequential stacks was created using Fiji ImageJ (v1.53c). A rectangle with the constant height of 12.5 microns was used to measure the average intensity in the

samples and the controls along the whole width of the wing pouch. To align the intensity profiles from different images along the anterior/posterior axis, the script (wing_disc-alignment.py) was used. The average intensity of the samples and the control were then compared using the script (wingdisc_comparison.py). Both scripts were generated by Etienne Schmelzer from the Affolter lab, and can be found on: https://etiennees.github.io/Wing_disc-alignment/. The resulting signal intensity profiles were generated on GraphPad Prism software (v.9.3.1(471)).

2.2.5 Counting the number and measuring the size of particles

To measure the number and sizes of particles an average intensity of 3 z-stacks from the images were created using Fiji ImageJ. The total area of controls and samples in which the particles were counted had a width of 20.16 and height of 34.17 microns. The images were filtered with the median of 2.0 to smoothen the edges, and a threshold of 21-255 was set on all images to outline and define the particles. The number and area of the particles were measured by the built-in "Analyze Particles" option on Fiji. The data were used to make box and whiskers graphs on GraphPad Prism. A ratio-paired t-test ($p<0.05$) was used for statistical analysis.

2.3 Genotyping

2.3.1 Nucleic acid extraction from adult flies

The buffer used to squish singles flies was prepared by adding 10 µL of 1M Tris-HCl (pH 7.5), 5 µL of 500mM EDTA (pH 8.0), 5 µL of 5M NaCl, 10 µL of Proteinase K (20 mg/mL), and added up to 1 mL with ddH2O. Single flies were anesthetized with CO_2 and transferred into a PCR tube and squished using a pipette tip in 50 µL of the squishing buffer. The samples were then incubated for 40 minutes at 37°C, followed by 2 minutes at 95°C to deactivate the Proteinase K. One microliter of the sample was then used as a DNA template for PCR reactions, following the One*Taq*® 2X Master Mix with Standard Buffer (New England BioLabs, M0482) protocol.

2.4 Designing Tkv with the extracellular tag

In order to visualize Tkv extracellularly, I tagged Tkv in the extracellular domain with the small HA tag. HA peptide is derived from the influenza virus hemagglutinin, is 9 amino acids in size, and has been extensively used in biochemical studies due to the availability of high-affinity monoclonal antibodies (Field et al. (1988) and Wilson et al. (1984), as cited in Vigano et al. (2021)). Due to the small size of the HA tag, and former successful tagging of different proteins with HA, I decided to also tag Tkv with this epitope. Previous attempts to tag Tkv extracellularly with mCherry have been unsuccessful and these flies were unable to become homozygous (Alborelli, 2016). Therefore, inserting a small tag in the correct position was critical. I used NCBI's Multiple Sequence Alignment program to align BMP type I receptor among different *Drosophila* species, to look for the presence of non-conserved regions, as these regions were likely to be the best location for inserting the tag without interrupting the functionality of the receptor. The amino acids 77-83 were the only non-conserved region in the extracellular domain of the receptor. Therefore, I designed to insert the HA tag after amino acid number 79, 165 bps upstream of the transmembrane domain of *tkv* (Fig. 2.1).

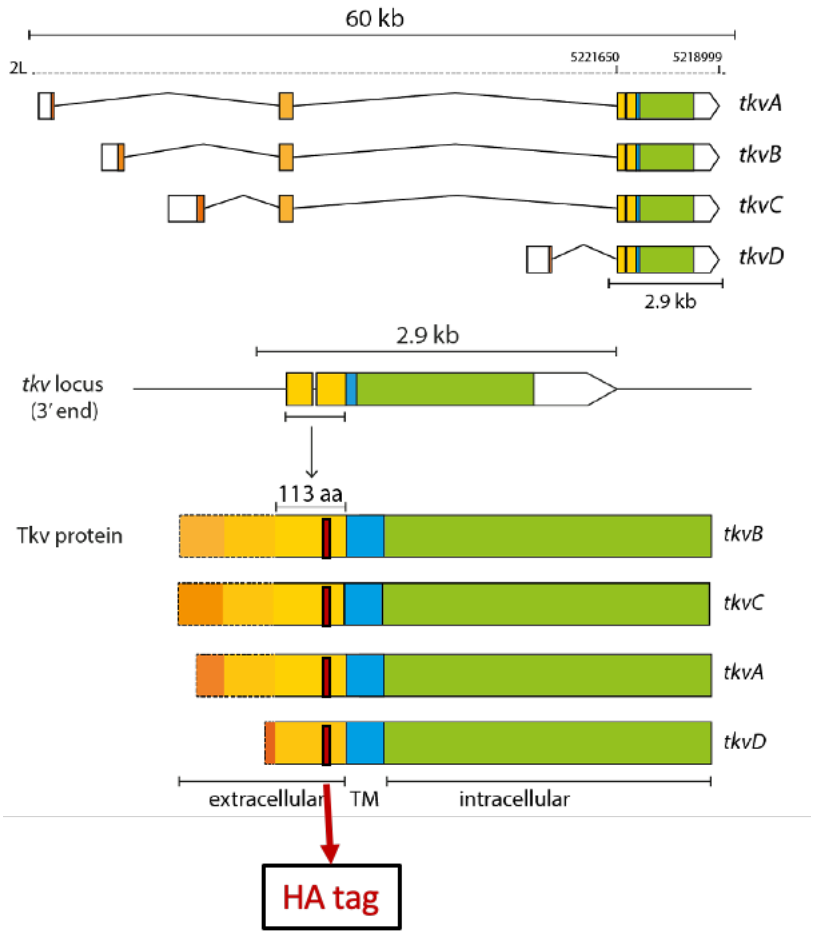

Figure 2.1: Insertion of the HA tag in tkv locus.
The HA tag is following amino acid number 79, ensuring its presence in all 4 Tkv isoforms. (Figure adapted from Alborelli (2016)).

As Tkv has 4 isoforms, I used NCBI's Multiple Sequence Alignment tool to ensure the HA tag can be present in all 4 isoforms, regardless of their alternative splicing. The established fly line with Tkv containing the extracellular HA tag was homozygous viable, and was used to visualize the extracellular Tkv in this study.

The fragment containing 1XHA tag in the extracellular region of Tkv is as followed and was produced by Genewiz Inc.:

Sequence of the HA tag: ACCCATACGACGTACCAGATTACGCT

The transmembrane domain:

CTGGCCGTCTTTGGCTCCATCATCATCTCCCTGTCCGTGTTTATGCTGATCGTGGCTAGCTTATGTTTC

Tkv extracellularly tagged with HA: (amino acid number 79, 46 amino acids upstream of the transmembrane domain)

CTCCACGAATTCTCCGGAGCGGCCGCTTTAAGTGCATTACTGCAACAGACGACTAGTTATTATAACCGGATATCATAAGGACA
TATTATAGGGGTCTTTGGGAAGCGTAAAGTCAGAAAAAGACGTTAAGGAAGCTAAGATCTTTTATTAGCTTAAAAGTCATGAC
CAATCCCATTTTCAGGCAGGAATAAATACGCAAGAGTCGTAAAATTGGTGATGTTAACAAGATAATTTGATTCTTACCAGACT
CTTCATTTCATATGGATTATCAATGAATGGTATATTAATTATATTCTGTTGCCATTTTAGCCCGCTCCCTAACCTGCTACTGC
GATGGCAGTTGTCCGGACAATGTAAGCAATGGAACCTGCGAGACCAGACCCGGTGGCAGTTGCTTCAGCGCAGTCCAACAGCT
TTACGATGAGACGACCGGGATGTACGAGGAGGAGCGTACATATGGATGCATGCCTCCCGAAGACAACGGTGGTTTTCTCATGG
TGAGTCCCCTATTAATCCATACAATAAATCCATAGCTAATGAAAATATCTTTTTGTTACAGTGCAAGGTAGCCGCTTACCCAT
ACGACGTACCAGATTACGCTGTACCCCACCTGCATGGCAAGAACATTGTCTGCTGCGACAAGGAGGACTTCTGCAACCGTGAC
CTGTACCCCACCTACACACCCAAGCTGACCACACCAGCGCCGGATTTGCCCGTGAGCAGCGAGTCCCTACACACGCTGGCCGT
CTTTGGCTCCATCATCATCTCCCTGTCCGTGTTTATGCTGATCGTGGCTAGCTTATGTTTCACCTACAAGCGACGCGAGAAGC
TGCGCAAGCAGCCACGTCTCATCAACTCAATGTGCAACTCACAGCTGTCGCCTTTGTCACAACTGGTGGAACAGAGTTCGGGC
TCCGGATCGGGATTACCATTGCTGGTGCAAAGAACCATTGCCAAGCAGATTCAGATGGTGCGACTGGTGGGCAAAGGACGATA
TGGCGAGGTCTGGCTGGCCAAATGGCGCGATGAGCGGGTGGCCGTCAAGACCTTCTTTACGACCGAAGAGGCTTCTTGGTTCC
GCGAGACTGAAATCTATCAGACAGTGCTGATGCGACACGACAATATCTTGGGCTTCATTGCCGCCGATATCAAGGGTAATGGT
AGCTGGACACAGATGTTGCTGATCACCGACTACCACGAGATGGGCAGCCTACACGATTACCTCTCAATGTCGGTGATCAATCC
GCAGAAGCTGCAATTGCTGGCGTTTTCGCTGGCCTCCGGATTGGCCCACCTGCACGACGAGATTTTCGGAACCCCTGGCAAAC
CAGCTATCGCTCATCGCGATATCAAGAGCAAGAACATTTTGGTCAAGCGGAATGGGCAGTGCGCTATTGCTGACTTCGGGCTG
GCAGTGAAGTACAACTCGGAACTGGATGTCATTCACATTGCACAGAATCCACGTGTCGGCACTCGACGCTACATGGCTCCAGA
AGTATTGAGTCAGCAGCTGGATCCCAAGCAGTTTGAAGAGTTCAAACGGGCTGATATGTATTCAGTGGGTCTCGTTCTGTGGG
AGATGACCCGTCGCTGCTACACACCCGTATCGGGCACCAAGACGACCACCTGCGAGGACTACGCCCTGCCCTATCACGATGTG
GTGCCCTCGGATCCCACGTTCGAGGACATGCACGCTGTTGTGTGCGTAAAGGGTTTCCGGCCGCCGATACCATCACGCTGGCA
GGAGGATGATGTACTCGCCACCGTATCCAAGATCATGCAGGAGTGCTGGCACCCGAATCCCACCGTTCGGCTGACTGCCCTGC
GCGTAAAGAAGACGCTGGGGCGACTGGAAACAGACTGTCTAATCGATGTGCCCATTAAGATTGTCTAACTCGAGTGGCGCGCC
GGTACC

2.4.1 Generation of Tkv with the extracellular tag

The *TkvHA* allele (Tkv tagged intracellularly before the stop codon with 3XHA) was previously described (Norman et al., 2016). The same plasmid was used as a vector to insert the designed fragment of Tkv tagged extracellularly with 1xHA. The designed fragment and the plasmid were both digested using EcoRI and AscI restriction enzymes, The cut vector and insert were both purified and ligated together at 18°C over night.

2.4.2 Generation of GrabFP tagged with v5

The plasmid morphotrap_intra from Emmanuel Caussinus in the Affolter lab which contains the nanobody fused to an mCherry tag was used to amplify the Vhh4 nanobody together with V5 tag instead of mCherry. The following primers were used to amplify the sequence using the Q5 Hotstart high-fidelity DNA polymerase:

Table 2.1: Primers used for amplifying the nanobody with the V5 tag

Acc65I_V5_mCD8_F	ggtaccGGTAAGCCTATCCCTAACCCTCTCCTCGGTCTCGATTCTACGGGCAGCAAGCCACAGGCACCCG
XbaI_nanobody_R	ccTCTAGattaGCTGGAGACGGTGACCTG

The amplified sequence was purified using the NucleoSpin Gel and PCR Clean-up kit (Macherey-Nagel, ref. 740609.50). The plasmid pLOT-CD8-Apa1.3ScFv was used as a vector to insert the V5-tagged nanobody. Both the purified sequence and the plasmid were digested using Acc65I and XbaI restriction enzymes. The cut vector and insert were both purified and ligated together at 18°C over night.

2.5 Generation of transgenic flies

2.5.1 Transformation

The salt concentration of the ligated DNA product was reduced by dialyzing for ten minutes against H2O on a 0.025µm membrane filter paper (Millipore®). After dialysis, 1µl of the DNA solution was mixed with 500µl of electro-competent *E.coli* bacteria on ice, and transferred into a 1 mm Gene Pulser cuvette. A Biorad Micropulser™ was used to induce an electric pulse and transform the bacteria. Following the transformation, the bacteria were transferred into 500µl of LB media and incubated inside a shaker at 37°C for one hour. The bacteria were then centrifuged for 30 seconds at 10,000 RPM, 300µl of the supernatant was discarded, and the pellet was resuspended in the remaining 200µl. The bacteria were platted on LB agar plates containing the required antibiotics, and incubated at 37°C over night.

2.5.2 Plasmid purification

Several single colonies from the transformed bacteria were taken from the LB agar plate and grown separately in 5mL of LB media containing 0.1% of the required antibiotics at 37°C over night. DNA from 4mL of the grown bacteria in LB media were then isolated using the protocol from the Miniprep NucleoSpin® Plasmid Kit (Machery-Nagel). The DNA sample containing the correct insert was chosen upon Sanger sequencing, and 5µl of the remaining bacteria culture was added to 100 mL of fresh LB media containing 0.1% of the required antibiotics, and incubated at 37°C over night. Plasmid DNA was isolated and purified using protocol 8.1 and 8.3 of the Midiprep NucleoBond® Xtra Midi EF (Macherey-Nagel). The concentration of the purified DNA was measured using a Nanotrop Photospectrometer. The DNA was diluted to the final concentration of 300ng/µl in 25µl of 10% 10xPBS, to prepare it for injection into the fly embryos.

2.5.3 Fly injection

The fly stock *yw M{vas-int.Dm}zh-2A;tkv[KO-attP]/CyO* (Norman et al., 2016) was used for injecting the constructs containing the extracellular tagged Tkv, and the *yw M{vas-int.Dm}zh-2A ; M{attP}zh-86Fb* was used to inject the construct containing the GrabFP tagged with V5.

Fly embryos to be injected were collected for 30 minutes on grape-juice agar plates containing one drop of yeast, and were dechorionated using a 30% sodium hypochloride solution for 1 minute. The embryos were then washed and aligned using a stereomicroscope, and adhered on a glass slide containing embryo glue (adhesive tape dissolved in heptane). Embryos were dried using a cold air blow drier for 5 minutes, and to avoid desiccation, they were covered with a layer of Voltalet PCTFE oil (Atofina). The prepared DNA solutions diluted in PBS were injected into the posterior pole using a glass needle, a pressure pump and a micromanipulator. The injected embryos were kept at 18°C for 3 days, and the survivors were collected in conventional fly vials containing polenta and yeast. Upon hatching, adult flies were collected and crossed with $y^{-}w^{-}$ flies, and the positively marked progeny were selected and crossed with balancer flies to establish balanced stocks.

2.6 UAS/Gal4 system

The UAS/Gal4 system is a useful tool derived from yeast, allowing ectopic expression of genes from any organism in a specific region in a tissue and in a temporal-specific manner (Sonnenfeld, 2009). This system is commonly used in *Drosophila* to drive expression of genes of interest in specific tissues. The UAS/Gal4 system was used in this study to express RNAis against targets of interest to knockdown their expression in a temporal-specific manner. Gal4 is a transcription factor binding to the Upstream Activating Sequence (UAS), activating an upstream situated gene. The Gal80 can be used to temporally control the activation of the genes of interest, as it represses the function of Gal4, thereby blocking the activation of UAS activated genes. The temperature-sensitive Gal80TS is functional at the permissive temperature of 18°C, negatively regulating the Gal4 transcriptional activator by binding to the Gal4 protein. However, at restrictive temperature of 29°C, Gal80TS can no longer bind to Gal4 and its repressive function is lost (Fig 2.2). Gal80TS can thus be used in combination with shifts in temperature to temporally regulate the UAS/Gal4 system. As expression of RNAis against different trafficking factors from early embryogenesis would have been lethal for the organism, Gal80TS was used in this study to temporally restrict expression of RNAis in tissues of interest. Different trafficking factors were knocked down in the dorsal compartment of the wing imaginal discs using the apterous driver, *ap-Gal4*, while allowing the ventral compartment of the wing imaginal discs to be used as an internal control.

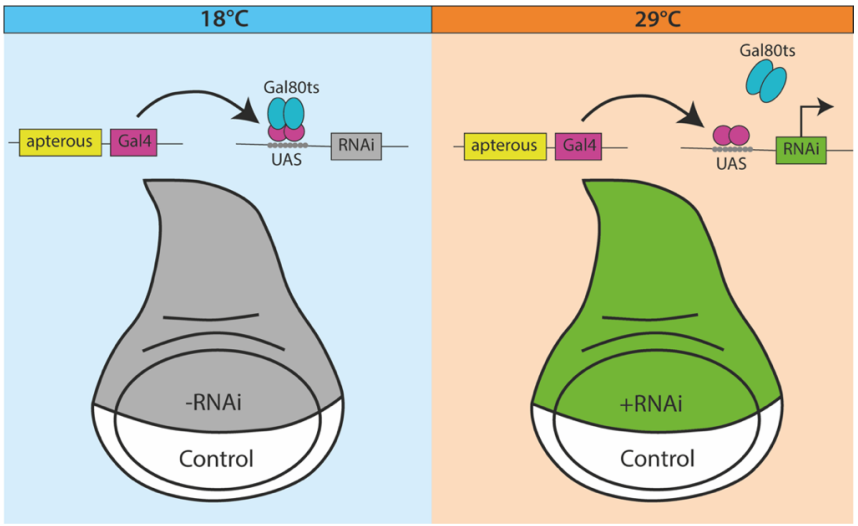

Figure 2.2: Schematic illustration of UAS/Gal4 system together with the use of tub-Gal80TS.
At permissive temperature of 18°C Gal80TS is functional and prevent the expression of the RNAi by binding to the Gal4 protein. At restrictive temperature of 29°C, Gal80TS can no longer bind to Gal4, allowing for a temporal control of RNAi expression.

3 Shaping and interpretation of Dpp morphogen gradient by endocytic trafficking

Paper manuscript:

Shaping and interpretation of Dpp morphogen gradient by endocytic trafficking

This paper has been submitted as a preprint to bioRxiv prior to the PhD examination.

Shaping and interpretation of Dpp morphogen gradient by endocytic trafficking

Sheida Hadji Rasouliha[1], Gustavo Aguilar[1], Cindy Reinger[1], Shinya Matsuda[1]

1. Growth & Development, Biozentrum, Spitalstrasse 41, University of Basel, 4056 Basel,

Email: shinya.matsuda@unibas.ch

Abstract

Dpp/BMP is a well-studied morphogen that controls patterning and growth in the Drosophila wing disc. However, how Dpp morphogen gradient is established and is interpreted by endocytic trafficking remains largely unclear. To address the role of trafficking in Dpp distribution, we generated endogenously tagged *dpp* alleles with the monomeric proteins mGreenLantern and mScarlet. Using these alleles, we found that blocking dynamin-dependent endocytosis expanded the extracellular Dpp gradient and impaired Dpp signaling. Also, blocking the early endosomal trafficking by knocking down Rab5 not only expanded the extracellular Dpp gradient, but also increased the range of Dpp signaling due to an impaired downregulation of its receptor Tkv. We demonstrated that blocking multivesicular bodies (MVBs) but not the late endosome formation, led to an accumulation of the internalized Dpp distribution and expanded its signaling range without affecting the extracellular gradient. We also showed that while recycling endosomes slightly affect the intracellular Dpp distribution, they minimally affect the extracellular Dpp gradient and its signaling activity. Our findings indicated that the early endocytic factors act as a sink for the extracellular Dpp gradient and are required to activate its signaling, while termination of Dpp signaling by sorting activated receptors into the intraluminal vesicles (ILVs) contributes to interpretation of the extracellular Dpp gradient. Taken together, our results reveal that extracellular Dpp morphogen gradient is shaped and interpreted by distinct endocytic trafficking pathways.

Keywords

Endosome, BMP, Drosophila, Trafficking, Gradient, Recycling, Degradation

Introduction

Morphogens are signaling molecules that are produced by a localized source of cells, and control the fate of their neighboring cells in a concentration dependent manner (Rogers & Schier, 2011). Among morphogens, Decapentaplegic (Dpp), the homologue of the vertebrate bone morphogenetic protein 2/4 (BMP2/4) has served as an excellent model system to understand morphogen function.

Dpp is produced in a stripe of cells in the anterior compartment along the anterior/posterior compartment boundary of the wing imaginal disc controls patterning and growth of the Drosophila wing. From the source cells, Dpp spreads and forms a concentration gradient in the tissue (Affolter & Basler, 2007; Lecuit et al., 1996; Matsuda et al., 2016; Nellen et al., 1996; Restrepo et al., 2014). Given the severe patterning and growth defects in *dpp* mutant flies, Dpp spreading from the stripe of cells has been thought to be essential for patterning and growth, especially in the posterior compartment (Matsuda et al., 2021). Furthermore, to date, how Dpp spreads remains controversial. A variety of extracellular and cell surface molecules have been shown to be required for Dpp gradient formation and signaling gradient, but their function remains to be further understood.

Dpp is thought to bind to the Type I and Type II receptors, Tkv and Punt on the cell surface to induce phosphorylation of Mad (pMad) in the target tissue. pMad is then translocated into the nucleus to control the expression of Dpp target genes. Also, pMad induces gene expression by repressing Brk, which acts as a repressor for Dpp target genes. Thus, the graded extracellular Dpp gradient is converted into the nuclear pMad gradient (Affolter et al., 2001) and the inverse-in-shape Brk gradient, which regulates the nested expression of the target genes to specify the position of the future adult wing veins L2 and L5 as well as growth at least in the posterior compartment (Cook et al., 2004; Müller et al., 2003; Pyrowolakis et al., 2004).

Endocytic trafficking and receptor-mediated internalization has been implicated in shaping gradients of different morphogens (Dubois et al., 2001; Scholpp & Brand, 2004; Strigini & Cohen, 2000; Yu et al., 2009). In the case of Dpp, several models have been proposed for the role of endocytosis on Dpp morphogen gradient. First, since Dpp was accumulated in *tkv* mutant clones, in cells that were close to the source, Dpp was thought to be transported by Tkv through repeated cycles of endocytosis and exocytosis (Entchev et al., 2000). Second, by using the nanobody internalization assay, it has recently been proposed that heparan sulfate proteoglycans such as Dally, but not Tkv, acts as a cell-surface receptor to internalize and recycle Dpp to contribute to the extracellular Dpp morphogen gradient

(Romanova-Michaelides et al., 2022). Although both models have been challenged, endocytic trafficking may control Dpp spreading through other cell surface factors. Third, Tkv-mediated endocytosis has been proposed to simply acts as a sink for Dpp, and Dally antagonizes this process to establish a long range Dpp gradient (Akiyama et al., 2018; Simon et al., 2023), Regardless of the role of extracellular and cell-surface factors on regulation of the extracellular Dpp gradient, if and how endocytic trafficking itself influences the extracellular Dpp gradient remains unclear.

It also remains unclear if and how extracellular Dpp gradient is interpreted at the cellular level. Interestingly, it has been shown that Dpp exists mainly intracellularly and Dpp signaling is lost in endocytosis deficient cells (González-Gaitán & Jäckle, 1999; Kicheva et al., 2007; Teleman & Cohen, 2000; Zhou et al., 2012), indicating the importance of internalized Dpp for its signal activation. However, it remains unclear in which endocytic compartment Dpp signaling is activated and shut off, and whether the duration of Dpp signaling is required to interpretate the extracellular Dpp gradient, partly due to the lack of tools to visualize the intracellular Dpp distribution. Recently, fluorophore-conjugated anti-GFP nanobody was used to label and trace only the internalized GFP-Dpp (Romanova-Michaelides et al., 2022). However, fluorescent protein tagged *dpp* alleles allowing to visualize both extracellular and intracellular Dpp distribution without manipulating Dpp were not available.

In this study, we generated such *dpp*, allowing us to directly visualize both extracellular and intracellular Dpp distribution under physiological conditions. Using these alleles, we investigated the role of endocytic trafficking on Dpp morphogen gradient formation and its signaling activity by interfering with the function of various trafficking factors.

We found that blocking dynamin-mediated endocytosis expanded the extracellular Dpp gradient and impaired Dpp signaling, while blocking the early endosomal trafficking expanded the extracellular Dpp gradient and its signaling range. This indicated that endocytosis acts as a sink for Dpp and activates Dpp signaling, but following the subsequent endosomal maturation and degradative pathway terminates Dpp signaling. We further show that blocking the formation of the multivesicular bodies (MVBs), but not lysosomal degradation, expanded the distribution of internalized Dpp and its signaling range without affecting the extracellular Dpp gradient. These results indicate that termination of Dpp signaling by sorting the activated receptors into the intraluminal vesicles (ILVs) contributes to interpretation of the extracellular Dpp gradient. Taken together, our results revealed the role of distinct endocytic factors in formation and interpretation of the extracellular Dpp morphogen gradient.

Results

Visualization of extracellular and intracellular endogenous Dpp gradient in the wing disc

We previously generated an endogenous GFP-dpp allele by inserting GFP after the last processing sites of Dpp to tag all the mature Dpp (Matsuda et al., 2021). However, the resulting GFP-Dpp signal was too weak to visualize the graded distribution (Fig. 1A). Similar results were obtained using the other GFP-dpp alleles (Romanova-Michaelides et al., 2022). To be able to better visualize the endogenous Dpp gradient, we then inserted mGreenLantern (mGL) (Campbell et al., 2020) or mScarlet (mSC) (Bindels et al., 2017) into the *dpp* locus to generate endogenous *mGL-dpp* and *mSC-dpp* alleles respectively. Interestingly, we found that the mGL-Dpp shows a brighter fluorescent signal than GFP-Dpp (Fig. 1A, B), and a graded distribution outside the stripe of Dpp source cells (Fig. 1B). Similar graded distribution of mSC-dpp signal was also observed (Fig. 1C).

Unlike the *GFP-dpp* allele, the two newly generated alleles were not haploinsufficient but semi-lethal. To overcome the partial embryonic lethality, we introduced a transgene called “JAX”, which contains the genomic region of *dpp*, which is critical for the early embryogenesis (Hoffmann & Goodman, 1987), but does not rescue the wing phenotypes of *dpp* mutants (Simon et al., 2023). We found that JAX greatly rescued the lethality of each allele and each allele easily becomes homozygous viable without obvious phenotypes (Fig. 1D, E). JAX did not affect Dpp signal in the functional *HA-dpp* (Matsuda et al., 2021) wing discs (Fig. 1F, G, J) and Dpp signal was comparable between *JAX;HA-dpp*, *JAX;mGL-dpp* and *JAX;mSC-dpp* wing discs (Fig. 1G-J). These results suggest that *mGL-dpp* and *mSC-dpp* allele are functional at least during wing development.

To address whether the mGL-Dpp signal is derived from extracellular or intracellular Dpp, we compared the extracellular mGL-Dpp distribution with the mGL-Dpp signal. In contrast to the higher mGL-Dpp signal in the center of wing disc (Fig. 1K), the extracellular mGL-Dpp showed a shallow graded distribution (Fig. 1K’). We found that the two signals rarely colocalize (Fig. 1K”), indicating that the majority of mGL-Dpp signal is derived from the intracellular Dpp. Consistently, the extracellular mGL-Dpp distribution, but not mGL-Dpp fluorescent signal, was sensitive to the acid wash, which efficiently removes extracellular proteins (Romanova-Michaelides et al., 2022) (Fig. S2).

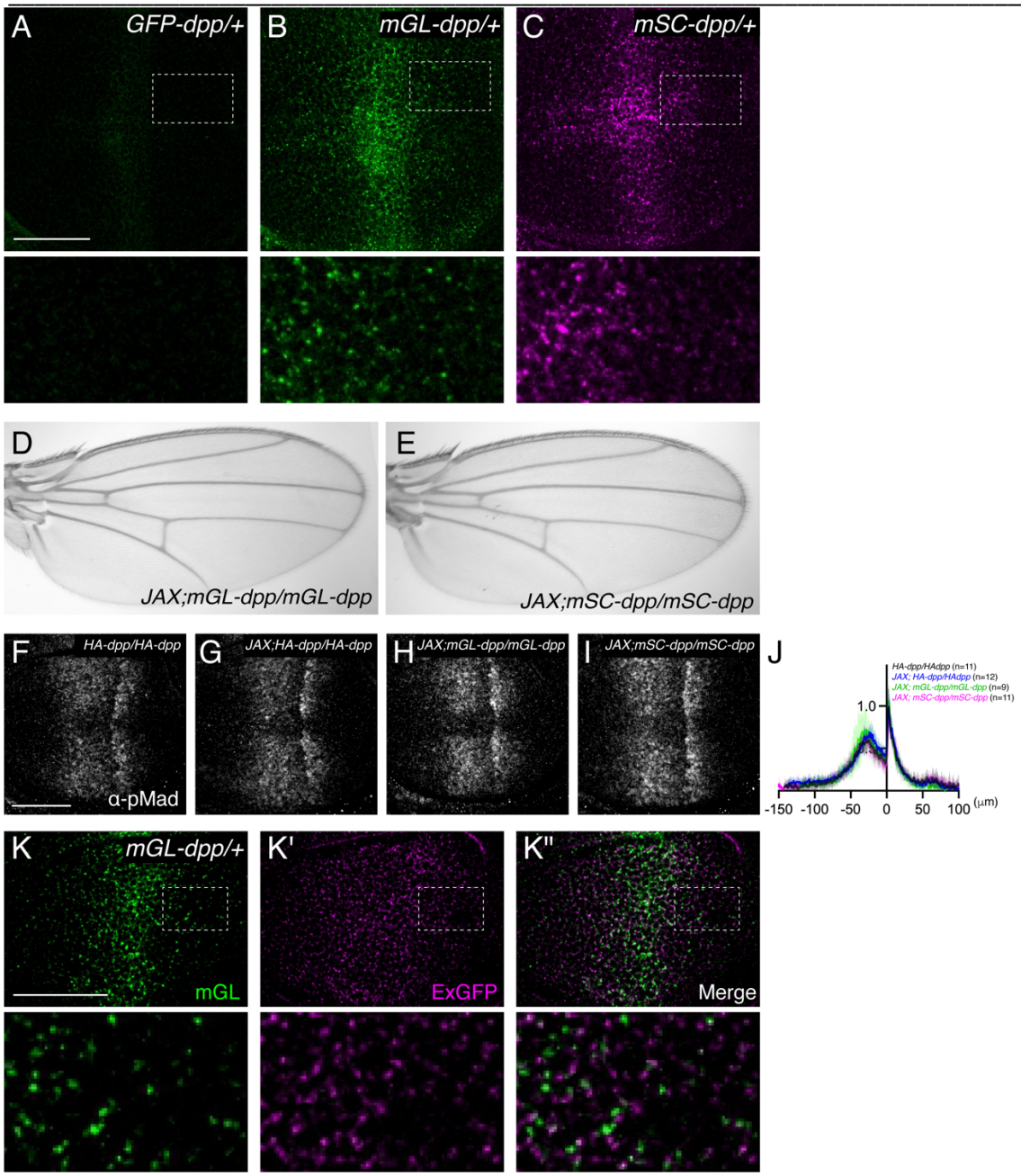

Figure 1: Visualization of endogenous Dpp morphogen gradient in the wing disc.

(A) GFP-Dpp signal from *GFP-dpp/Cyo, p23*. (A), mGL-Dpp signal from *mGL-dpp/+* wing disc (B) mSC-Dpp signal from *mSC-dpp/+*. (D) Adult wing of *JAX; mGL-dpp/mGL-dpp*. (E) Adult wing of JAX; *mSC-dpp/mSC-dpp*. (F-I) α-pMad staining of *HA-dpp/HA-dpp* (F), *JAX; HA-dpp/HA-dpp* (G), *JAX; mGL-dpp/mGL-dpp* (H), *JAX; mSC-dpp/mSC-dpp* (I) wing disc. (J) Average fluorescence intensity profile of (F-I). Data are presented as mean +/- SD. (K) mGL-Dpp signal (K), extracellular α-GFP staining (K'), and merge (K") of *mGL-dpp/+* wing disc. Scale Bar: 50um.

To test where the endogenous Dpp is localized within the cells, we compared the endogenous mSC-Dpp localization with different Rab proteins tagged with eYFP (Fig. 2). The Mander's coefficient (M1) revealed that mSC-Dpp colocalizes with the early endosome marker Rab5-eYFP (Fig. 2A'), the late endosome marker Rab7-eYFP (Fig. 2B'), the fast recycling endosome marker Rab4-eYFP (Fig. 2C'), and the slow recycling endosome marker Rab11-eYFP (Fig. 2D') to different extents, showing that the internalized Dpp is trafficked to different endocytic compartments.

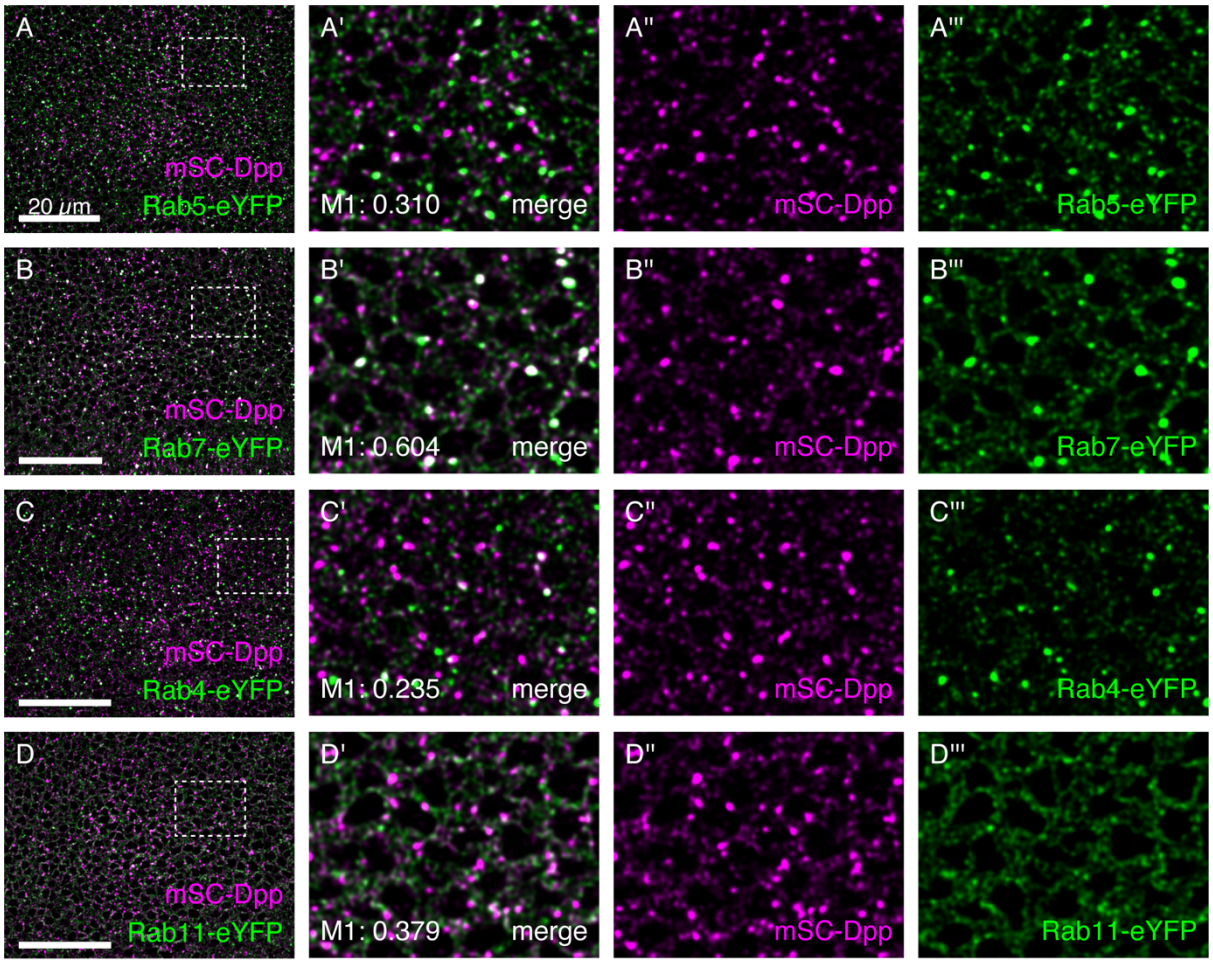

Figure 2: Colocalization of mSC-Dpp with different Rabs.

(A-D) Comparison of mSC-Dpp signal with Rab5-eYFP (A), Rab7-eYFP (B), Rab4-eYFP (C), Rab11-eYFP (D) in the late third instar wing imaginal discs. Mander's coefficient (M1) indicates the percentage of overlap of mSC-Dpp with different Rabs.

Rab5 is required for shutting down Dpp signal

To study how different endocytic compartments contribute to Dpp gradient formation and signaling, we first knocked down Dynamin GTPase (*Drosophila* homologue: shibire), a critical factor to excise the formed vesicles and separate them from the plasma membrane (Koenig & Ikeda, 1989). Consistent with the idea that endocytosis is required for Dpp signaling (Belenkaya et al., 2004), we found that the temperature-sensitive allele of shibire (shi^{ts1}) led to a complete loss of Dpp signaling at restrictive temperatures for 2h (Fig. 3A-C). Previous results showed that loss of Rab5 by dominant negative form of Rab5 reduced Dpp signaling and its target gene expression, indicating that Dpp is transported through endocytosis (Entchev et al., 2000), or Dpp signaling is activated at the level of the early endosome or below (Moreno et al., 2002).

In stark contrast, we surprisingly found that temporally knocking down Rab5 by RNAi by using the temperature-sensitive Gal80 repressor in the dorsal compartment of the wing discs resulted in an increase in Dpp signaling activity compared with the control ventral compartment (Fig. 3D-F). Similar results were obtained using different RNAi lines against Rab5 or the dominant negative form of Rab5 used in the previous studies (Fig.3, G-J). Inducing *rab5* null clones ($rab5^{2}$, (Wucherpfennig et al., 2003)) also led to a reduction in Brk intensity (Fig. 3K-K'), consistent with an increase of Dpp signaling. These results suggest that early endocytosis and/or the following trafficking is required for shutting down Dpp signaling.

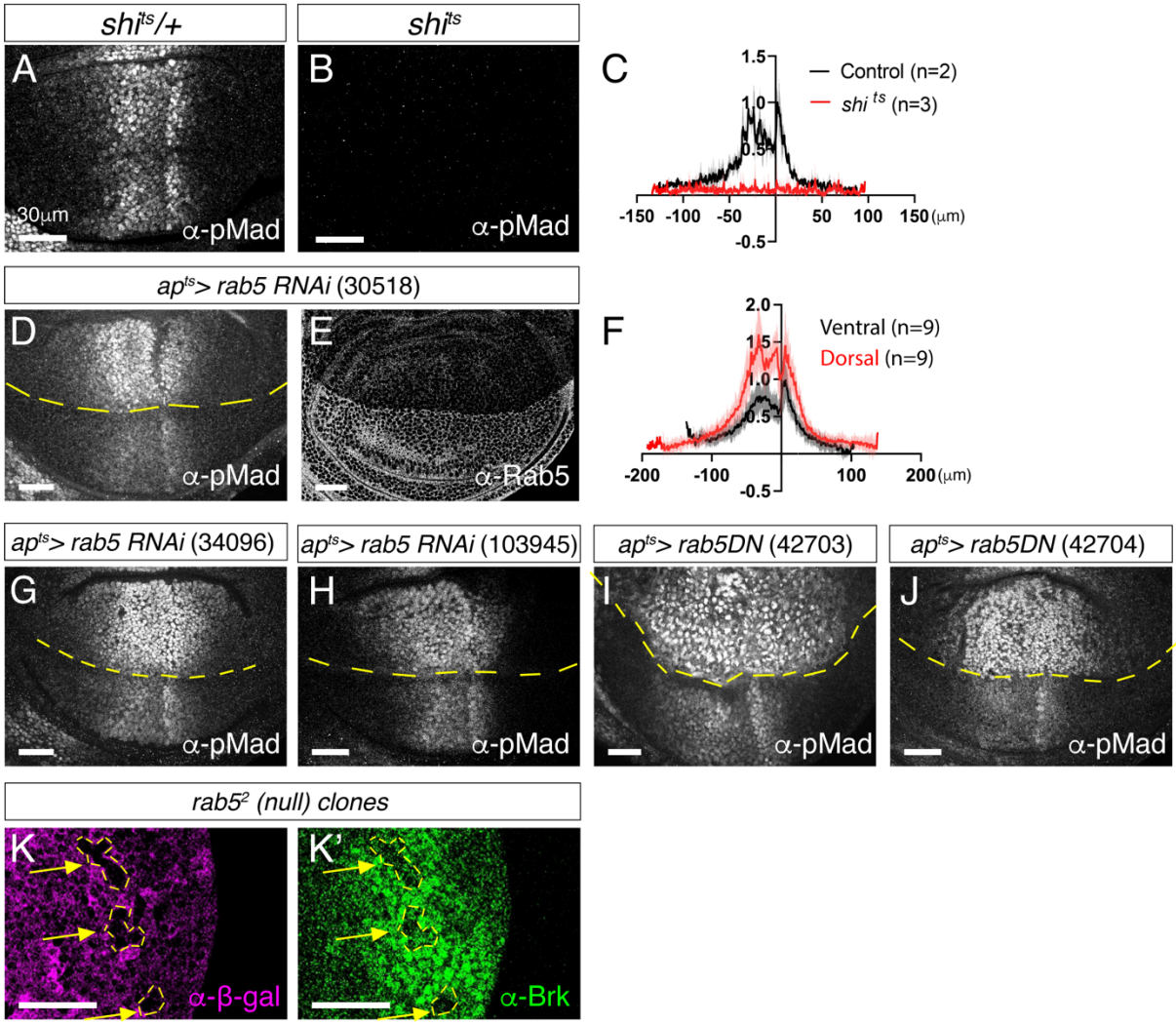

Figure 3: Rab5 is required for shutting down Dpp signaling.

(A-B) α-pMad staining of *shi^{ts}/+* wing disc (control)(A) and *shi^{ts}* wing disc (B) upon 2h at restrictive temperatures. (C) Average fluorescence intensity profile of (A, B). Data are presented as mean +/- SD. (D, E) α-pMad staining (D) and α-Rab5 staining (E) of *ap^{ts}>rab5RNAi* (30518). (F) Average fluorescence intensity profile of (D). Data are presented as mean +/- SD. (G-J) α-pMad staining of *ap^{ts}>rab5RNAi* (34096) (G), *ap^{ts}>rab5RNAi* (103945) (H), *ap^{ts}>rab5DN* (42703) (I), and *ap^{ts}>rab5DN* (42704) (J). (K) *rab5^{2}* null clones generated in the peripheral regions visualized via absence of α-β-gal staining (K) and α-Brk staining (K'). Scale bar:30μm.

The effects of Rab5 on Dpp distribution

How does loss of Rab5 lead to an increase in Dpp signaling? To test if *dpp* is involved in the increase of pMad range and intensity upon knocking down Rab5, we knocked down Rab5 in the dorsal compartment in *dpp, brk* double mutants, in which the wing disc could grow in the absence of Dpp signal. We found that pMad was not upregulated under this condition, indicating that the observed phenotype was dependent on Dpp (Fig. 4A).

To test if changes in *dpp* transcription were involved, we then followed a *dpp* transcription reporter *dpp-lacZ* upon knocking down Rab5 via RNAi, and found no changes in *dpp* transcription (Fig. 4B), indicating that upregulation of *dpp* transcription was not the cause of increase of Dpp signaling upon knocking down Rab5.

We then asked if the changes in Dpp distribution and/or trafficking affect Dpp signaling in this condition. When Rab5 was knocked down, the extracellular mGL-Dpp increased (Fig. 4, C-E), consistent with defects in endocytosis in *rab5* mutants (Bucci et al., 1992). Visualizing cross-sections from the wing imaginal discs showed that the extracellular mGL-Dpp increased in the basolateral side, especially outside of the Dpp producing cells (Fig. 4D, yellow arrowheads). This increase of extracellular Dpp could lead to activation of Dpp signaling. However, blocking endocytosis by shi^{ts1} led to a similar increase of extracellular mGL-Dpp (Fig. 4F, G, & Fig. S1) while Dpp signaling was completely lost after 2 hours at restrictive temperatures (Fig. 3B), indicating that Dynamin-mediated endocytosis of Dpp is required to activate Dpp signaling (Belenkaya et al., 2004). Thus, the accumulation of the extracellular Dpp is unlikely the direct cause of increase in Dpp signaling activity in absence of Rab5.

In contrast, we found that, upon knocking down Rab5 by RNAi, the number of mGL-Dpp puncta decreased in the lateral side (Fig. 4I, M), but increased in the basal side of the disc (Fig. 4J, N), where the extracellular Dpp was also increased (Fig. 4C, D). To ensure that the observed signal was not coming from the extracellular mGL-Dpp, the acid wash protocol was followed to remove the extracellular molecules (Romanova-Michaelides et al., 2022). While the reduction in the number of mGL-Dpp puncta is consistent with the idea that loss of Rab5 disrupts the formation of the early endosome and the following endosomal trafficking, the increase in number of mGL-Dpp puncta in the basal side suggests that in absence of Rab5, Dpp is internalized (Bucci et al., 1992; Morrison et al., 2008; Wucherpfennig et al., 2003) but not eliminated without the function of the early endosome, especially from the basal side of the wing disc.

Similarly, in absence of Rab5 the number of intracellular Tkv-YFP puncta decreased in the lateral side (Fig. 4K, O), but increased in the basal side of the wing discs (Fig. 4L, P). Taken together, these results raise the possibility that Dpp signaling is initiated but not terminated in the absence of Rab5-mediated trafficking.

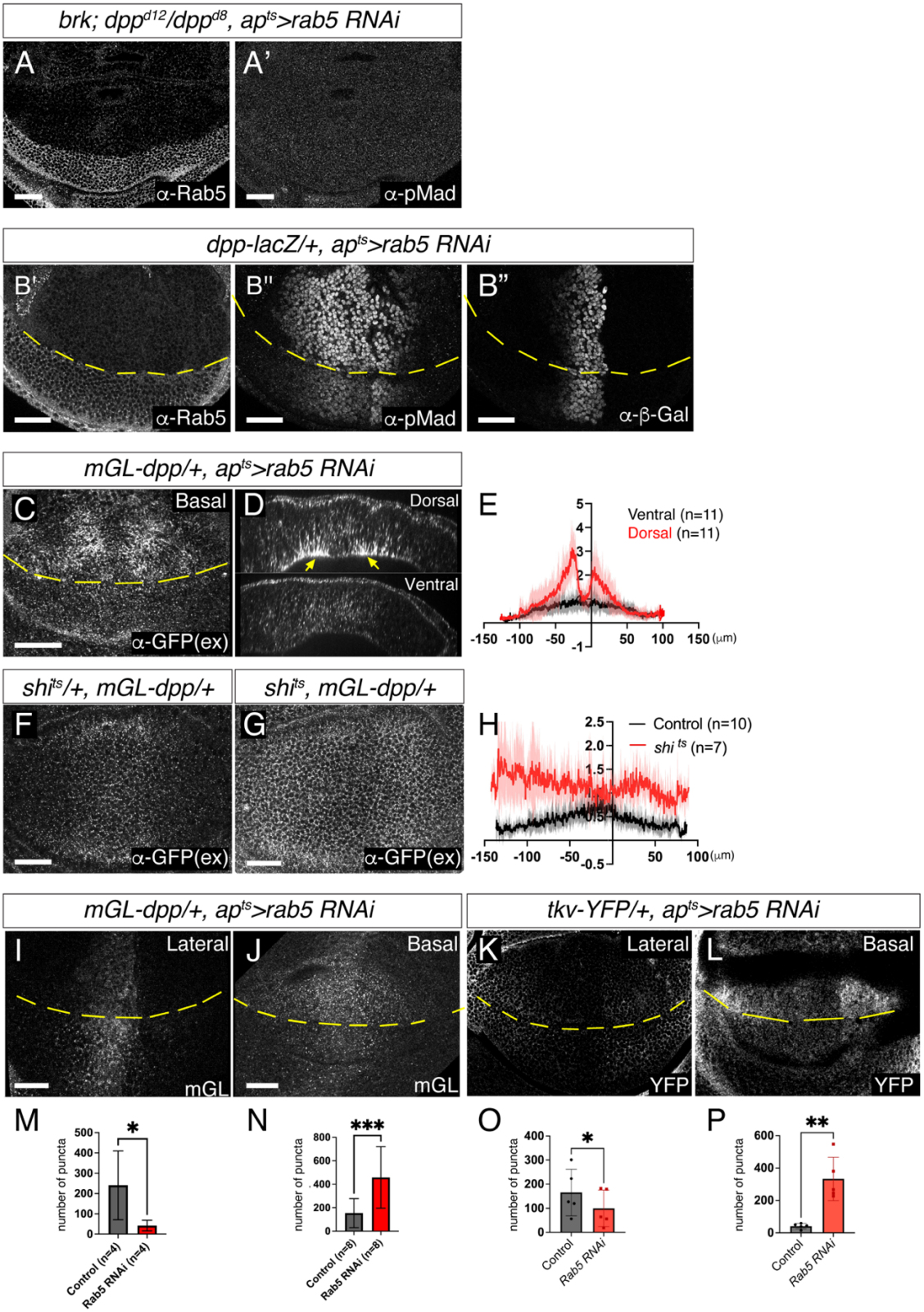

Figure 4: Changes in Dpp distribution in absence of Rab5.

(A) α-Rab5 staining (A) and α-pMad staining (A') in *brk, dpp^{d8}/dpp^{d12}, ap^{ts}>Rab5 RNAi* wing disc. (B) α-Rab5 staining (B), α-pMad staining (B'), and α-β-gal staining (B") in *dpp-lacZ/+, ap^{ts}>Rab5 RNAi*. (C) Extracellular α-GFP staining in *mGL-dpp/+, ap^{ts}>Rab5 RNAi*. (D) Optical cross-section of (C). (E) Average fluorescence intensity profile of (C). Data are presented as mean +/- SD. (F, G) Extracellular α-GFP staining in *shi^{ts}/+, mGL-dpp/+* wing disc (F) and *shi^{ts}, mGL-dpp/+* (G) after 2h at restrictive temperature of 34°C. (H) Average fluorescence intensity profile of (F, G). Data are presented as mean +/- SD. (I, J) mGL-Dpp intracellular signal in the lateral side (I) and basal side (J) in *mGL-dpp/+, ap^{ts}>rab5 RNAi* wing disc. (K, L) Tkv-YFP (total) signal of lateral side (K) and basal side (L) of *tkv-YFP/+, ap^{ts}>rab5 RNAi* wing disc. (M-P) Comparison of the number of puncta of (I-L). Ratio-paired t-test with $p<0.05$ was used for the comparison; p=0.0383 (n=4) (M), p=0.0001 (n=8) (N), p=0.0123 (n=5) (O) p=0.0010 (n=5) (P). Scale bar: 30µm.

Rab5 terminates Dpp signaling via degradation of Tkv

If Rab5-mediated trafficking downregulates the activated Tkv, the increased pMad intensity in Rab5 mutant or knockdown conditions could be due to the prolonged activation of Tkv. In this case, artificial removal of the receptor could rescue the increase in Dpp signaling in absence of Rab5. To test this, we applied deGradHA, a genetically encoded method to deplete HA-tagged proteins (Vigano et al., 2021). Since Tkv is the critical receptor for Dpp signaling, we used the deGradHA tool to degrade only one copy of Tkv-HA-eGFP in the dorsal compartment in the wing imaginal discs (Fig. 5).

While pMad intensity was similar between the dorsal and the ventral compartment in the control wing discs (Fig. 5A), knocking down Rab5 via RNAi in the dorsal compartment led to an increase in pMad intensity compared to the ventral compartment (Fig. 5B). In contrast, simultaneous knocking down of Rab5 via RNAi and partially degrading Tkv in the dorsal compartment rescued the dorsal pMad intensity comparable to the ventral pMad signal (Fig. 5C). Partially degrading Tkv via deGradHA alone did not affect the pMad gradient except a slight decrease along the A/P compartment boundary, likely due to the low levels of Tkv in that region (Fig. 5D). These results suggest that trafficking of Tkv through the early endosome is required to terminate Dpp signaling.

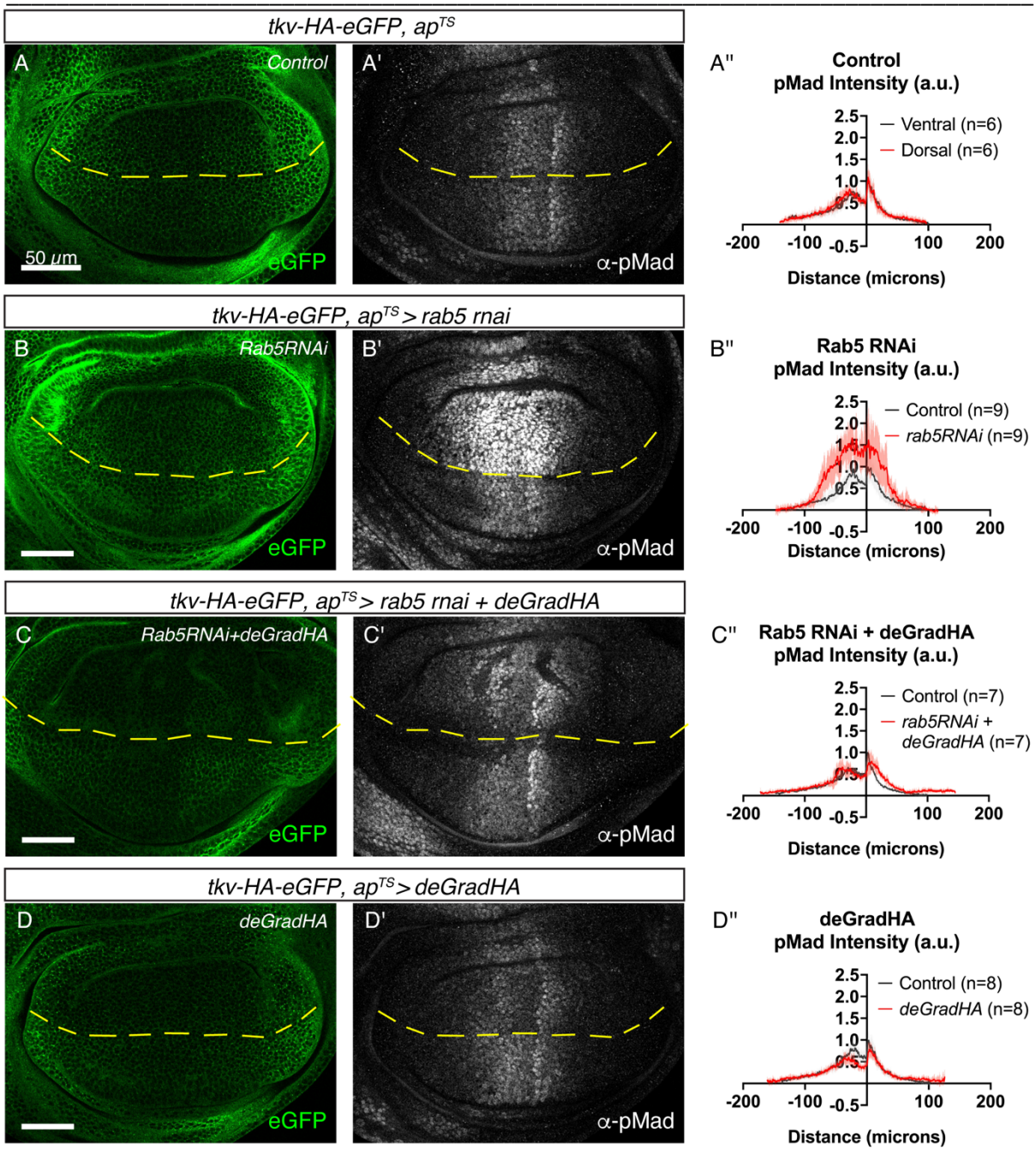

Figure 5: Rescue of increase of Dpp signaling upon knocking down Rab5 by artificial removal of one copy of Tkv.

(A-D) Tkv-HA-eGFP signal (A-D) and α-pMad staining (A'-D') of *tkv-HA-eGFP/+, ap^{ts}>+* wing disc (Control) (A), *tkv-HA-eGFP/+, ap^{ts}>rab5 RNAi* wing disc (B), *tkv-HA-eGFP/+, ap^{ts}>rab5 RNAi, deGradHA* wing disc (C) and *tkv-HA-eGFP/+, ap^{ts}>deGradHA* wing disc (D). (A"-D") Average fluorescence intensity profiles of (A'-D'). Data are presented as mean +/- SD. Scale bar: 50µm.

Late endosomal trafficking is not involved in terminating Dpp signaling

Given the role of endocytosis in protein degradation, we investigated the effect of late endosomal trafficking in termination of Dpp and its signaling. To address this, we first asked if the lysosomal degradation is involved in shutting off Dpp signaling. Inducing clones that were mutant for *rab7* (null mutant, (Cherry et al., 2013) or knocking down Rab7 by RNAi (Fig. 6A-D) reduced Rab7 but did not affect Dpp signaling activity. Consistently, the extracellular and the intracellular mGL-Dpp signal remained unchanged upon knocking down Rab7 by RNAi (Fig. 6E-G). These results suggest that lysosomal degradation does not contribute to termination of Dpp signaling or Dpp distribution.

Formation of MVBs is required for Dpp signaling termination

As the early endosome matures into the late endosome, the ESCRT components recognize and sort ubiquitinated proteins into the intraluminal vesicles (ILVs) to form the MVBs (Bucci & Stasi, 2016). The late endosome containing MVBs are then fused with lysosome to degrade the contents of MVBs (Bucci & Stasi, 2016). MVB formation has been proposed to downregulate a variety of signaling pathways including Dpp signaling through lysosomal degradation (Jékely & Rørth, 2003; Thompson et al., 2005).

Indeed, we found that knocking down ESCRT-II component TSG101, ESCRT-III component Shrub, or Vps4 by RNAi in the dorsal compartment led to an increase in range and intensity of the pMad signal compared to the ventral compartment (Fig. 7A-C). Consistent with the defects in sorting of ubiquitinated receptors, Tkv and ubiquitin accumulated and highly colocalized upon knocking down Vps4 (Fig. 7D, Fig. S3), but not upon knocking down Rab7 (Fig. 7E). In contrast to previous studies (Thompson et al., 2005), these results indicate that sorting of activated receptors into MVBs itself rather than their lysosomal degradation is the key to terminating Dpp signaling probably through separating activated receptors from Mad in cytosol.

We then tested if blocking formation of MVBs affected extracellular or intracellular Dpp distribution. Consistent with the defects in sorting of Dpp, we found that the intracellular mGL-Dpp accumulated as large puncta without affecting the extracellular mGL-Dpp gradient upon knocking down Vps4 (Fig. 7F-H). These results suggest that termination of Dpp signaling at the level of MVBs contributes to the interpretation of extracellular Dpp gradient.

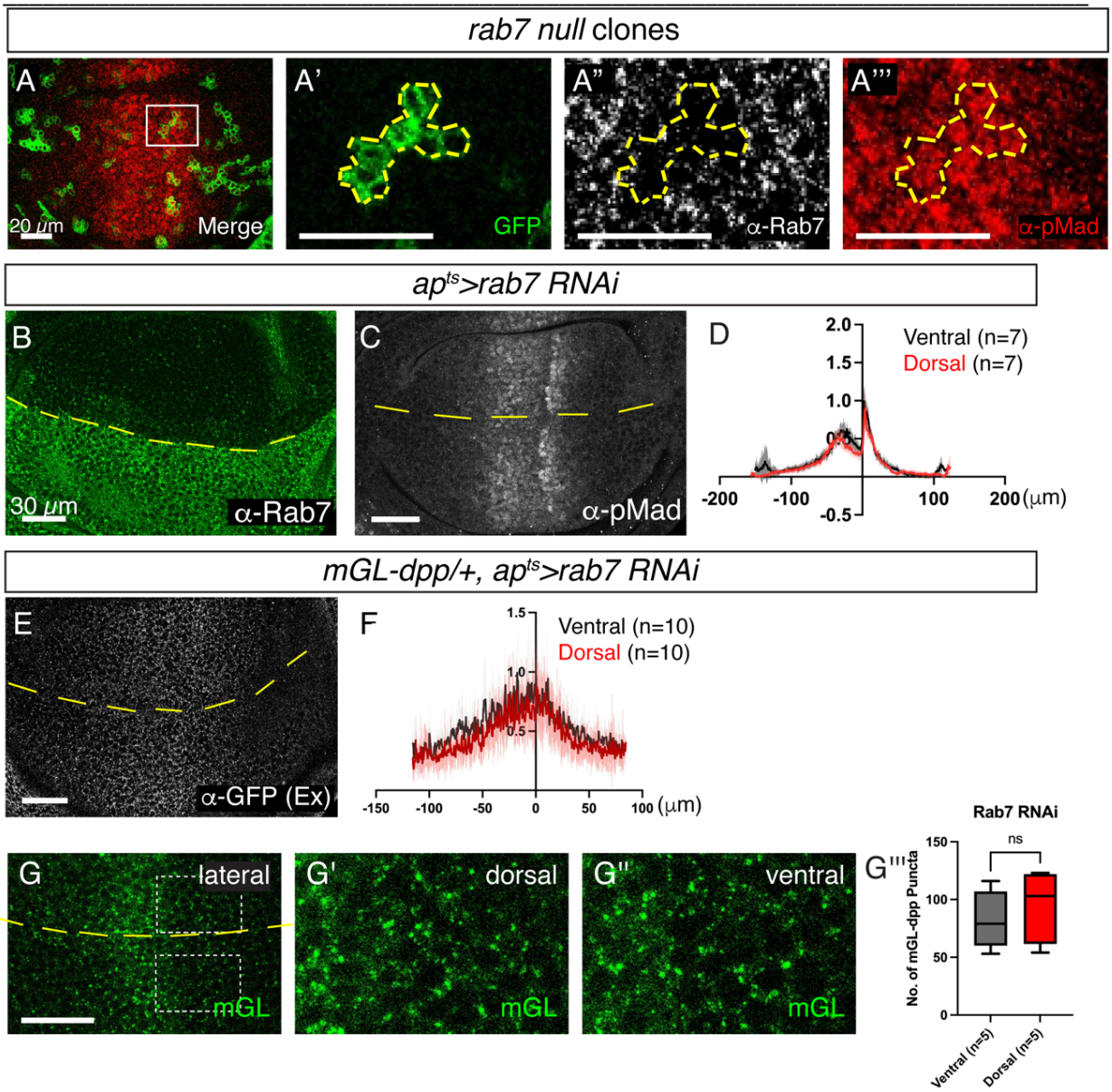

Figure 6: Late endosomal trafficking is not involved in terminating Dpp signaling

(A) merge (A), GFP signal (A'), α-Rab7 staining (A"), and α-pMad staining (A"') of rab7 null clones (labeled by GFP signal) generated by MARCM (Lee and Luo 2001). (B, C) α-Rab7 staining (B) and α-pMad staining (C) of *ap^{ts}>rab7 RNAi* wing disc. (D) Average fluorescence intensity profiles of (C). Data are presented as mean +/- SD. (E) Extracellular α-GFP staining of *mGL-dpp/+, ap^{ts}>rab7 RNAi* wing disc. (F) Average fluorescence intensity profiles of (E). Data are presented as mean +/-SD. (G) mGL-Dpp signal from apical side (G), magnified region in the dorsal compartment (G'), and magnified region in the ventral compartment (G") of *mGL-dpp/+, ap^{ts}>rab7 RNAi* wing disc. (G"') Comparison of number of mGL-Dpp puncta, ratio-paired t-test with $p<0.05$ was used for the comparison; non-significant $p=0.2083$ (n=5).

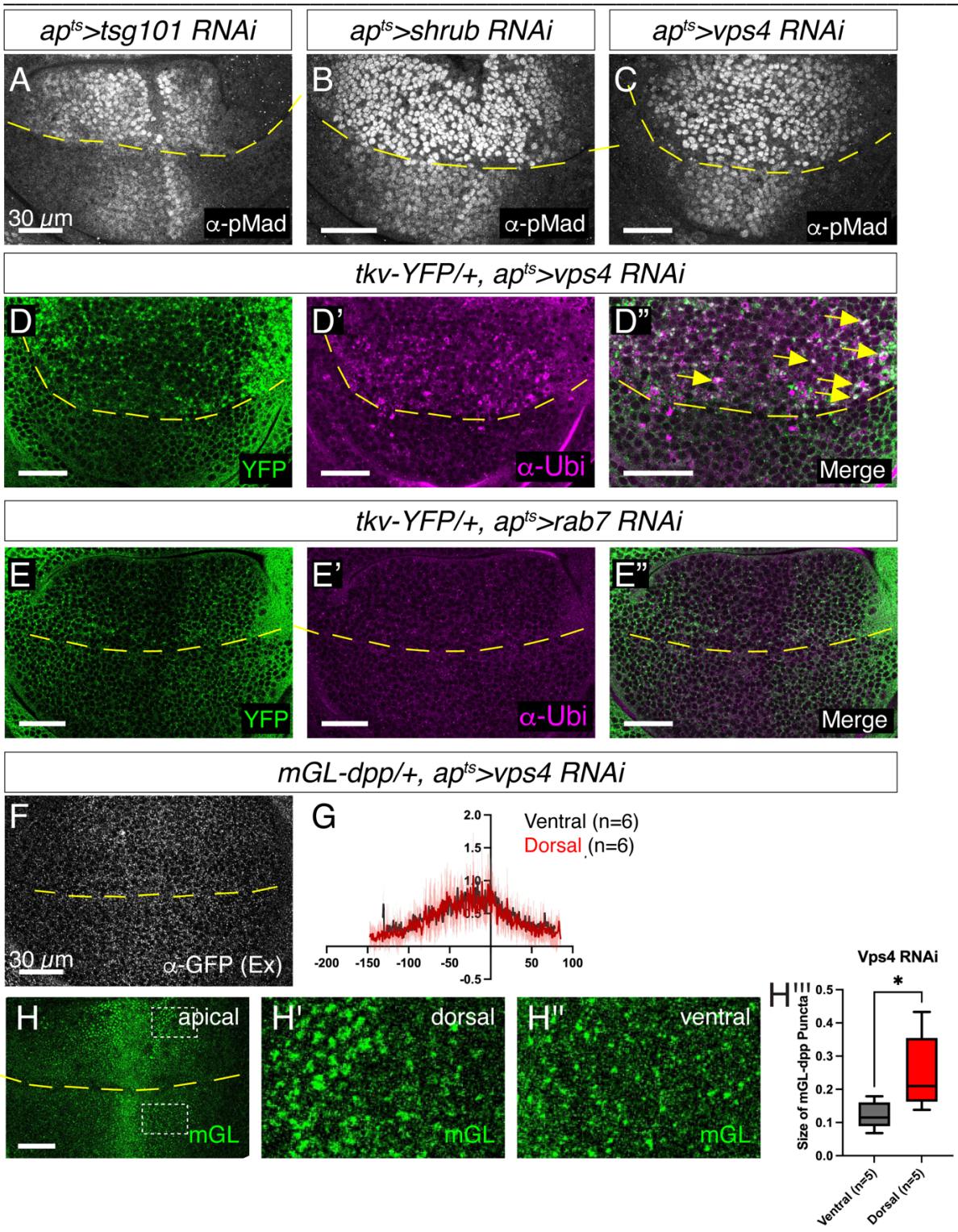

Figure 7. Formation of MVBs is required for Dpp signaling termination.

(A-C) α-pMad staining of *ap^ts>tsg101 RNAi* (A), *ap^ts>shrub RNAi* (B), and *ap^ts>Vps4 RNAi* (C) wing disc. (D) Tkv-YFP signal (D), α-Ubiquitin staining (D'), and merge (D") in *tkv-YFP/+, ap^ts>vps4 RNAi* wing disc. (E) Tkv-YFP signal (E), α-Ubiquitin staining (E'), and merge (E") in *tkv-YFP/+, ap^ts>rab7 RNAi* wing disc.

(F) Extracellular α-GFP staining of *mGL-dpp/+, ap^{ts}>Vps4 RNAi* wing disc. (G) Average fluorescence intensity profiles of (F). Data are presented as mean +/- SD. (H) mGL-Dpp signal from apical side (H), with magnified region in the dorsal compartment (H'), and the ventral compartment (H") of *mGL-dpp/+, ap^{ts}>Vps4 RNAi* wing disc. (H''') Comparison of size of mGL-Dpp puncta in H' and H'', ratio-paired t-test with $p<0.05$ was used for the comparison; $p=0.0325$ ($n=5$).

Recycling is largely dispensable for Dpp gradient formation and signaling

Our findings suggested that, early endocytic factors regulate extracellular Dpp and act as a sink, while the late endocytic factors terminate Dpp signaling and do not affect the extracellular Dpp distribution. Recently, it has been proposed that knocking down Rab4 or Rab11 severely affected GFP-Dpp distribution upon its overexpression, indicating that the recycling endosomes are involved in the extracellular Dpp gradient formation (Romanova-Michaelides et al., 2022). Indeed, we found co-localization of Dpp with Rab4 and Rab11 (Fig. 2C-D). To test if the recycling endosomes were involved in formation of the endogenous extracellular Dpp distribution and Dpp signaling, we knocked down Rab4 and Rab11 by RNAi in the dorsal compartment and investigated the extracellular and intracellular mGL-Dpp distribution.

We found that knocking down Rab4 by RNAi did not affect Dpp signaling (Fig. 8A, C) nor the intracellular Dpp (Fig. 8K-L), but showed a slight decrease in the extracellular Dpp distribution at the basal side and not the lateral side of the wing disc (Fig. 8B-B', D, E). We also found that knocking down Rab11 by RNAi did not affect extracellular Dpp distribution nor Dpp signaling (Fig.8F-J), while the internalized Dpp accumulated as large puncta especially in the basal side of the discs (Fig. 8O-R). These results suggest that Rab4 or Rab11 do not greatly contribute to the extracellular Dpp distribution or Dpp signaling.

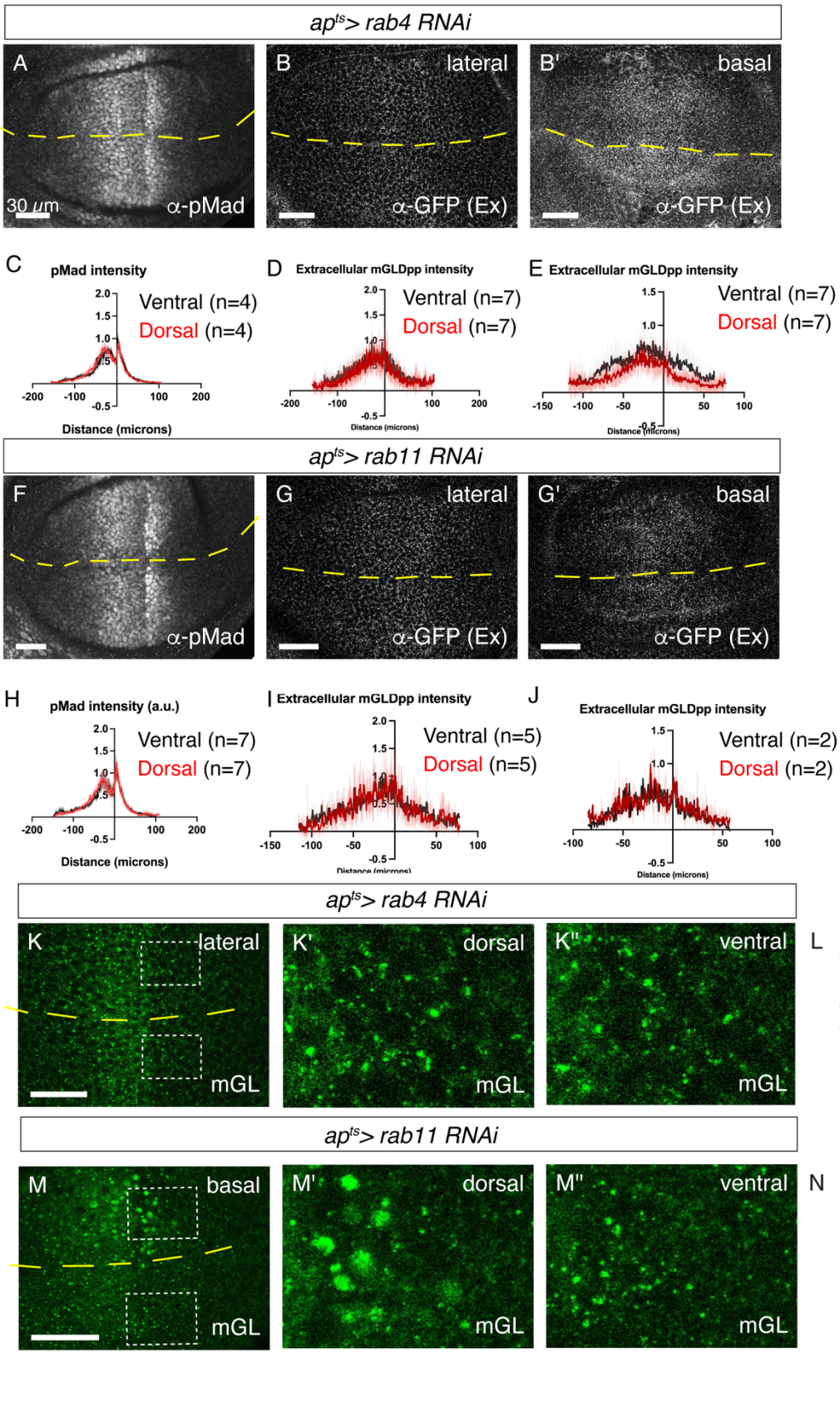
ap^ts> rab4 RNAi
A
30 μm
α-pMad
B
lateral
α-GFP (Ex)
B'
basal
α-GFP (Ex)
C
pMad intensity
Ventral (n=4)
Dorsal (n=4)
Distance (microns)
D
Extracellular mGLDpp intensity
Ventral (n=7)
Dorsal (n=7)
Distance (microns)
E
Extracellular mGLDpp intensity
Ventral (n=7)
Dorsal (n=7)
Distance (microns)
ap^ts> rab11 RNAi
F
α-pMad
G
lateral
α-GFP (Ex)
G'
basal
α-GFP (Ex)
H
pMad intensity (a.u.)
Ventral (n=7)
Dorsal (n=7)
Distance (microns)
I
Extracellular mGLDpp intensity
Ventral (n=5)
Dorsal (n=5)
Distance (microns)
J
Extracellular mGLDpp intensity
Ventral (n=2)
Dorsal (n=2)
Distance (microns)
ap^ts> rab4 RNAi
K
lateral
mGL
K'
dorsal
mGL
K''
ventral
mGL
L
Rab4 RNAi
ns
No. of mGL-dpp Puncta
Ventral (n=5)
Dorsal (n=5)
ap^ts> rab11 RNAi
M
basal
mGL
M'
dorsal
mGL
M''
ventral
mGL
N
Rab11 RNAi
**
Size of mGL-dpp Puncta
Control (n=5)
Rab11 RNAi (n=5)

Figure 8: Recycling is largely dispensable for Dpp gradient formation and signaling.

(A-B') pMad staining (A), extracellular α-GFP staining in the lateral side (B), and extracellular α-GFP staining in the basal side (B') of *ap^{ts}>rab4 RNAi*. (C-E) Average fluorescence intensity profiles of (A-B'). Data are presented as mean +/- SD. (F-G') pMad staining (F), extracellular α-GFP staining in the lateral side (G), and extracellular α-GFP staining in the basal side (G') of *ap^{ts}>rab11 RNAi*. (H-J) Average fluorescence intensity profiles of (F-G'). Data are presented as mean +/- SD. (K-L) mGL-Dpp (total) signal of lateral side (K), with magnified region in the dorsal compartment (K') and ventral compartment (K''), and comparison between the number of mGL-Dpp puncta in K' and K'' (L) in *ap^{ts}>rab4 RNAi*. Ratio-paired t-test with $p<0.05$ was used for the comparison; non-significant $p=0.8317$ (n=5) (L). (M-N) mGL-Dpp (total) signal of basal side (M), with magnified region in the dorsal compartment (M') and the ventral compartment (M'') in *ap^{ts}>rab11 RNAi*. (N) Comparison of the size of mGL-Dpp puncta in M' and M''. Ratio-paired t-test with $p<0.05$ was used for the comparison; $p=0.006$ (n=5).

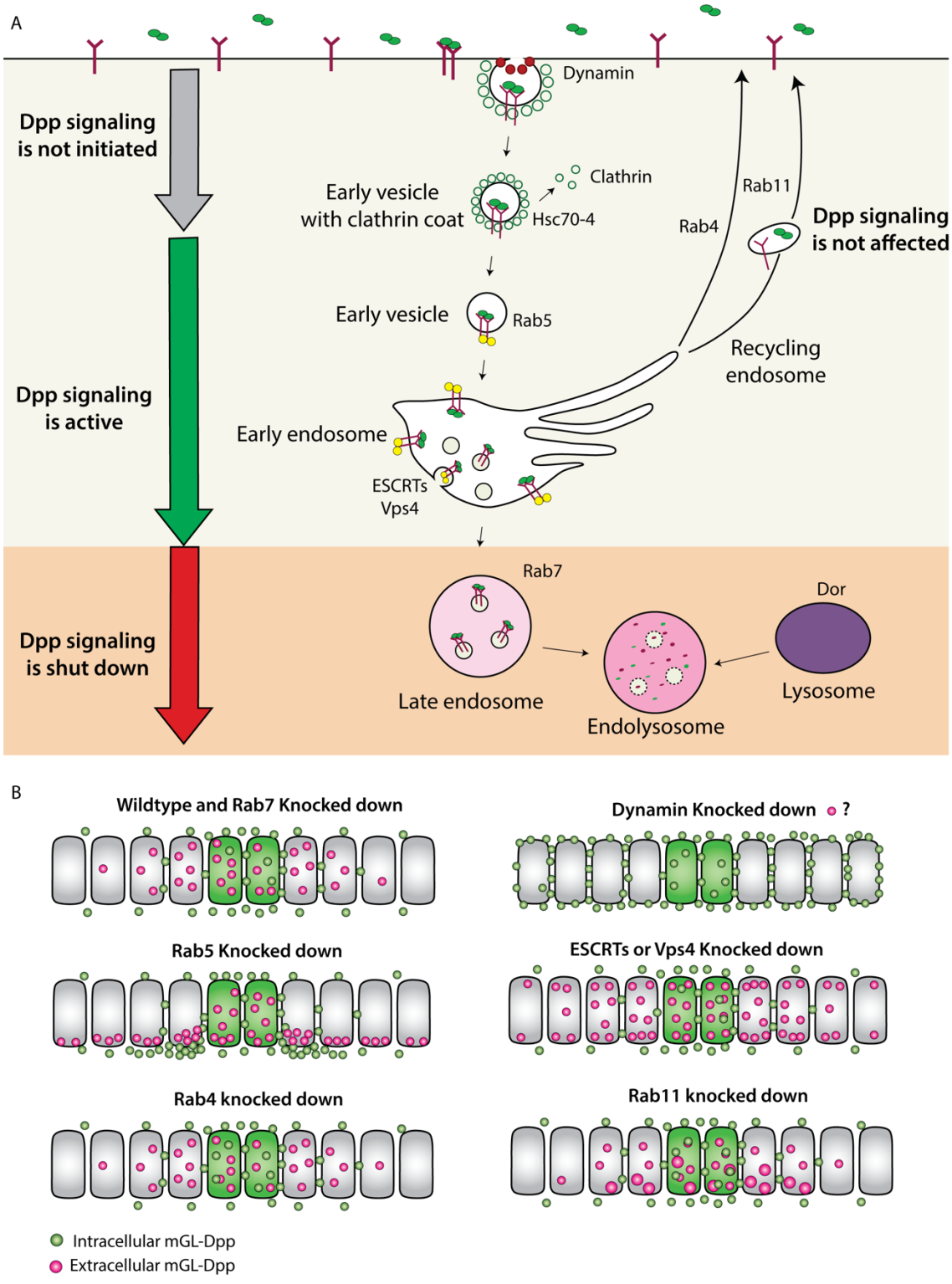

Figure 9: Model for the role of trafficking factors on Dpp signaling and Dpp extracellular gradient formation. (A) Endocytic pathway for the Dpp/Tkv complex inside the receiving cells. (B) Extracellular (in magenta) and intracellular (in green) Dpp gradient change upon knocking down different trafficking factors.

Discussion

In this study, we generated novel *dpp* alleles to visualize both extracellular and intracellular Dpp distributions. Using these alleles, we addressed the role of endocytic trafficking in extracellular and intracellular Dpp gradient formation and its interpretation. Our results suggest that endocytosis has a major contribution in Dpp gradient formation via the active removal of Dpp from the extracellular space, and it terminates Dpp signaling by sorting Tkv into the intraluminal vesicles, contributing to the interpretation of the extracellular Dpp gradient.

Role of endocytic trafficking in extracellular Dpp gradient formation

Endocytic trafficking has been proposed to regulate extracellular Dpp gradient formation through receptor-mediated transcytosis (Entchev et al., 2000), recycling (Romanova-Michaelides et al., 2022), and sink (Simon et al., 2023). We found that the extracellular Dpp distribution expanded upon blocking early endocytosis and not the following endocytic trafficking such as MVBs formation, late endosome, or recycling, supporting that early endocytosis simply acts as a sink for Dpp. Given the expansion of the extracellular Dpp distribution upon loss of *tkv* (Simon et al., 2023), Tkv-mediated internalization of Dpp likely acts as a sink to regulate Dpp morphogen gradient.

Role of endocytic trafficking in interpretation of the extracellular gradient

Contrary to the previous results (Entchev et al., 2000; Moreno et al., 2002), we surprisingly found that loss of Rab5 led to an increase in Dpp signaling activity due to the impaired downregulation of activated receptors (Fig. 3-5), indicating that the Dpp signaling is initiated before the formation of the early endosome and is terminated at the level of the early endosome or the following endocytic trafficking. We speculate that the loss of Dpp signaling in absence of Rab5 in previous studies is partly due to pleiotropic effects. In this study we utilized the temperature sensitive Gal80 to carefully knock down Rab5 in a temporally controlled manner, while Rab5 was constantly knocked down in the previous study, although the temperature was controlled to reduce pleiotropic effects (Entchev et al., 2000). We speculate that constant despite the weak expression of the dominant negative form of Rab5, it may have nevertheless caused pleiotropic effects affecting Dpp signaling activity. Supporting

this interpretation, we found that longer downregulation of Rab5 caused cell extrusion or aberrant tissue architecture (data not shown).

In contrast to the idea that BMP signal is terminated through lysosomal degradation (Aoyama et al., 2012), our results suggest that Dpp signaling is terminated at the level of MVB formation but not through lysosomal degradation (Fig. 6, 7). We speculate that sorting activated receptors into the ILVs itself separates the receptors from its target Mad in the cytosol. It has been shown that multiple signaling pathways are activated upon blocking MVBs formation. It would be interesting to test if this is due to the impaired sorting of the activated receptors or impaired lysosomal degradation. Interestingly, Dpp signaling was upregulated without affecting the extracellular Dpp gradient upon blocking MVBs formation, indicating that extracellular Dpp gradient is interpreted by the duration of Dpp signaling

Novel tools to visualize Dpp morphogen gradient

Dpp morphogen gradient has been intensively studied using GFP-Dpp. When expressed in the anterior stripe of cells, the main *dpp* source, GFP-Dpp showed highest fluorescent signal in the source cells and shallow graded signal in both sides as punctate signal (Entchev et al., 2000; Teleman & Cohen, 2000). While the punctate signal was shown to be mainly from the internalized GFP-Dpp (Kicheva et al., 2007; Teleman & Cohen, 2000; Zhou et al., 2012), extracellular staining revealed distinct extracellular-specific Dpp morphogen gradient (Belenkaya et al., Cell 2004). Using FRAP and FCS, the parameters for Dpp gradient formation have been measured, including diffusion coefficient, degradation rates, etc (Kicheva et al., 2007; Zhou et al., 2012). However, given the unphysiological level of overexpression (estimated 400 times higher than the physiological level) (Romanova-Michaelides et al., 2022), it has been questioned how much the obtained results from overexpression of Dpp reflects the way the endogenous Dpp gradient is established (Simon et al., 2023). Nevertheless, these results suggested that Dpp gradient consists of extracellular (bound and unbound) and internalized populations.

Recently, with the advances in genome engineering methods, it has become possible to insert a tag in *dpp* locus (Bosch et al., 2017; Matsuda et al., 2021; Romanova-Michaelides et al., 2022). Endogenous *GFP-dpp* allele revealed that the fluorescent signal was too low to visualize the graded Dpp distribution (Fig. 1A) and to apply FRAP assay to measure the parameters of Dpp gradient formation (Romanova-Michaelides et al., 2022). Similarly, an endogenous *HA-dpp* allele revealed a shallow extracellular HA-Dpp distribution and the conventional immunostaining failed to visualize the Dpp distribution outside the main source cells (Matsuda et al., 2021). The nanobody internalization assay was able to visualize

the internalized Dpp but it is not clear if the nanobody bound GFP-Dpp reflects the functional ligand that undergoes proper endocytic trafficking given that GFP-dpp is not fully functional (Romanova-Michaelides et al., 2022).

mGL-dpp and *mSC-dpp* alleles can overcome these shortcomings. These alleles are functional at least during wing development and their brighter fluorescent signal allows for visualization of the endogenous Dpp distribution (mostly internalized Dpp) without any manipulation (Fig. 1). Using the *mGL-dpp* allele also allows for visualization of the extracellular Dpp distribution through anti-GFP antibody staining. FRAP assays, morphotrap, and live imaging have already been successfully applied to characterize the role of mGL-Dpp in the Drosophila testis (Ridwan et al., 2022 Biorxiv). By applying these assays in the wing disc, it would be of interest to re-investigate the parameters of Dpp morphogen gradient formation using these alleles.

Materials and methods

Fly stocks

Flies for experiments were kept in standard fly vials containing polenta and yeast. Embryos from fly crosses for experiments including Gal80ts were collected for 24h and kept at 18°C, until shifted to 29°C prior to dissection of 3rd instar larvae. To induce *Rab5*^{2} clones, third instar larvae were subjected to heat shock (37°C) for 8 minute and incubated at 25°C for 24 hours prior to dissection. The following fly lines were used: *shibire*^{ts1} (BDSC 7068), *mGL-dpp* (this study), *mSC-dpp* (this study), *ap-Gal4* (M. Affolter), *tub-GAL80TS* (M. Affolter), *tkv-3xHA* (G. Pyrowolakis), *tkv-YFP* (G. Pyrowolakis), *tkv-1xHAeGFP* (G. Pyrowolakis), *brk*^{XA} (G. Campbell & A. Tomlinson), *UAS-rab5-RNAi* (BDSC 30518, VDRC 34096, 103945), *UAS-rab5.S43N* (BDSC 42703 & 42704), *UAS-rab4 RNAi* (VDRC 24672), *UAS-rab11-RNAi* (VDRC 22198), *UAS-vps4-RNAi* (VDRC 105977), *UAS-tsg101-RNAi* (BDSC 35710), *UAS-shrub-RNAi* (BDSC 38305*), UAS-rab7-RNAi* (BDSC 27051), *dpp-LacZ* (M.Affolter), *UAS-LOT-deGradHA* (G. Pyrowolakis & M. Affolter), *rab5-eYFP* (BDSC 62543*), rab7-eYFP* (BDSC 62545), *rab4-eYFP* (BDSC 62542*), rab11-eYFP* (BDSC 62549), *FRT82b, rab7*$^{Gal4\text{-}Knock\text{-}in}$ null allele (P. R. Hiesinger), *hsFlp,UAS-GFP,w;FRT42D,tub-Gal80;tub-Gal4,FRT82B,tub-Gal80* (BDSC 86318), *hsFlp;tub>CD2>Gal4,UAS-lacZ* (B. Bello), *hsFlp, rab5*^{2}*, FRT40* (BDSC 42702), *yw, dpp*^{d8} and *dpp*^{d12} are described from Flybase.

Genotypes by figures

Fig.1, A; *GFPdpp/Cyo, p23*
Fig.1, B; *mGL-dpp/+*
Fig.1, C; *mSC-dpp/+*
Fig.1, D; *JAX; mGL-dpp/mGL-dpp*
Fig.1, E; *JAX; mSC-dpp/mSC-dpp*
Fig.1, F; *HA-dpp/HA-dpp*
Fig.1, G; *JAX; HA-dpp/HA-dpp*
Fig.1, H; *JAX; mGL-dpp/mGL-dpp*
Fig.1, I; *JAX; mSC-dpp/mSC-dpp*
Fig.1, K; *mGL-dpp/+*
Fig.2, A; *mSC-dpp / rab5-eYFP*
Fig.2, B; *mSC-dpp / +; rab7-eYFP/ +*
Fig.2, C; *mSC-dpp / rab4-eYFP*
Fig.2, D; *mSC-dpp / +; rab11-eYFP/ +*
Fig.3, A; *HA-dpp, ap-Gal4 / +; UAS-rab5-RNAi (30518) / tub-Gal80ts* (29h at 29°C)
Fig.3, B; *tkv-YFP, ap-Gal4 / +; UAS-rab7-RNAi (27051) / tub-Gal80ts* (43h at 29°C)
Fig.3, C; *HA-dpp, ap-Gal4 / +; UAS-rab11-RNAi (22198) / tub-Gal80ts* (42h at 29°C)
Fig.3, D; *HA-dpp, ap-Gal4 / +; UAS-rab4-RNAi (24672) / tub-Gal80ts* (42h at 29°C)
Fig.3, E; *HA-dpp, ap-Gal4 / +; UAS-rab5-RNAi (34096) / tub-Gal80ts* (29h at 29°C)

Fig.3, F; *HA-dpp, ap-Gal4 / +; UAS-rab5-RNAi (103945) / tub-Gal80ts* (24h at 29°C)
Fig.3, G; *HA-dpp, ap-Gal4 / UAS-rab5.S43N (42703); tub-Gal80ts* / + (18h at 29°C)
Fig.3, H; *Ollas-dpp, ap-Gal4 / +; UAS-rab5.S43N (42704)/ tub-Gal80ts* (13.5h at 29°C)
Fig.3, I; *hsFlp, rab5^{2} FRT40/arm-LacZ, m(2)Z FRT40*
Fig.3, J; *hsFlp; tub>CD2>Gal4 UAS-lacZ / +; UAS-rab5.S43N (42704) / tub-Gal80TS*
Fig.4, A; *brk^{XA}; dpp^{d8}, apGal4 / dpp^{d12}; UAS-rab5-RNAi (30518) / tub-Gal80TS* (29h at 29°C)
Fig.4, B; *apGal4 / dpp-LacZ; UAS-rab5-RNAi (30518) / tub-Gal80TS* (29h at 29°C)
Fig.4, C; *mGL-dpp, apGal4/ +; UAS-rab5-RNAi (30518) / tub-Gal80TS* (29h at 29°C)
Fig.4, D; *yw; tkv-YFP* (2h heat shock at 34°C)
Fig.4, E; *shi^{TS}; tkv-YFP* (2h heat shock at 34°C)
Fig.4, G; *shi^{TS} /+; mGL-dpp /+* (2h heat shock at 34°C)
Fig.4, H; *shi^{TS}; mGL-dpp /+* (2h heat shock at 34°C)
Fig.4, J, L, N; *dpp-mGL, apGal4 / +; UAS-rab5-RNAi (30518)/ tub-Gal80TS* (29h at 29°C)
Fig.4, O, Q; *tkv-YFP, apGal4; UAS-rab5-RNAi (30518)/ tub-Gal80TS* (29h at 29°C)
Fig.5, A; *yw, tkv-HA-eGFP, apGal4 / +; tub-Gal80TS / +* (29h at 29°C)
Fig.5, B; *tkv-HA-eGFP, apGal4 / +; UAS-rab5-RNAi (30518) / tub-Gal80TS* (29h at 29°C)
Fig.5, B; *tkv-HA-eGFP, apGal4 / +; UAS-rab5-RNAi (30518), tub-Gal80TS/ +* (29h at 29°C)
Fig.5, C; *tkv-HA-eGFP, apGal4 / +; UAS-rab5-RNAi (30518), tub-Gal80TS/ UAS-deGradHA* (29h at 29°C)
Fig.5, D; *tkv-HA-eGFP, apGal4 / +; UAS-deGradHA/ tub-Gal80TS* (29h at 29°C)
Fig.6, A; *hsFlp, UAS-GFP; FRT82b, tub-Gal4 / FRT82b rab7 Gal4-Knock-In*
Fig.6, B; *HA-dpp, apGal4; UAS-rab7-RNAi (27051)/ tub-Gal80TS* (42h at 29°C)
Fig.6, C, D; *mGL-dpp, apGal4; UAS-rab7-RNAi (27051)/ tub-Gal80TS* (42h at 29°C)
Fig.6, E; *tkv-YFP, apGal4; UAS-tsg101-RNAi (35710)/ tub-Gal80TS* (44h at 29°C)
Fig.6, F; *tkv-YFP, apGal4/ UAS-shrub-RNAi (38305); tub-Gal80TS / +* (28h at 29°C)
Fig.6, G, H; *tkv-YFP, apGal4 / UAS-vps4-RNAi (105977); tub-Gal80TS / +* (30h at 29°C)
Fig.6, I; *tkv-YFP, apGal4; UAS-rab7-RNAi (27051)/ tub-Gal80TS* (42h at 29°C)
Fig.6, J, K; *mGL-dpp, apGal4 / UAS-vps4-RNAi (105977); tub-Gal80TS / +* (30h at 29°C)

Generation of *mGL-dpp* and *mSC-dpp*

The detail procedure to generate endogenously tagged dpp alleles were previously reported (Matsuda et al., 2021). In brief, utilizing the attP sites in a MiMIC transposon inserted in the dpp locus (MiMIC dppMI03752, BDSC 36399), about 4.4 kb of the dpp genomic sequences containing the second (last) coding exon of dpp including a tag and its flanking sequences was inserted in the intron between dpp's two coding exons. The endogenous exon was then removed using FLP-FRT to keep only the tagged exon. mGL (mGreenLantern (Campbell et al., 2020)) was inserted after the last processing site to tag all the Dpp mature ligands. mGL-dpp homozygous flies show no obvious phenotypes.

Immunohistochemistry

Visualization of mGL-Dpp and mSC-Dpp

To visualize the (total) mGL-Dpp and mSC-Dpp signal, third instar larvae were dissected in ice-cold Phosphate Buffered Saline (PBS). The dissected larvae were washed with HCl with pH 3.0 following

the acid wash protocol (Romanova-Michaelides et al., 2022) to remove the extracellular proteins prior to fixation in 4.0% Paraformaldehyde (PFA) for 25min on a shaker at room temperature (25°C). The discs were washed three times for ten minutes with PBS at 4°C, and mounted in Vectashield on glass slides.

Total staining

Third instar larvae were dissected in ice-cold Phosphate Buffered Saline (PBS) and fixed in 4.0% Paraformaldehyde (PFA) for 25min on a shaker at room temperature (25°C). After fixation, the discs were washed three times for ten minutes with PBS at 4°C, and three times with PBST (0.3% Triton-X in PBS) to permeabilize the tissues. The discs were then blocked in 5% normal goat serum (NGS) in PBST for 30min. The primary antibodies were added to 5% NGS in PBST for incubation of the discs at 4°C overnight. The next day, the primary antibody was carefully removed, and the samples were washed three times with PBST. Secondary antibodies were added to5 % NGS in PBST and the discs were incubated for 2h in the dark at room temperature. At last, the samples were washed three times for 15 minutes with PBST at room temperature, two times with PBS, and mounted in Vectashield on glass slides.

Extracellular staining

Wing discs from third instar larvae were dissected in ice-cold Schneider's Drosophila medium (S2). The discs were then blocked in cold 5% NGS in S2 medium on ice for 10min. The blocking solution was carefully removed and the primary antibody was added for 1h on ice. To ensure an even distribution of the primary antibody, the tubes were tapped every 10min during the incubation time. The antibody was then removed and the samples were washed at least 6 times with cold S2 medium and another two times with cold PBS to remove excess primary antibody. Wing discs were then fixed with 4% PFA in PBS for 25min on the shaker at room temperature (25°C). After fixation the protocol continued as described in total staining.

Acid wash

The protocol was adapted from Romanova-Michaelides et al. (2022). In order to remove the extracellular proteins prior to fixation, the dissected wing discs were washed three times ten seconds with ice-cold Schneider's Drosophila medium (S2), pH dropped down to 3 by HCl. To remove the stripped membrane-bound proteins, the discs were washed three times 15min with ice-cold S2 medium (pH 7.4), and fixed in 4% PFA.

Antibodies

Primary antibodies: Rabbit anti-phospho-Smad 1/5 (Cell signaling 9516S; 1:200), mouse anti-patched (DSHB; 1:40), mouse anti-wingless (4D4, DSHB; 1:120), rabbit anti-GFP (Abcam ab6556; 1:2000 for total staining, 1:200 for extracellular staining,), guinea pig anti-rab5 (provided by Akira Nakamura; 1:1000), rabbit anti-rab11 (provided by Akira Nakamura; 1:8000), mouse anti-rab7 (DSHB; 1:30), mouse anti-ubiquitin (Enzo PW8810-0100; 1:1000), mouse anti-beta galactosidase (Promega Z378825580610; 1:500), guinea pig anti-brk (provided by from Gines Morata; 1:1000), mouse anti-V5 (Invitrogen; 1:5000).

The following secondary antibodies were used at 1:500 dilutions in this study: Goat anti-rabbit IgG (H+L) Alexa Fluor™ 488 (A11008 Thermo Fischer), goat-anti-rabbit IgG (H+L) Alexa Fluor™ 568 (A11011 Thermo Fischer), goat-anti-rabbit IgG (H+L) Alexa Fluor™ 680 (A21109 Thermo Fischer), goat anti-mouse IgG (H+L) Alexa Fluor™ 488 (A11001 Thermo Fischer), goat anti-mouse IgG (H+L) Alexa Fluor™ 568 (A11004 Thermo Fischer), goat anti-mouse IgG (H+L) Alexa Fluor™ 680 (A10038 Thermo Fischer), goat-anti-guinea pig IgG (H+L) Alexa Fluor™ 568 (A11075 Thermo Fischer), goat-anti-guinea pig IgG (H+L) DyLight 680 (SA5-10098 Invitrogen).

Imaging

Wing imaginal discs were imaged using a Leica SP5-II MATRIX and an Olympus Spinning Disk (CSU-W1), and images were analyzed using Fiji (ImageJ). Figures were obtained using OMERO and Adobe Illustrator.

Quantification of pMad and extracellular mGL-dpp intensity

To quantify the intensity of pMad and extracellular mGL-dpp gradient in the images, an average intensity of three sequential stacks was created using Fiji ImageJ (v1.53c). Each signal intensity profile collected in Excel (Ver. 16.51) was aligned along A/P compartment boundary (based on anti-Ptc or pMad staining) and average signal intensity profile from different samples was generated and plotted by the script (wing_disc-alignment.py). The average intensity of the samples and the control were then compared using the script (wingdisc_comparison.py). Both scripts were generated by E. Schmelzer, and can be found on: https://etiennees.github.io/Wing_disc-alignment/. The resulting signal intensity profiles (mean with SD) were generated on GraphPad Prism software (v.9.3.1(471)). Figures were prepared using OMERO (ver5.9.1) and Adobe Illustrator (24.1.3).

Quantification of mGL-dpp and Tkv-YFP positive puncta

To measure the number particles an average intensity of 3 z-stacks from the images were created using Fiji ImageJ. The number and area of the particles were measured by the built-in "Analyze Particles" plug-in on Fiji. The data were used to make the graphs on GraphPad Prism. A ratio-paired t-test ($p<0.05$) was used for statistical analysis.

Reproducibility

All experiments were independently repeated at least two time, with consistent results. Statistical significance was assessed by the GraphPad Prism software (v.9.3.1(471)).

Acknowledgements

The authors would like to thank Markus Affolter for his continuous support throughout the course of this project. We thank Developmental Studies Hybridoma Bank (DSHB) at The University of Iowa for providing us with the primary antibodies, and Bloomington Drosophila Stock Center (BDSC) for providing us with fly stocks. We would also like to thank Dr. Giorgos Pyrowolakis, Prof. Peter Robin Hiesinger and Prof. Isabel Guerrero for providing us with fly lines and Prof. Akira Nakamura for providing us with primary antibodies. We thank Dr. Etienne Schmelzer for providing us with scripts for quantifications. We would like to thank Bernadette Bruno, Gina Evora, Karin Mauro and Dario Dörig for their constant and reliable supply of the world's best fly food. We thank the Biozentrum Imaging Core Facility (IMCF), especially Dr. Oliver Biehlmaier, Dr. Alexia Loyton-Ferrand, Dr. Sara Roig, Dr. Kai Schleicher, Laurent Guerard, Nikolaus Ehrenfeuchter and Dr. Sébastien Herbert for their constant support with the microscopes and image analysis.

References

Affolter, M., & Basler, K. (2007). The Decapentaplegic morphogen gradient: from pattern formation to growth regulation. *Nat Rev Genet*, *8*(9), 663-674. https://doi.org/10.1038/nrg2166

Akiyama, T., User, S. D., & Gibson, M. C. (2018). Somatic clones heterozygous for recessive disease alleles of BMPR1A exhibit unexpected phenotypes in Drosophila. *Elife*, *7*, e35258. https://doi.org/10.7554/eLife.35258

Aoyama, M., Sun-Wada, G. H., Yamamoto, A., Yamamoto, M., Hamada, H., & Wada, Y. (2012). Spatial restriction of bone morphogenetic protein signaling in mouse gastrula through the mVam2-dependent endocytic pathway. *Dev Cell*, *22*(6), 1163-1175. https://doi.org/10.1016/j.devcel.2012.05.009

Belenkaya, T. Y., Han, C., Yan, D., Opoka, R. J., Khodoun, M., Liu, H., & Lin, X. (2004). Drosophila Dpp morphogen movement is independent of dynamin-mediated endocytosis but regulated by the glypican members of heparan sulfate proteoglycans. *Cell*, *119*(2), 231-244. https://doi.org/10.1016/j.cell.2004.09.031

Bosch, P. S., Ziukaite, R., Alexandre, C., Basler, K., & Vincent, J. P. (2017). Dpp controls growth and patterning in Drosophila wing precursors through distinct modes of action. *Elife*, *6*. https://doi.org/10.7554/eLife.22546

Bucci, C., Parton, R. G., Mather, I. H., Stunnenberg, H., Simons, K., Hoflack, B., & Zerial, M. (1992). The small GTPase rab5 functions as a regulatory factor in the early endocytic pathway. *Cell*, *70*(5), 715-728. https://doi.org/https://doi.org/10.1016/0092-8674(92)90306-W

Bucci, C., & Stasi, M. (2016). Endosome to Lysosome Transport. In R. A. Bradshaw & P. D. Stahl (Eds.), *Encyclopedia of Cell Biology* (pp. 408-417). Academic Press. https://doi.org/https://doi.org/10.1016/B978-0-12-394447-4.20041-2

Campbell, B. C., Nabel, E. M., Murdock, M. H., Lao-Peregrin, C., Tsoulfas, P., Blackmore, M. G., Lee, F. S., Liston, C., Morishita, H., & Petsko, G. A. (2020). mGreenLantern: a bright monomeric fluorescent protein with rapid expression and cell filling properties for neuronal imaging. *Proc Natl Acad Sci U S A*, *117*(48), 30710-30721. https://doi.org/10.1073/pnas.2000942117

Cherry, S., Jin, E. J., Ozel, M. N., Lu, Z., Agi, E., Wang, D., Jung, W. H., Epstein, D., Meinertzhagen, I. A., Chan, C. C., & Hiesinger, P. R. (2013). Charcot-Marie-Tooth 2B mutations in rab7 cause dosage-dependent neurodegeneration due to partial loss of function. *Elife*, *2*, e01064. https://doi.org/10.7554/eLife.01064

Dubois, L., Lecourtois, M., Alexandre, C., Hirst, E., & Vincent, J. P. (2001). Regulated endocytic routing modulates wingless signaling in Drosophila embryos. *Cell*, *105*(5), 613-624. https://doi.org/10.1016/s0092-8674(01)00375-0

Entchev, E. V., Schwabedissen, A., & González-Gaitán, M. (2000). Gradient formation of the TGF-beta homolog Dpp. *Cell*, *103*(6), 981-991. https://doi.org/10.1016/s0092-8674(00)00200-2

González-Gaitán, M., & Jäckle, H. (1999). The range of spalt-activating Dpp signalling is reduced in endocytosis-defective Drosophila wing discs. *Mech Dev*, *87*(1-2), 143-151. https://doi.org/10.1016/s0925-4773(99)00156-2

Hoffmann, F. M., & Goodman, W. (1987). Identification in transgenic animals of the Drosophila decapentaplegic sequences required for embryonic dorsal pattern formation. *Genes Dev*, *1*(6), 615-625. https://doi.org/10.1101/gad.1.6.615

Jékely, G., & Rørth, P. (2003). Hrs mediates downregulation of multiple signalling receptors in Drosophila. *EMBO Rep*, *4*(12), 1163-1168. https://doi.org/10.1038/sj.embor.7400019

Kicheva, A., Pantazis, P., Bollenbach, T., Kalaidzidis, Y., Bittig, T., Jülicher, F., & González-Gaitán, M. (2007). Kinetics of morphogen gradient formation. *Science*, *315*(5811), 521-525. https://doi.org/10.1126/science.1135774

Koenig, J. H., & Ikeda, K. (1989). Disappearance and reformation of synaptic vesicle membrane upon transmitter release observed under reversible blockage of membrane retrieval. *J Neurosci*, *9*(11), 3844-3860. https://doi.org/10.1523/jneurosci.09-11-03844.1989

Lecuit, T., Brook, W. J., Ng, M., Calleja, M., Sun, H., & Cohen, S. M. (1996). Two distinct mechanisms for long-range patterning by Decapentaplegic in the Drosophila wing. *Nature*, *381*(6581), 387-393. https://doi.org/10.1038/381387a0

Li, W., Yao, A., Zhi, H., Kaur, K., Zhu, Y. C., Jia, M., Zhao, H., Wang, Q., Jin, S., Zhao, G., Xiong, Z. Q., & Zhang, Y. Q. (2016). Angelman Syndrome Protein Ube3a Regulates Synaptic Growth and Endocytosis by Inhibiting BMP Signaling in Drosophila. *PLoS Genet*, *12*(5), e1006062. https://doi.org/10.1371/journal.pgen.1006062

Matsuda, S., Harmansa, S., & Affolter, M. (2016). BMP morphogen gradients in flies. *Cytokine Growth Factor Rev*, *27*, 119-127. https://doi.org/10.1016/j.cytogfr.2015.11.003

Matsuda, S., Schaefer, J. V., Mii, Y., Hori, Y., Bieli, D., Taira, M., Plückthun, A., & Affolter, M. (2021). Asymmetric requirement of Dpp/BMP morphogen dispersal in the Drosophila wing disc. *Nat Commun*, *12*(1), 6435. https://doi.org/10.1038/s41467-021-26726-6

Moreno, E., Basler, K., & Morata, G. (2002). Cells compete for decapentaplegic survival factor to prevent apoptosis in Drosophila wing development. *Nature*, *416*(6882), 755-759. https://doi.org/10.1038/416755a

Morrison, H. A., Dionne, H., Rusten, T. E., Brech, A., Fisher, W. W., Pfeiffer, B. D., Celniker, S. E., Stenmark, H., & Bilder, D. (2008). Regulation of early endosomal entry by the Drosophila tumor suppressors Rabenosyn and Vps45. *Mol Biol Cell*, *19*(10), 4167-4176. https://doi.org/10.1091/mbc.e08-07-0716

Nellen, D., Burke, R., Struhl, G., & Basler, K. (1996). Direct and long-range action of a DPP morphogen gradient. *Cell*, *85*(3), 357-368. https://doi.org/10.1016/s0092-8674(00)81114-9

Restrepo, S., Zartman, J. J., & Basler, K. (2014). Coordination of patterning and growth by the morphogen DPP. *Curr Biol*, *24*(6), R245-255. https://doi.org/10.1016/j.cub.2014.01.055

Rogers, K. W., & Schier, A. F. (2011). Morphogen Gradients: From Generation to Interpretation. *Annual Review of Cell and Developmental Biology*, *27*(1), 377-407. https://doi.org/10.1146/annurev-cellbio-092910-154148

Romanova-Michaelides, M., Hadjivasiliou, Z., Aguilar-Hidalgo, D., Basagiannis, D., Seum, C., Dubois, M., Jülicher, F., & Gonzalez-Gaitan, M. (2022). Morphogen gradient scaling by recycling of intracellular Dpp. *Nature*, *602*(7896), 287-293. https://doi.org/10.1038/s41586-021-04346-w

Scholpp, S., & Brand, M. (2004). Endocytosis controls spreading and effective signaling range of Fgf8 protein. *Curr Biol*, *14*(20), 1834-1841. https://doi.org/10.1016/j.cub.2004.09.084

Schwank, G., Dalessi, S., Yang, S. F., Yagi, R., de Lachapelle, A. M., Affolter, M., Bergmann, S., & Basler, K. (2011). Formation of the long range Dpp morphogen gradient. *PLoS Biol*, *9*(7), e1001111. https://doi.org/10.1371/journal.pbio.1001111

Simon, N., Safyan, A., Pyrowolakis, G., & Matsuda, S. (2023). Dally is not essential for Dpp spreading or internalization but for Dpp stability by antagonizing Tkv-mediated Dpp internalization. *bioRxiv*, 2023.2001.2015.524087. https://doi.org/10.1101/2023.01.15.524087

Strigini, M., & Cohen, S. M. (2000). Wingless gradient formation in the Drosophila wing. *Curr Biol*, *10*(6), 293-300. https://doi.org/10.1016/s0960-9822(00)00378-x

Teleman, A. A., & Cohen, S. M. (2000). Dpp gradient formation in the Drosophila wing imaginal disc. *Cell*, *103*(6), 971-980. https://doi.org/10.1016/s0092-8674(00)00199-9

Vigano, M. A., Ell, C. M., Kustermann, M. M. M., Aguilar, G., Matsuda, S., Zhao, N., Stasevich, T. J., Affolter, M., & Pyrowolakis, G. (2021). Protein manipulation using single copies of short peptide tags in cultured cells and in Drosophila melanogaster. *Development*, *148*(6). https://doi.org/10.1242/dev.191700

Wartlick, O., Kicheva, A., & González-Gaitán, M. (2009). Morphogen gradient formation. *Cold Spring Harb Perspect Biol*, *1*(3), a001255. https://doi.org/10.1101/cshperspect.a001255

Wucherpfennig, T., Wilsch-Bräuninger, M., & González-Gaitán, M. (2003). Role of Drosophila Rab5 during endosomal trafficking at the synapse and evoked neurotransmitter release. *J Cell Biol*, *161*(3), 609-624. https://doi.org/10.1083/jcb.200211087

Yu, S. R., Burkhardt, M., Nowak, M., Ries, J., Petrásek, Z., Scholpp, S., Schwille, P., & Brand, M. (2009). Fgf8 morphogen gradient forms by a source-sink mechanism with freely diffusing molecules. *Nature*, *461*(7263), 533-536. https://doi.org/10.1038/nature08391

Zhou, S., Lo, W. C., Suhalim, J. L., Digman, M. A., Gratton, E., Nie, Q., & Lander, A. D. (2012). Free extracellular diffusion creates the Dpp morphogen gradient of the Drosophila wing disc. *Curr Biol*, *22*(8), 668-675. https://doi.org/10.1016/j.cub.2012.02.065

Supplementary materials

Shaping and interpretation of Dpp morphogen gradient by endocytic trafficking

Hadji Rasouliha et al. 2023

Supplementary Figures 1-3

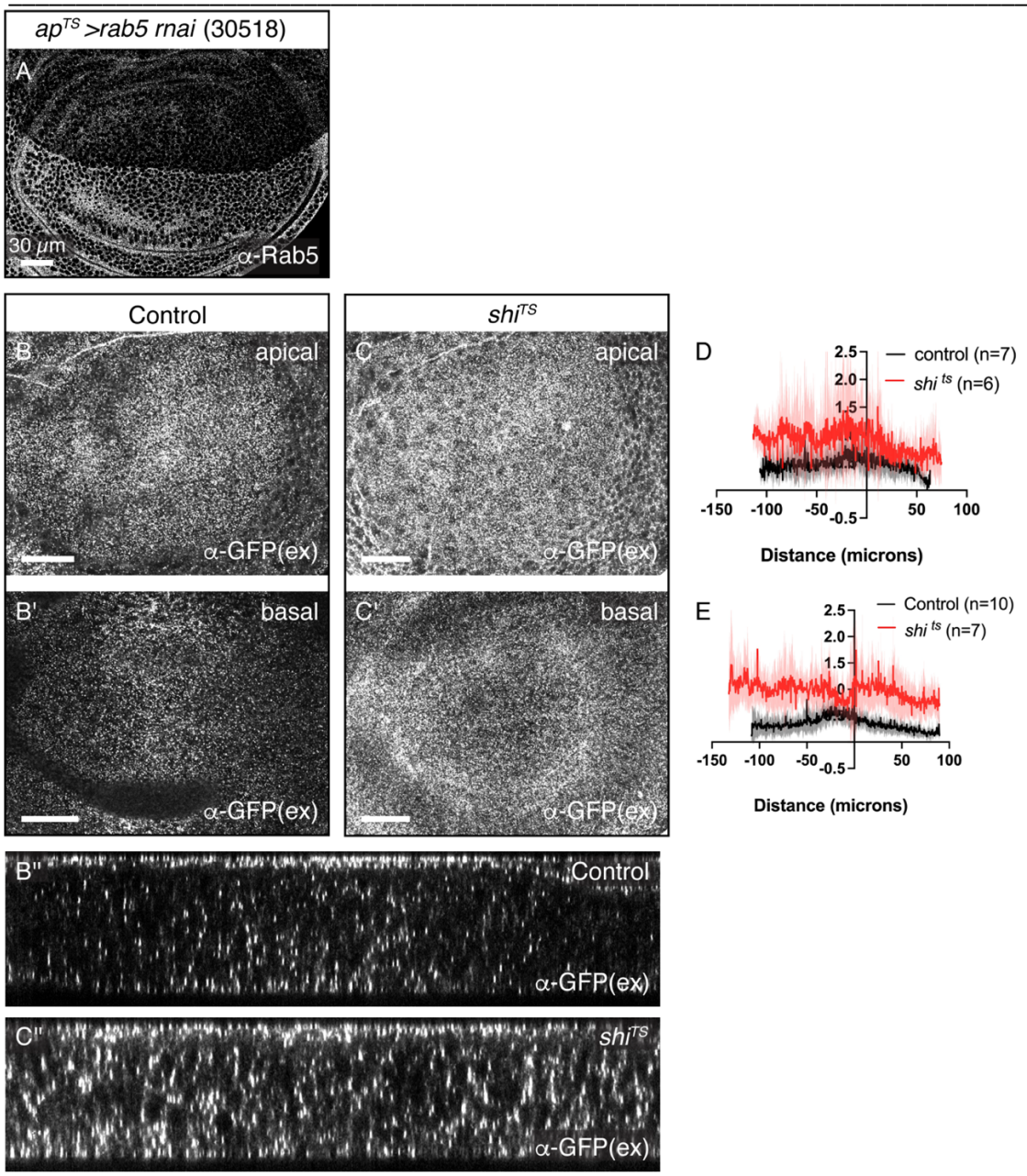

Figure S1: Rab5 RNAi validation, and accumulation of extracellular Dpp in *sh^{ts1}* mutant allele: (A) Antibody staining against Rab5 in *ap^{TS}>rab5 rnai*. (B-E) Extracellular mGL-Dpp via α-GFP antibody staining in (B) apical side in the control heterozygous *shi^{ts1}* (B') basal side in the control heterozygous *shi^{ts1}*, (C) apical side in hemizygous *shi^{ts1}*, (C') basal side in hemizygous *shi^{ts1}*. (B''-C'') Optical cross-sections of the wing imaginal disc in heterozygous *shi^{ts1}* (B'') and hemizygous *shi^{ts1}* (C''). (D-E) Quantification of extracellular mGL-Dpp in the apical (D) and the basal (E) side in B-C. All flies in B-C were subjected to 2h of heat shock at 34°C.

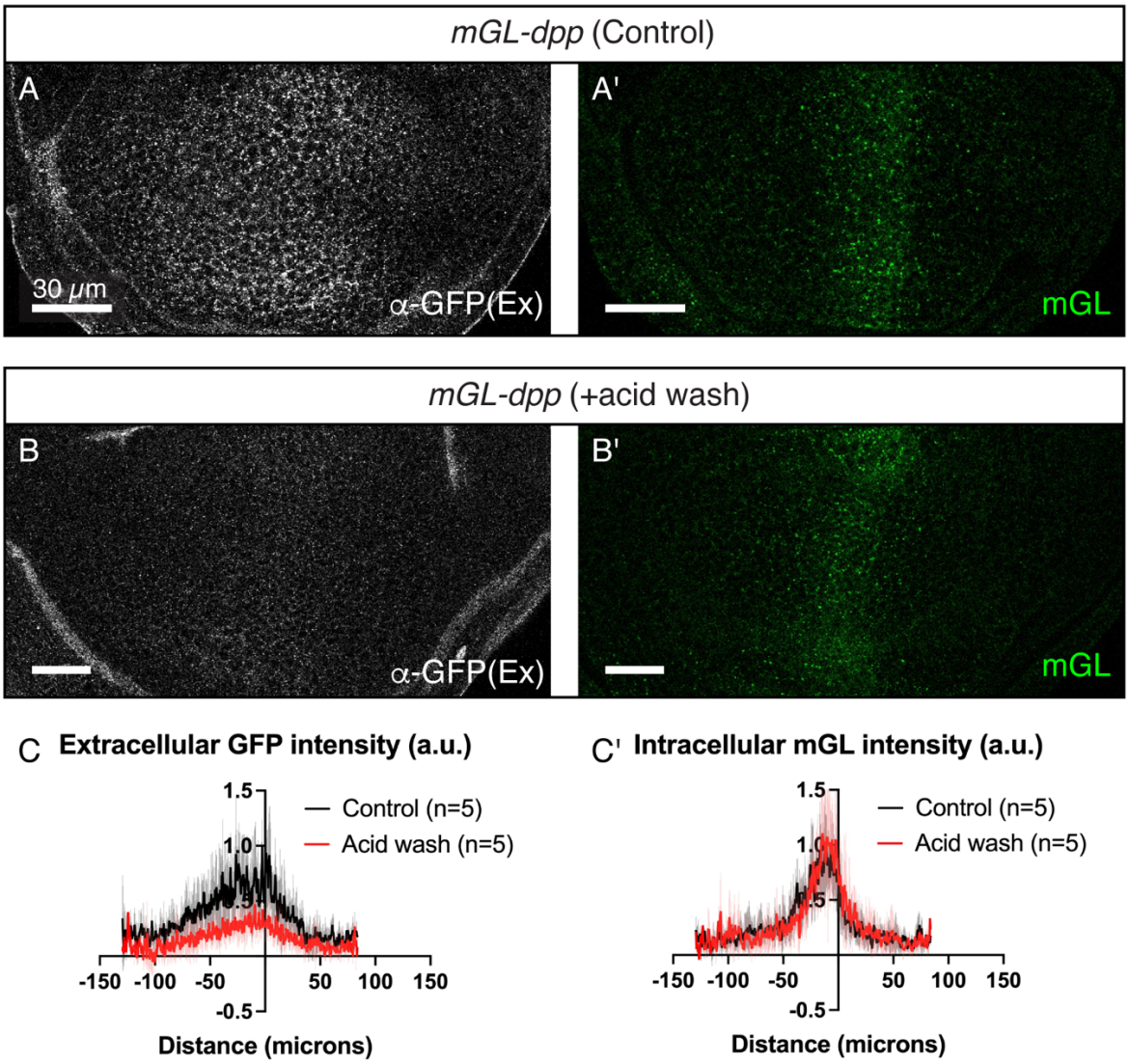

Figure S2: Acid wash removes extracellularly bound proteins but does not alter the intracellular proteins: (A) Extracellular mGL-Dpp observed through an α-GFP antibody staining in the control condition in absence of the acid wash, (A') total mGL-Dpp signal in absence of the acid wash, (B) Extracellular mGL-Dpp observed through an α-GFP antibody staining after the acid wash, (B') total mGL-Dpp after the acid wash. (C-C') Quantification of the extracellular mGL-Dpp signal intensity in A and B (C), and the intracellular mGL-Dpp signal in A' and B' (C').

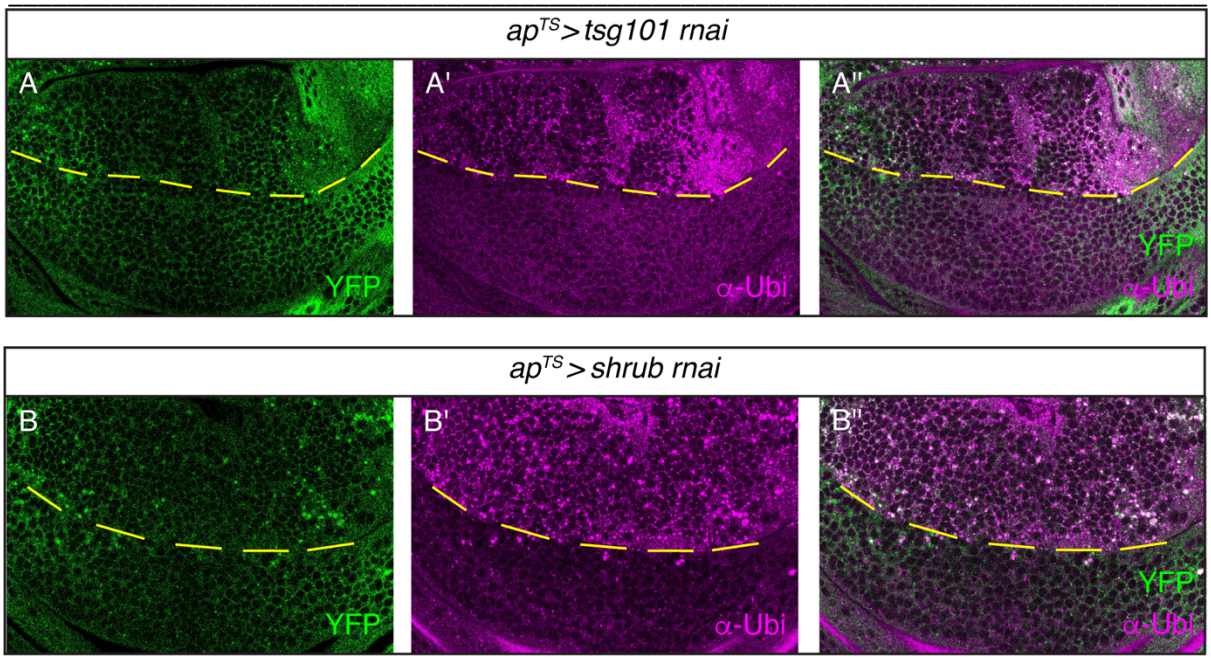

Figure S3: Knocking down the ESCRT components TSG101 and shrub leads to an accumulation of Tkv and ubiquitin in puncta. (A-A'') Tkv-YFP signal (A), ubiquitin signal (A') and the merged image (A'') in *ap^{TS}>tsg101 rnai* flies. (B-B'') Tkv-YFP signal (B), ubiquitin signal (B') and the merged image (B'') in *ap^{TS}>shrub rnai* flies.

4 Additional results

4.1 Role of endocytosis in Dpp signaling and gradient formation

4.1.1 Tkv tagged extracellularly with HA

To be able to visualize the extracellular localization of Tkv and know if it colocalizes with the ligand in the extracellular space, we generated *HA-tkv,* (named HA-Tkv from here on) by inserting an HA tag 165 bps upstream of the transmembrane domain, after the amino acid number 79 in the non-conserved region. The insertion was proven to be successful, as the flies were homozygous viable, the adult wings showed no aberrant phenotype (Fig.4.1, C-C') and the HA staining for HA-Tkv in the wing imaginal discs resembled the Tkv expression pattern.

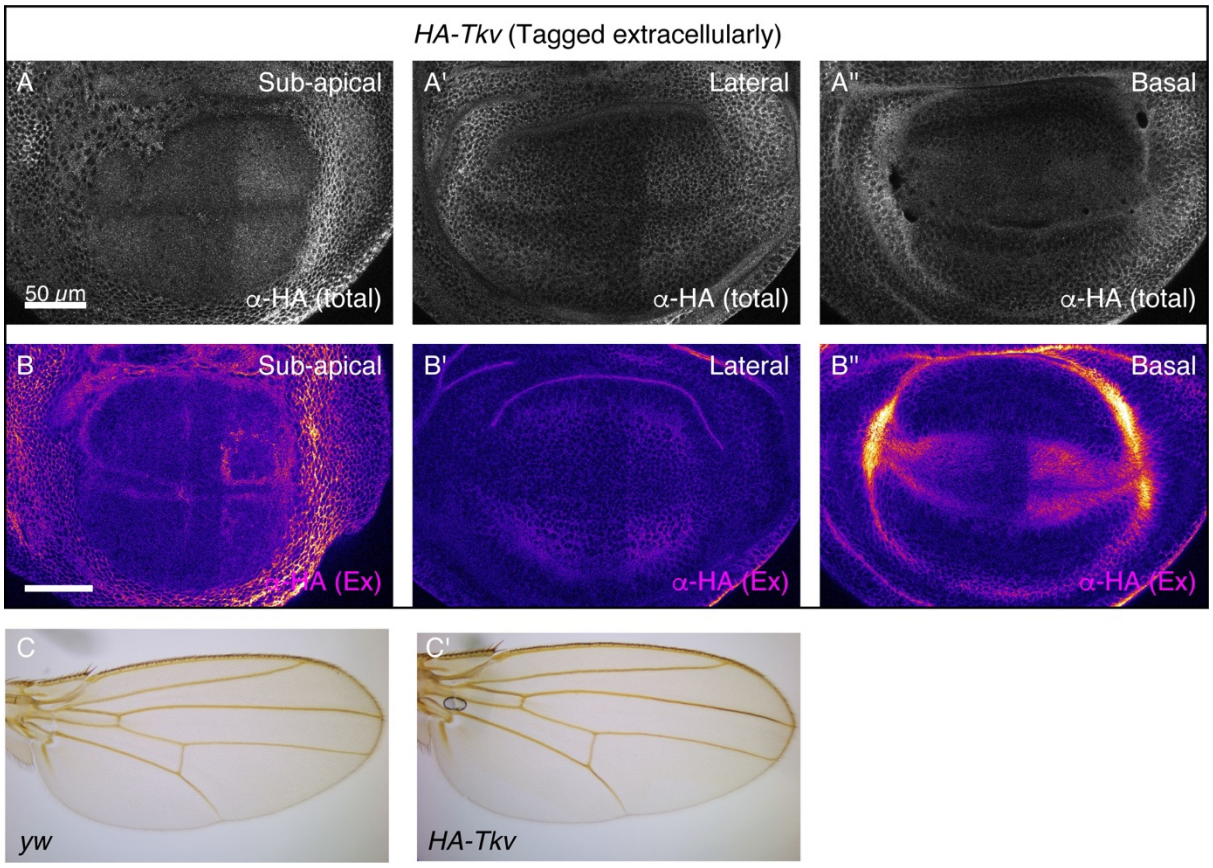

Figure 4.1: Total and extracellular HA staining for the generated extracellularly tagged HA-Tkv
(A-A'') Total HA-Tkv visualized via total HA staining in the sub-apical (A), lateral (A') and basal (A'') side of the wing imaginal disc. (B-B'') Extracellular HA visualized via an extracellular HA staining in the sub-apical (B), lateral (B') and basal (B'') side of the wing imaginal disc. (C-C') Comparison between the adult wings of the control yw flies (C) with the HA-tkv flies (C').

The newly generated extracellularly tagged HA-Tkv showed a similar staining to Tkv-3xHA (Intracellular) and Tkv-YFP and resembled the Tkv expression pattern (Fig.4.1, A-A''). Also, an extracellular staining against HA showed the presence of extracellular HA-Tkv throughout the pouch, also resembling the expected expression pattern of Tkv (Fig.4.1, B-B'), with a more prominent presence in the basal and the sub-apical region (Fig.4.1, B, B'').

4.1.2 Is Tkv the internalizing receptor of Dpp?

With the generation of the extracellularly tagged *HA-tkv*, it was possible to visualize the extracellular mGL-Dpp and HA-Tkv together (Fig.4.2). As expected, HA-Tkv is localized apically (some also in the peripodial membrane), but also to a large extent in the basolateral region (Fig.4.2, A). Also, mGL-Dpp is mostly localized laterally, and follows a gradient towards the periphery, but is also present in the peripodial membrane (Fig.4.2, A'). The colocalization map indicates the positions in which HA-Tkv and mGL-Dpp colocalize (Fig.4.2, A'''), and the colocalized positions seem to be mostly apical/in the peripodial membrane, as well as basolateral where majority of HA-Tkv is localized. Due to the high affinity of Tkv for Dpp, it is highly likely that HA-Tkv and mGL-Dpp interact and bind together extracellularly.

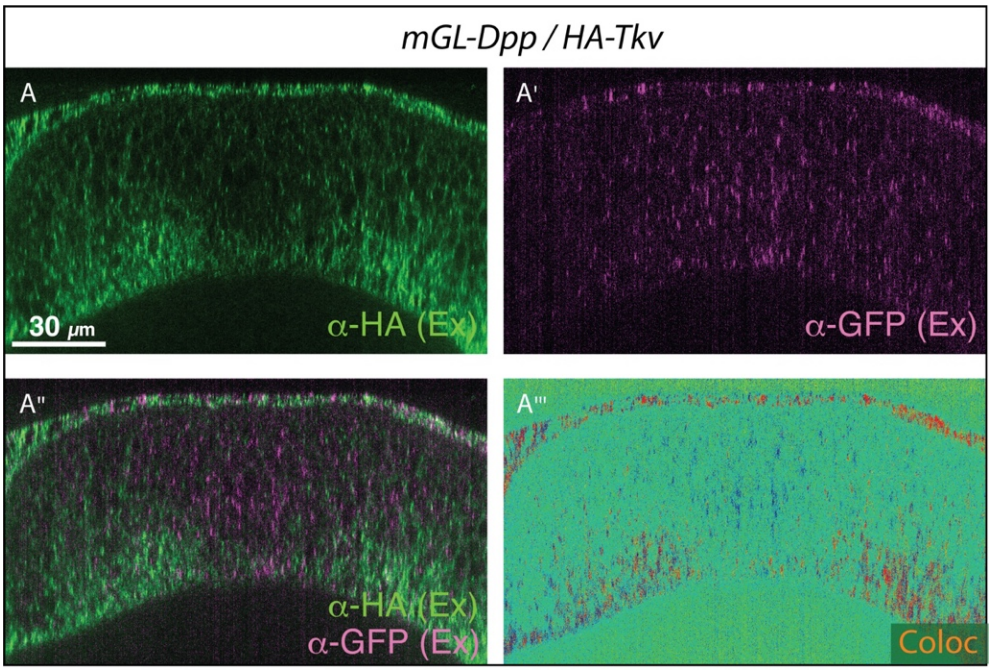

Figure 4.2: mGL-Dpp and HA-Tkv colocalize extracellularly.
(A) Extracellular HA-Tkv, (A') Extracellular mGL-Dpp, visualized through an extracellular GFP antibody staining, (A'') merged image of Extracellular mGL-Dpp and HA-Tkv, (A'') colocalization map, showing regions of overlap between the extracellular HA-Tkv and extracellular mGL-Dpp.

A recent study has suggested that Tkv is not the internalizing receptor for Dpp, and that Dpp signaling is initiated once the internalized Dpp and Tkv encounter each other inside the trafficking endosomes (Romanova-Michaelides et al., 2022). However, the recent study done by Simon et al. (2023) has challenged this idea. Also, the observed colocalization between the extracellular Tkv and Dpp suggests that the two already interact on the cells, possibly prior to internalization.

Also, to further address whether Tkv is indeed the internalizing receptor for Dpp, we knocked down Tkv by RNAi to investigate if Dpp is internalized in absence of this receptor. As seen in Figure 4.3, knocking down Tkv via RNAi for 24 hours in the dorsal compartment of the wing imaginal discs led to a decrease in the number of mGL-Dpp puncta. To ensure the puncta signal did not include the extracellular mGL-Dpp, the acid wash protocol was used to remove the extracellular molecules prior to the tissue fixation. Knocking down Tkv led to a complete loss of Dpp signaling activity, and a decrease in the number of mGL-Dpp puncta, suggesting that Tkv is the internalizing receptor of Dpp (Fig.4.3, B).

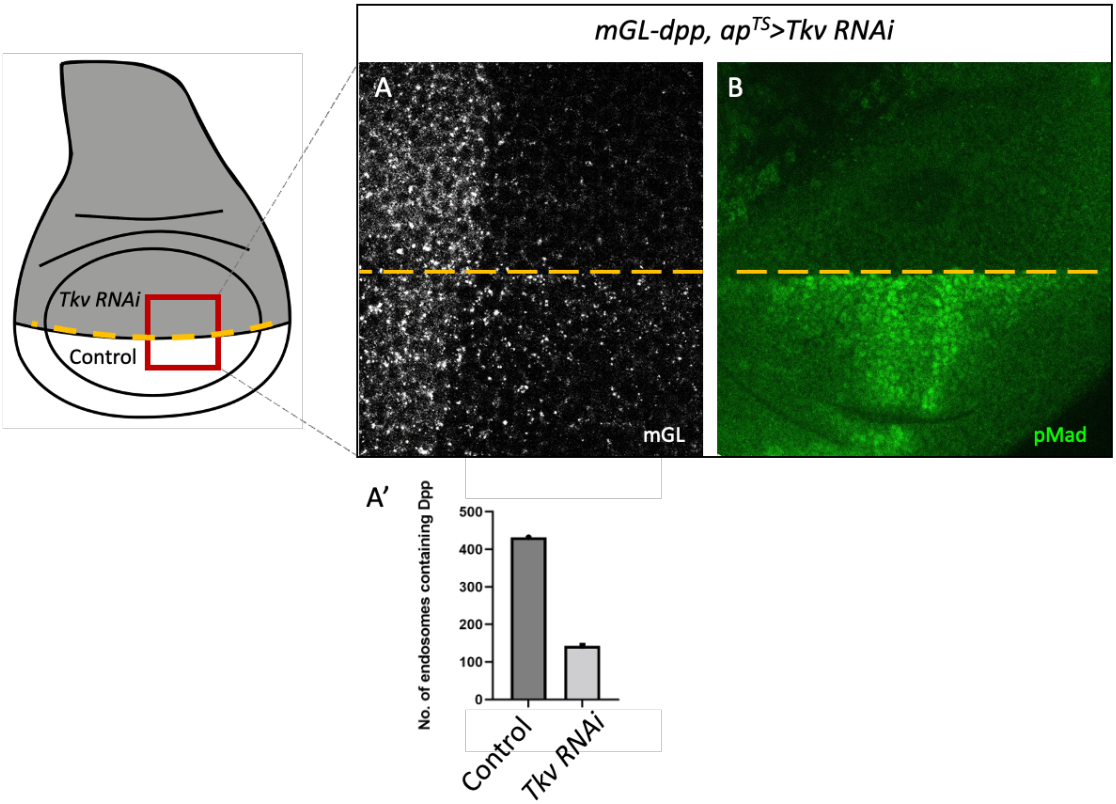

Figure 4.3: Knocking down Tkv leads to reduced number of mGL-Dpp positive puncta.
(A-A') By knocking down Tkv in the dorsal compartment of the wing imaginal disc via RNAi for 24 hours, the number of mGL-positive puncta, after acid wash was decreased. (B) Knocking down Tkv via RNAi for 24 hours led to a complete loss of pMad signal in the dorsal compartment.

4.1.3 Tkv accumulates extracellularly in the early endocytic factors

Tkv was found to be accumulated extracellularly in the wing discs in hemizygous *shi^{ts1}* flies upon 2h of heat shock at 34°C (Fig4.4, A-B), indicating that Tkv, similar to Dpp, is also internalized via dynamin-dependent endocytosis. Also, knocking down Rab5 in the dorsal compartment of the wing imaginal discs not only led to an accumulation of the extracellular ligand, but also to an accumulation of Tkv (Fig4.4, C-D). Visualizing HA-Tkv via an extracellular staining in absence of Rab5 showed that HA-Tkv accumulated in the dorsal compartment (Fig.4.4) including the apical (seen in the optical cross-sectioning in Fig.4.4, C''), lateral (Fig.4.4, C), and the basal (Fig.4.4, C') side of the disc, with the exception of the A/P boundary.

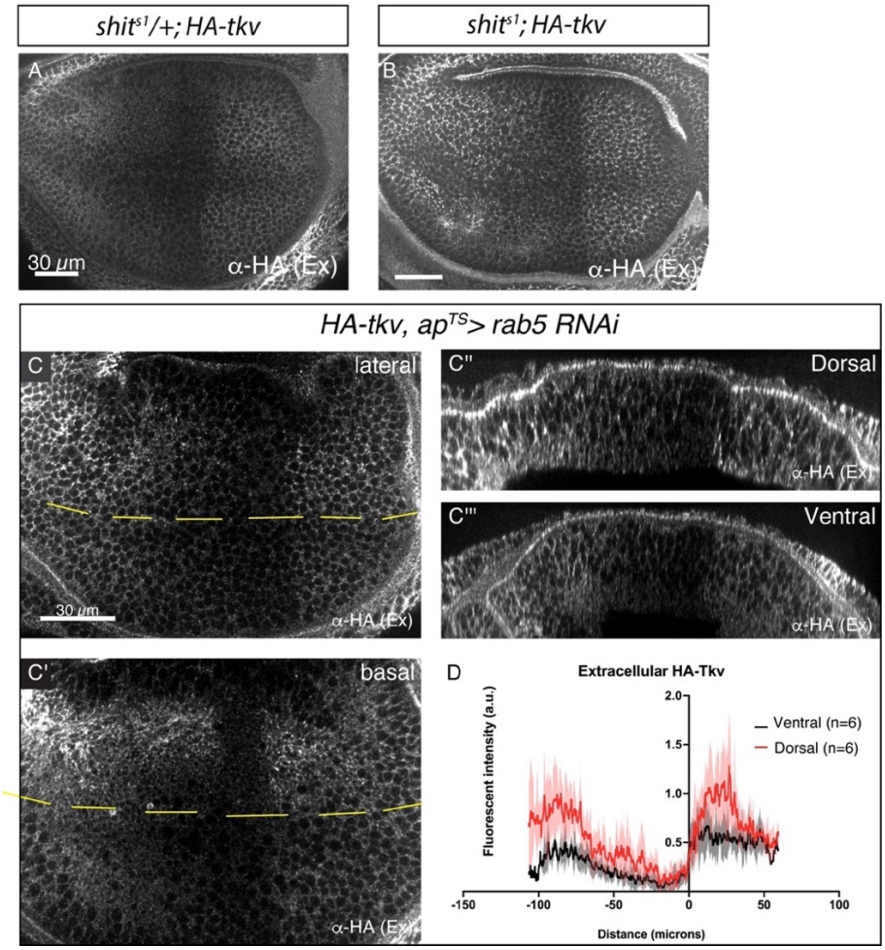

Figure 4.4: HA-Tkv accumulates extracellularly in absence of dynamin or Rab5.
(A-B) Extracellular HA staining in heterozygous (A) and hemizygous (B) shi^{ts1} flies. Knocking down Rab5 via RNAi in the dorsal compartment of the wing imaginal discs leading to an accumulation of extracellular HA-Tkv in the lateral (A) and basal (A') side of the discs. (A'') Optical cross-sectioning from the dorsal compartment, showing an accumulation of extracellular HA-Tkv in the whole tissue section, compared to (A''') showing the optical cross-sectioning from the ventral compartment used as an internal control. (B) Quantification of extracellular HA-Tkv signal intensity taken from the lateral side of the wing discs, showing an increase in signal intensity in absence of Rab5.

4.1.4 Knocking down Rab5 disrupts the lysosomal degradation pathway

Knocking down Rab5 via RNAi in the dorsal compartment of the wing imaginal disc not only showed a drastic decrease in Rab5 intensities visualized via an antibody staining against Rab5 (Fig.4.5, A), but also led to a decrease in Rab7 signal intensities observed through an antibody staining against Rab7 (Fig.4.5, A'). A decreased intensity in the late endosomal marker Rab7 points towards a decreased rate of endolysosomal fusion and lysosomal degradation.

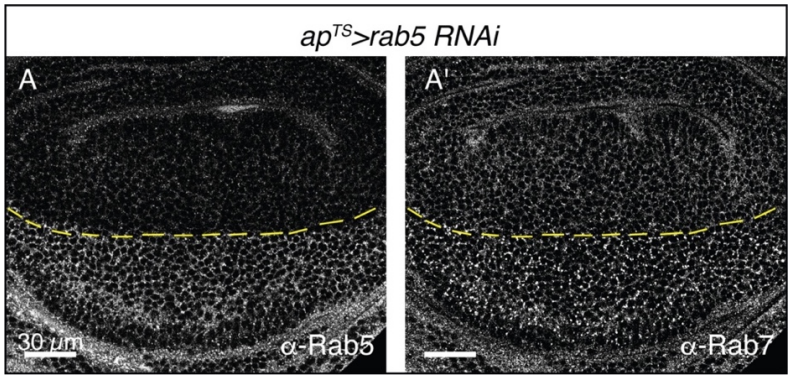

Figure 4.5: Knocking down Rab5 leads to a reduction of Rab7 signal intensity.
(A) Knocking down Rab5 via RNAi in the dorsal compartment of the wing imaginal discs leads to a drastic reduction in Rab5. (B) Knocking down Rab5 also leads to a decrease in Rab7 signal intensity, observed through an antibody staining.

Knocking down Rab5 via RNAi in the dorsal compartment of the wing discs led to an accumulation of Ubiquitin (Fig.4.6). As proteins that are fated to be degraded are ubiquitinated and are sorted into ILVs via the function of the ESCRT components and MVBs formation, knocking down Rab5 may disrupt this degradation pathway and lead to an accumulation of ubiquitinated proteins.

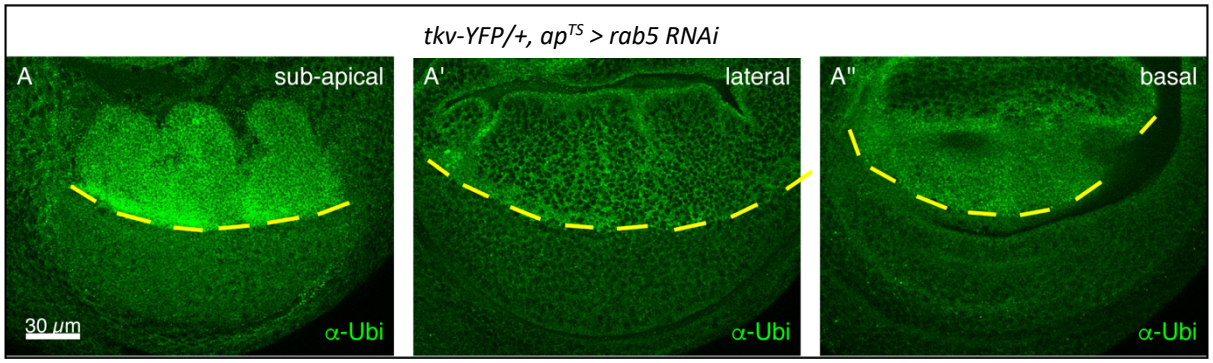

Figure 4.6: Knocking down Rab5 leads to an accumulation of Ubiquitin.
Rab5 was knocked down via RNAi in the dorsal compartment of the wing imaginal discs, and Ubiquitin was accumulated throughout the whole wing ouch, including the sub-apical (A), the lateral (A'), and the basal (A'') side.

4.1.5 Knocking down Rab5 leads to an accumulation of Spalt and Omb

Previous studies have used an antibody staining against Spalt as a measure for the Dpp signaling range, and they observed a decrease in this range when the dominant negative form of Rab5 (Rab5S43N) was overexpressed (Entchev et al., 2000). However, in this study, upon knocking down Rab5 via different RNAis, over-expressing $Rab5^{DN}$, and inducing $Rab5^{2}$ or $Rab5^{DN}$ clones, we observed an increase in pMad range and intensity. Antibody staining against pMad is an indicator for Dpp signaling activity. However, to ensure consistency of our results, we also checked the signal intensities of Omb and Spalt (Fig.4.7, A-A'). Knocking down Rab5 via RNAi in the dorsal compartment of the wing imaginal discs also led to an increase in the signal intensities from Omb (Fig.4.7, A) as well as Spalt (Fig.4.7, A').

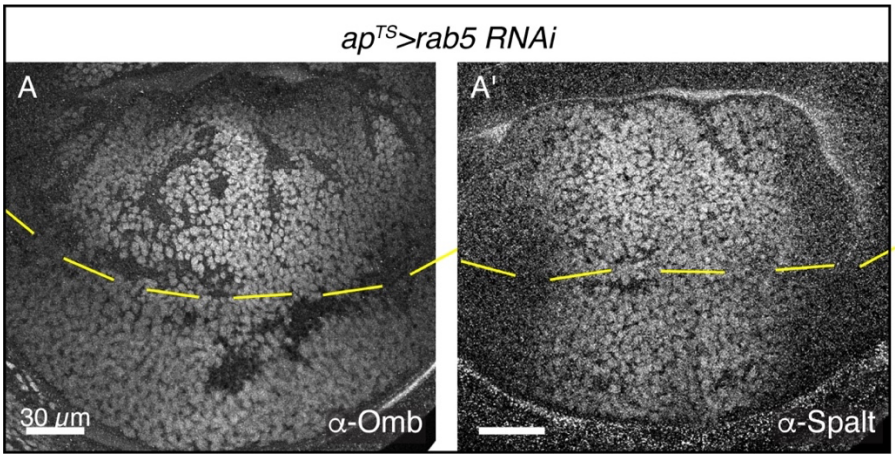

Figure 4.7: Knocking down Rab5 leads to an increase in Omb and Spalt intensities.
(A) Antibody staining against Omb showed an increase in Omb signal intensity in the dorsal compartment of the wing imaginal disc. (B) Antibody staining against Spalt showed an increase in Spalt signal intensity in the dorsal compartment.

4.1.6 Dally and Dlp accumulate upon knocking down Rab5

Dally and Dlp are glypicans known for their role in Dpp and Wg gradient formation (Akiyama et al., 2008; Han et al., 2005; Simon et al., 2023), and as cell-surface molecules, they are also internalized through cellular trafficking. Therefore, it was expected that altering the rate of endocytosis and degradation by knocking down Rab5 could lead to an accumulation of these proteins.

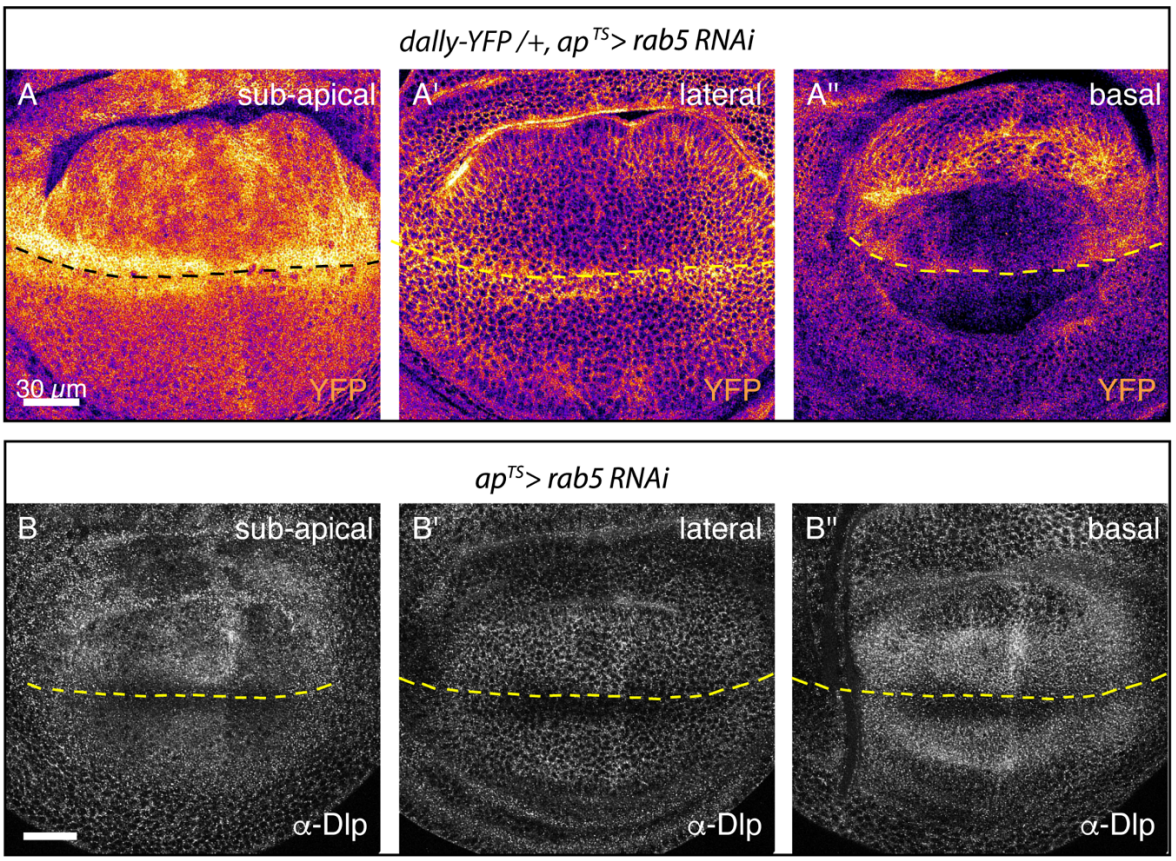

Figure 4.8: Knocking down Rab5 leads to an accumulation of Dally and Dlp.
(A-A'') Knocking down Rab5 via RNAi in the dorsal compartment of the wing imaginal discs leads to an accumulation of Dally-YFP in the sub-apical (A)region, to some extent in the lateral (A') and the basal (A'') region. (B-B'') Knocking down Rab5 via RNAi in the dorsal compartment of the wing imaginal discs leads to an accumulation of Dlp in the sub-apical (B), lateral (B') and the basal (B'') region.

To test this, we knocked down Rab5 via RNAi in the dorsal compartment and visualized an increase in Dally-YFP and Dlp signal intensities in the wing discs (Fig.4.8, A-A'', B-B''). Dally-YFP and Dlp were mostly increased in the sub-apical (Fig.4.8 A & B) and the basal (Fig.4.8, A'' & B'') region of the wing discs.

4.1.7 Increase in Dpp signaling in absence of Rab5 is independent of dally

Dally is a cells surface proteoglycan and it interacts with Dpp. The internalization of Dally via Pent has already been shown to be important in establishment of the long-range Dpp gradient (Norman et al., 2016). As we observed an accumulation of Dally in the absence of Rab5, it was of interest to know if the observed increase in Dpp signaling range and intensity in absence of Rab5 was dependent on Dally accumulation. Therefore, we knocked down Rab5, dally, and Rab5 together with dally in the dorsal compartment of the wing imaginal discs via RNAis, and compared the pMad signal intensities between the dorsal and the ventral compartments, while having the normal Dally-YFP and pMad signal as a control (Fig.4.9, A-D’’).

While the pMad gradient and intensities between the dorsal and the ventral compartment were identical in the control wing discs (Fig.4.9, A-A’’), knocking down Rab5 in the dorsal compartment led to an accumulation of Dally-YFP, as well as an increase in range and intensity of pMad (Fig.4.9, B-B’’). However, knocking down Rab5 and Dally simultaneously via RNAis in the dorsal compartment did not rescue the increase in Dpp signaling in absence of Rab5 (Fig.4.9, C-C’’). In absence of Dally and Rab5 together, the range and intensity of pMad was reduced in the lateral regions of the disc, possibly because Dpp could not reach that region in the absence of Dally, and Rab5 could not activate Dpp signaling in that region in the absence of Dpp. Also, the medial pMad intensity remained higher than the ventral compartment (Fig.4.9, C’-C’’), indicating that the absence of Dally does not prevent the increase in pMad signal intensity upon knocking down Rab5. Furthermore, knocking down Dally via RNAi in the dorsal compartment did not decrease the pMad intensity, but only led to a more restricted range of pMad in the periphery. These results suggest that the increase in Dpp signaling in the absence of Rab5 is independent of Dally.

To further verify that Dally has little role in the increase of Dpp signaling in absence of Rab5, we knocked down Rab5 via RNAi in the dorsal compartment of the wing imaginal discs that were mutant for *dally* (Fig.4.9, E-E’’). In the absence of Dally and Rab5, pMad intensities continued to be increased, suggesting that dally plays no role in the increase in Dpp signaling in absence of Rab5.

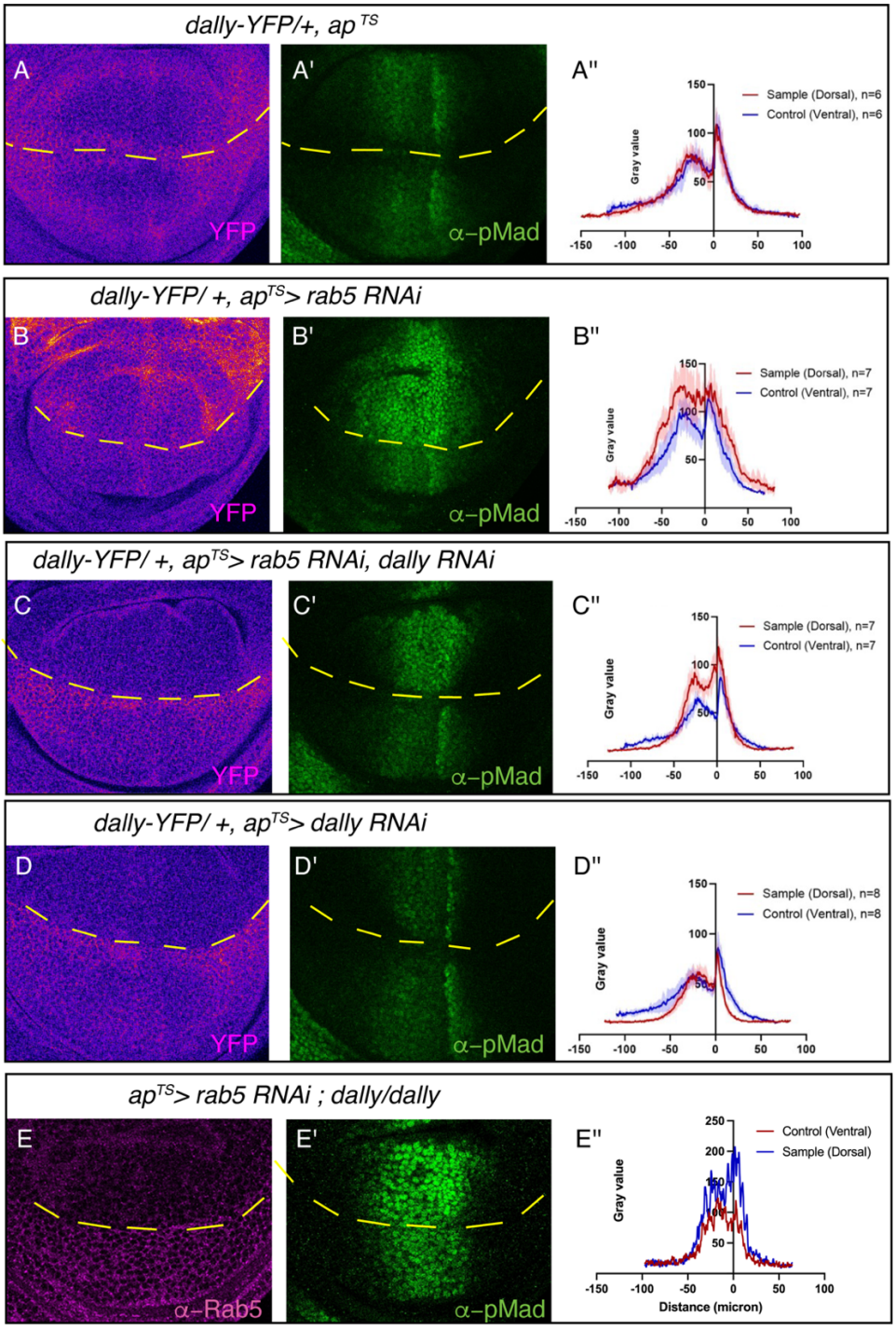

Figure 4.9: Increase in Dpp signaling activity upon knocking down Rab5 is independent of Dally.
(A-A''') Control condition showing Dally-YFP (A), pMad intensity (A') and quantification of pMad intensity in A'. (B-B'') Knocking down Rab5 in the dorsal compartment leads to an accumulation of Dally-YFP (B) and an increased pMad intensity (B'), while quantifications show an increase in pMad intensity in the dorsal compartment compared to the ventral (B''). (C-C'') Knocking down Rab5 and Dally simultaneously via RNAi leading to a decrease in Dally-YFP intensity (C), and an increase in pMad intensity (C'), and the quantification showing an increased pMad intensity in the dorsal compartment compared to the ventral (C''). (D-D'') Knocking down Dally via RNAi, showing a decrease in Dally-YFP intensity (D), a decrease in pMad range (D'), and the quantification showing the decrease in range of pMad in the dorsal compartment compared to the ventral (D''). (E-E'') Knocking down Rab5 in a dally mutant condition shows the decrease in Rab5 through an antibody staining (E), increase in pMad intensity (E'), and the quantification showing the increase in pMad intensity in the dorsal compartment compared to the ventral (E'').

4.1.8 Dpp is internalized via clathrin-mediated endocytosis

It has been proposed that Dpp is internalized via clathrin-mediated endocytosis, as absence of clathrin heavy chain and α-Adaptin led to a reduced range of Dpp-signaling activity (González-Gaitán & Jäckle, 1999). Since our findings regarding the role of Rab5 were contradicting to previous reports, to ensure the role of clathrin-mediated internalization, and clathrin-coated vesicles on Dpp, I knocked down Hsc70-4, the factor that is required for uncoating and recycling of clathrin triskelion from the early endocytosed clathrin-coated vesicles (Chang et al., 2002). Hsc70-4 is a constitutively expressed member of the Hsc70 protein family, and promotes the release of clathrin from clathrin-coated vesicles by binding to it and disrupting the clathrin cage concomitant through ATP hydrolysis (Chang et al., 2002; Schlossman et al., 1984). In absence of Hsc70-4, clathrin coated structures are completely lost and membrane protein internalization is disrupted (Chang et al., 2002).

Indeed, knocking down Hsc70-4 via RNAi in the dorsal compartment of the wing imaginal disc led to a reduction in pMad signal intensity hence Dpp signaling activity (Fig.4.10), and we can confirm that Dpp needs to be internalized via clathrin-mediated endocytosis for Dpp signaling to be initiated.

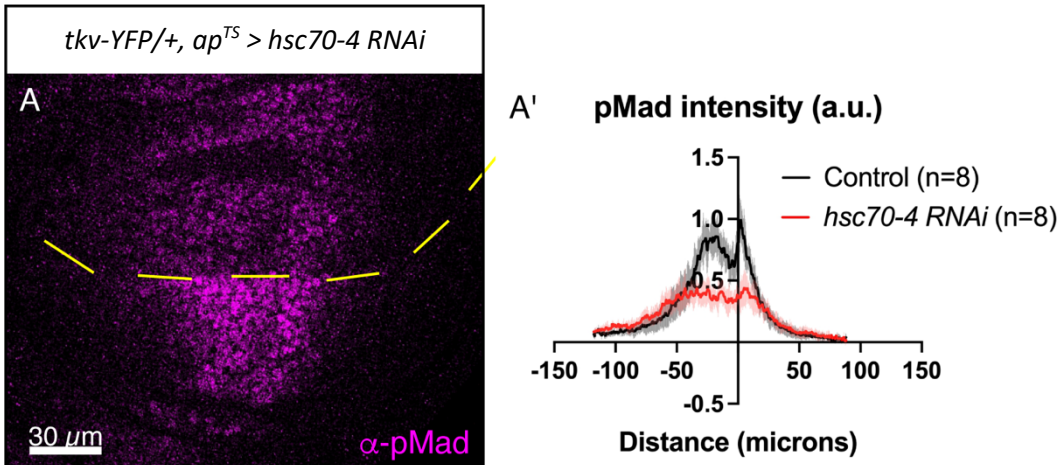

Figure 4.10: Dpp in internalized through clathrin-mediated endocytosis.
Knocking down Hsc70-4 via RNAi in the dorsal compartment of the wing imaginal disc led to reduction in pMad signal intensity and Dpp signaling activity (A-A').

4.1.9 Tkv and Ubiquitin accumulate on the early endosome in the absence of Vps4

Following up with the studies done on the role of Hrs (ESCRT-0 component) on downregulation of multiple signaling pathways (Jékely & Rørth, 2003), and the observations made in Figure 3.7, Vps4 was knocked down to study its role in sorting of Tkv. Vps4 is an AAA family ATPase, responsible for endosomal sorting of cargo into the multivesicular body for lysosomal degradation. Knocking down Vps4 via RNAi in the dorsal compartment of the wing imaginal discs, led to an accumulation of Tkv, Ubiquitin and Rab5 in puncta. (Fig.4.11, A-A'').

To have a complete overview of the cells from the apical to the basal side, optical cross-sections from the dorsal compartment of the wing pouch expressing Vps4 RNAi, and from the ventral compartment which was used as an internal control were obtained. Tkv-YFP and Ubiquitin were both accumulated throughout the tissue (Fig.4.11, C-C'), and compared to the control (Fig.4.11, B-B'''), showed a higher degree of colocalization between Tkv-YFP and Ubiquitin (Fig.4.11, C'''). Studies in yeast, HeLa cells and mouse embryos have shown that a dysfunctional ESCRT leads to an increase in Rab5 activity on the early endosomes, driving membrane accumulation and altering endosome morphology (Komada & Soriano, 1999; Raiborg et al., 2008; Raymond et al., 1992; Rieder et al., 1996; Schuh & Audhya, 2014). Consistently, knocking down Vps4 led to an increased Rab5 intensity, and a higher degree of colocalization between Rab5 and Tkv-YFP (Fig.4.11, D-D''', and E-E''').

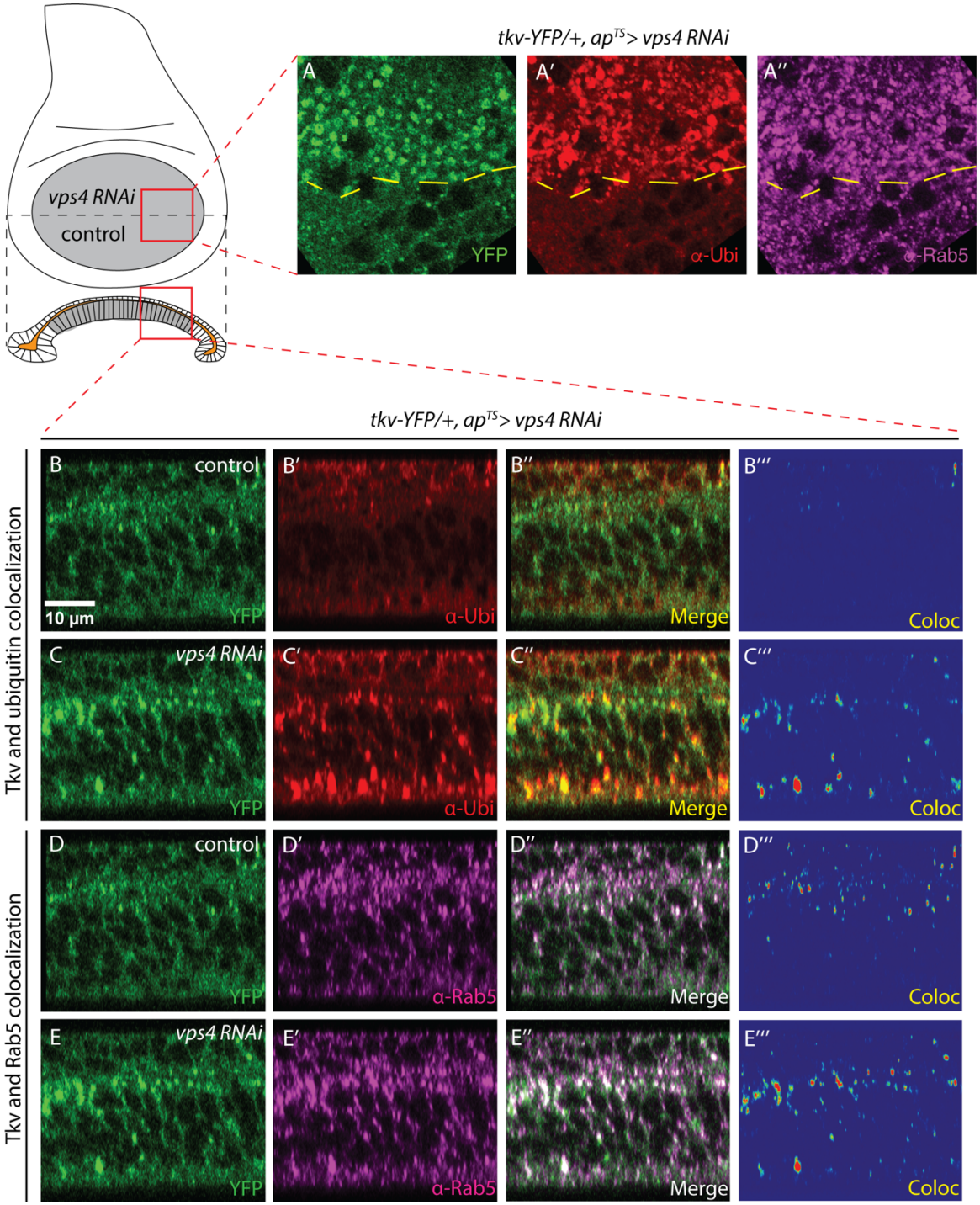

Figure 4.11: Tkv-YFP colocalizes with Ubiquitin and Rab5 when MVB formation is interrupted.
(A-A'') Knocking down vps4 via RNAi in the dorsal compartment of the wing imaginal discs leads to an accumulation of Tkv-YFP (A), Ubiquitin (A') and Rab5 (A''). (B-B''') Cross-sections from the ventral compartment used as an internal control. showing Tkv-YFP (B), Ubiquitin (B'), merged image of Tkv-YFP and Ubiquitin (B'') and the colocalization map showing colocalized spots between Tkv-YFP and Ubiquitin (B'''). (C-C''') Cross-sections from the dorsal compartment expressing vps4 RNAi, showing an accumulation of Tkv-YFP (C), Ubiquitin (C'), merged image of Tkv-YFP and Ubiquitin (C'') and the colocalization map showing colocalized spots between Tkv-YFP and Ubiquitin (C'''). (D-D'') Cross-sections from the ventral compartment used as an internal control. showing Tkv-YFP (D), Rab5 (D'), merged image of Tkv-YFP and Rab5 (D'') and the colocalization map showing colocalized spots between Tkv-YFP and Rab5 (D'''). (E-E''') Cross-sections from the dorsal compartment expressing vps4 RNAi, showing an accumulation of Tkv-YFP (E), Rab5 (E'), merged image of Tkv-YFP and Rab5 (E'') and the colocalization map showing colocalized spots between Tkv-YFP and Rab5 (E''').

4.2 Effects of re-localization of Smad to the cell membrane

Upon contact with an activated type-I receptor, Smad (*Drosophila* Mad) becomes phosphorylated and is re-localized into the nucleus for activation or inactivation of downstream target genes. With the availability of the endogenously tagged form of *Drosophila* Mad with GFP (gift from Prof. Brian McCabe) and the nanobody-based toolset for re-localizing proteins (Harmansa et al., 2017), it was of interest to know if Mad is able to become phosphorylated if re-localized to the cell membrane, where it can come in closer contact to Dpp receptors.

In order to do so, we applied GrabFP (Intra), which consists of a nanobody specifically recognizing GFP (vhhGFP4), and the mouse CD8 transmembrane protein, designed such that the nanobody is presented intracellularly along the cell surface (Fig.4.12, A) (Harmansa et al., 2017). GrabFP (Intra) was expressed in the dorsal compartment of the wing imaginal discs using the *ap-Gal4* driver, and the ventral compartment was used as an internal control (Fig.4.12, B). Expression of GrabFP (Intra) in flies heterozygous for GFP-Mad, led to a relocalization of GFP-Mad, and the ubiquitous GFP signal was re-localized to the cell membranes (Fig.4.12, B'). Subsequently, the pMad signal expanded but the expanded pMad was found outside of the nucleus (Fig.4.12, B''). To ensure the absence of a bleed-through from the mCherry signal into the pMad channel during image acquisition at the microscope, some of the wing discs were imaged without the addition of a secondary antibody for pMad (Fig.4.12, C-C''). When homozygous *Mad-GFP* was re-localized using GrabFP (Fig.4.12, D-D'''), no nuclear pMad signal was observed in the nucleus (Fig.4.12, D''), and the dorsal compartment was smaller, consistent with the idea that pMad acts in the nucleus to control growth. By having a closer look, the pMad signal was observed in small puncta (Fig.4.12, D'''), indicating that Mad is able to become phosphorylated when re-localized to the cell membrane, but in the presence of GrabFP, it cannot be translocated to the nucleus (Fig.4.12, D''').

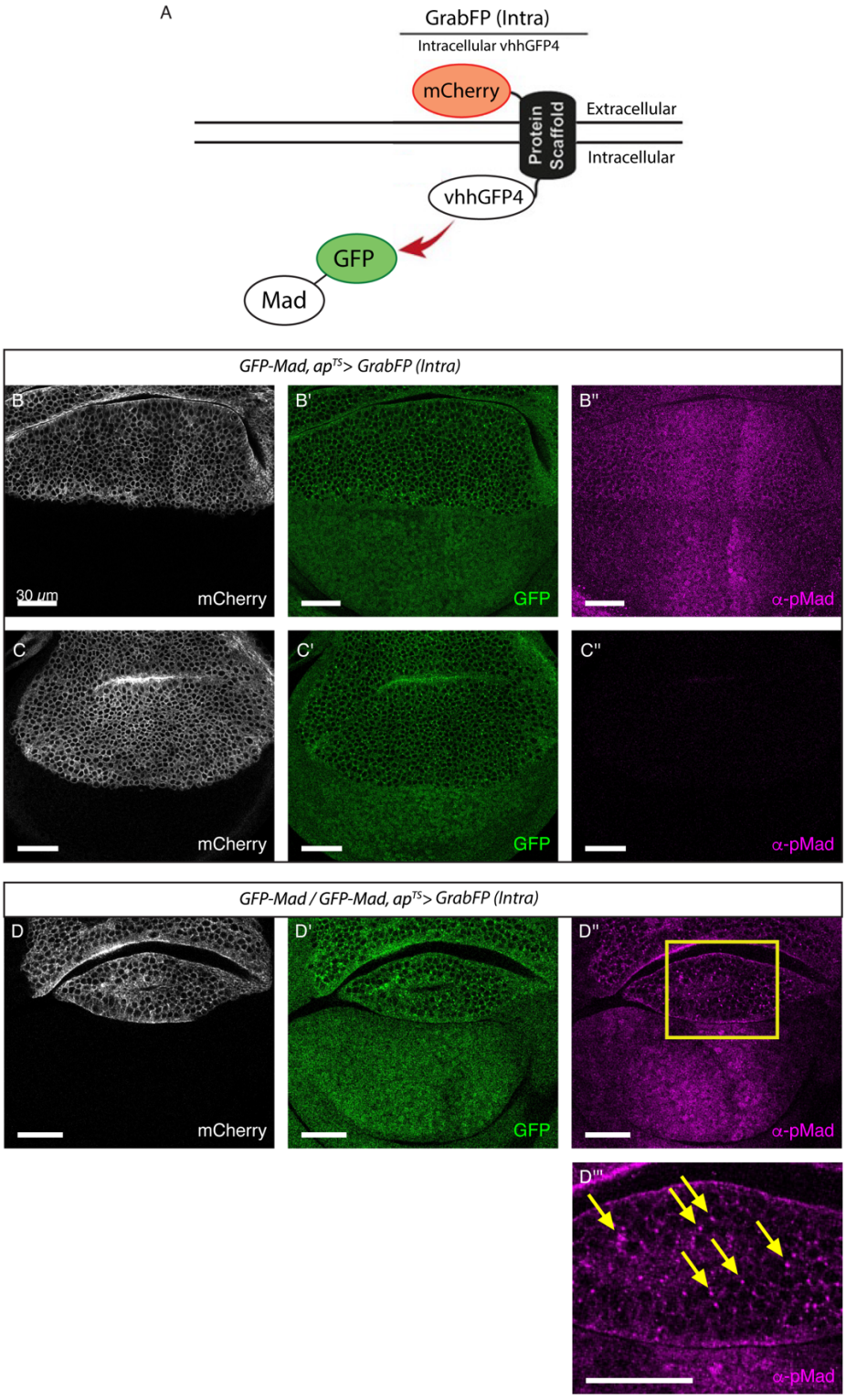

Figure 4.12: Re-localizing one copy of Mad to the cell membrane leads to an increase in membranous pMad. *(A) Illustration of GrabFP (Intra) with the mCherry tag. (B-B'') Expression of GrabFP (Intra) tagged with mCherry in the dorsal compartment (B) leads to relocalization of GFP-Mad to the inner cell membrane (B') and a general increase in membranous pMad signal (B''). (C-C'') Similar to (B-B''), except no secondary antibody was added for pMad staining (C'') to ensure the absence of a bleed-through from the mCherry signal into the channel observing pMad. (D-D'') Expression of GrabFP (Intra) tagged with mCherry in the dorsal compartment (D), and re-localizing GFP-Mad in a homozygous condition (D') leads to a reduction in the dorsal compartment's size and a complete absence of nuclear pMad signal (D''), while the pMad signal is observed in small puncta (D'''). GrabFP (Intra) was expressed for 24h prior to dissection and fixation of the wing discs.*

The fact that re-localizing Mad-GFP to the cell membrane via GrabFP (Intra) led to puncta signal from pMad was surprising, as we were expecting to observe only a membranous pMad signal. However, membranous proteins, including GrabFP (Intra) containing the CD8 transmembrane protein may constantly be internalized into cells via the trafficking machinery, and as endosomal compartments are derived from the cell membrane, presence of GrabFP/pMad on endosomal compartments can be expected. It was therefore of interest to know if Mad was becoming phosphorylated on the endosomes, and if so, on which endosomes. However, technical limitations from the image acquisition and microscopy could not allow us to use GrabFP (Intra) tagged with mCherry for this experiment as all the available channels for acquisition were occupied.

Therefore, we decided to replace the mCherry tag from GrabFP (Intra) with a V5 tag (Fig.4.13, A), making it possible to add additional stainings for endosomal markers and study colocalization between the endosomal markers and pMad. As indicated in Fig.4.13, the V5 tagged form of GrabFP (Intra) expressed in the dorsal compartment of the wing imaginal disc was able to re-localize Mad-GFP to the cell membrane (Fig.4.13, B'') in flies heterozygous for *mad-GFP* and the pMad signal intensity was slightly increased throughout the whole dorsal compartment (Fig.4.13, B').

Re-localizing Mad-GFP to the cell surface in flies homozygous for *mad-GFP* via GrabFP (Intra) with a V5 tag also led to a puncta signal from pMad (Fig.4.13, C). By co-staining these discs for Rab5 and Rab7, the colocalization between pMad and the early and late endosomal markers were analyzed (Fig.4.13, D-D''& E-E''). The Rab5 and the puncta pMad signal were highly colocalized (Fig.4.13, D-D'', white arrowheads), indicating that Mad is being phosphorylated on the early endosomes marked by Rab5 when re-localized using the GrabFP (Intra). Furthermore, the antibody staining against Rab7 indicated that majority of the puncta pMad signal was not colocalized with Rab7 (Fig.4.13, E'', yellow arrowhead). Although to a lower extent than Rab5, pMad was also occasionally colocalized with Rab7 (Fig.4.13, E'', white arrowhead), which could indicate that Mad may be able to be phosphorylated on the maturing/late endosome.

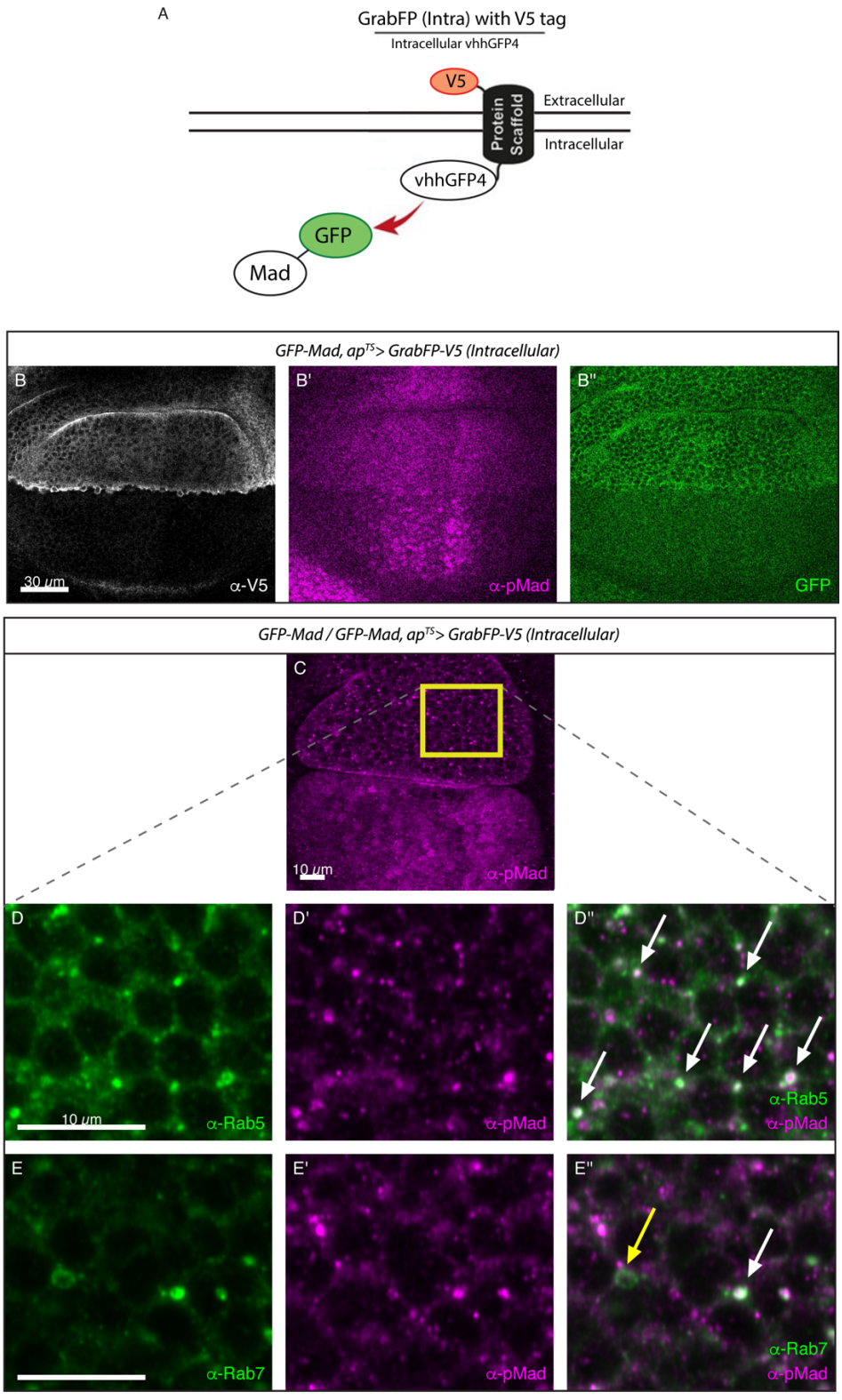

Figure 4.13: Puncta pMad signal colocalizes with Rab5.
(A) Illustration of GrabFP (Intra) with the V5 tag. (B-B') Re-localizing GFP-Mad in flies heterozygous for GFP-Mad with GrabFP (Intra) with the V5 tag in the dorsal compartment of the wing discs (B) also leads to a slight increase in the pMad signal (B'). (C) Trapping GFP-Mad in flies homozygous for GFP-Mad leads to a smaller dorsal compartment and pMad no longer has a nuclear signal, and is observed in small puncta. (D-D'') The puncta signal from pMad observed in higher magnification and resolution, showing a high degree of colocalization between the puncta pMad signal and Rab5 (white arrow heads). (E-E'') The puncta signal from pMad showing a lower degree of colocalization with Rab7 (white arrow head), and at points, completely avoiding each other (yellow arrow head).

5 Discussion

5.1 Summary of results

Since the discovery of morphogens and their ability to provide positional information, developmental biologists have extensively studied the mechanisms by which morphogens form gradients in developing tissues. Through the years, several mechanisms have been proposed to be involved in the establishment of extracellular morphogen gradients, including extracellular ligand diffusion, receptor binding, internalization, recycling, and intracellular degradation (Wartlick et al., 2009). Cellular trafficking plays an important role in possibly all of the above mechanisms, as trafficking factors are required for exocytosis and secretion of the ligand, internalization of the receptor/ligand complexes, recycling the factors back to the cell membrane or the extracellular space, and degrading ligand/activated receptors. These mechanisms are not necessarily similar amongst different morphogens or organisms. For example, although Dpp is one of the best and longest studied morphogens, the role that cellular trafficking plays in its gradient formation and signaling remains unclear.

In this thesis, I used novel genetic tools to investigate the role of cellular trafficking on the intra- and extracellular Dpp gradient in *Drosophila* wing imaginal discs. In addition, I have explored the role of these factors in Dpp signaling activation and termination. With the generation of endogenous *mGL-dpp* and *mSC-dpp* alleles, it has become possible to study the endogenous Dpp localization intra- and extracellularly. By utilizing different eYFP-tagged-Rab proteins as markers, I found that mSC-Dpp was localized on different endosomal compartments (Chapter 3-Fig.1). These endosomes included but were not limited to the early endosomes (marked with Rab5), the maturing/late endosomes (marked with Rab7), and the recycling endosomes (marked with Rab4 for fast recycling, and Rab11 for slow recycling).

In order to know what role these endosomes were playing in Dpp signaling activity, their endosomal Rab “markers” were knocked down via RNAi in the dorsal compartment of the wing imaginal discs, and the pMad levels were compared to that of the ventral compartment (internal control). Knocking down the late and the recycling endosomal markers did not affect Dpp signaling activity, and only minimally affected the extracellular Dpp gradient. However, knocking down Rab5 led to an increase in the intensity and the range of the pMad gradient, indicating an increase in Dpp signaling activity (Chapter 3-Fig.3). This observation was

surprising, as it was contradicting with previous reports where over-expression of dominant negative form of Rab5 led to a decrease in Dpp signaling range (Entchev et al., 2000). To ensure the consistency of this observation, Rab5 was knocked down/ knocked out using several different methods, all of which showed an increase in Dpp signaling activity. Also, this phenotype was dependent on Dpp and was not caused by an increase in Dpp expression levels (Chapter 3-Fig.4).

It was of interest to assess the role of Dpp distribution on Dpp signaling activity, as knocking down Rab5 also led to an accumulation of extracellular Dpp on the basolateral side of the wing imaginal disc, along the Dpp-producing cells (Chapter 3-Fig.4). However, it has been assumed in the field that Rab5, the marker for the early endosome is required for internalization to take place. So how could knocking down Rab5 which led to an accumulation of Dpp extracellularly, also lead to an increase in Dpp signaling activity? By analyzing pMad intensities in wing discs mutant for Dynamin GTPase (shi^{ts1}), it was ensured that Dpp indeed needs to be internalized for its signaling activity to be initiated. It was also demonstrated that in the absence of Rab5, internalization was still taking place, although possibly at a lower rate (Chapter 3-Fig.4).

Since knocking down Rab5 also led to an accumulation of Tkv, prolonged activation and continuation of signaling from the internalized receptors was a possibility for the increased Dpp signaling activity. Since degradation/formation of the late endosome is hindered in Rab5 knockdown condition and the Ubiquitin signal is also accumulated, indicating that ubiquitinated cargo is not degraded (Fig.4.5, Fig.4.6), the internalized and activated receptors could remain active on the early vesicles. Therefore, artificial removal of the receptor could rescue the increase in Dpp signaling in absence of Rab5. In order to assess this, deGradHA, was used to remove one copy of the receptor Tkv-HA-eGFP. Degrading one copy of the receptor rescued the Rab5 knock down phenotype (Chapter 3-Fig.5). These results suggested that Rab5-mediated trafficking is required to shut off activated Tkv.

Furthermore, it was found that Dpp signaling is shut down prior to the formation of the late endosome, as knocking down/knocking out Rab7 did not affect pMad signal intensities. This also did not have any effect on the extracellular mGL-Dpp gradient, nor did it drastically affect the intracellular mGL-Dpp signal (Chapter 3-Fig.6).

As the early endosome matures into the late endosome, intra-luminal vesicles (ILVs) are shaped from the membrane of the early endosome, giving the distinct multi-vesicular body (MVB) characteristic to the late endosome. Formation of the ILVs is mostly directed through ESCRT components that recognize the Ubiquitin signal from the cargo that is destined for degradation. It had been reported that Hrs, a member of ESCRT-0 is responsible for shutting down multiple signaling receptors, including Tkv (Jékely & Rørth, 2003). Following up on this observation, knocking down different ESCRT components, including TSG101, Shrub and Vps4, showed an increase in Dpp signaling activity. Tkv and Ubiquitin were accumulated in these conditions, and the two showed a higher degree of colocalization (Chapter 3-Fig.7). The intracellular mGL-Dpp was also accumulated and showed a larger puncta signal in the apical and basal side of the wing discs, while the extracellular mGL-Dpp gradient was not affected. These results indicated that formation of MVBs are essential for shutting down Dpp signaling activity, likely through internalization of the activated and ubiquitinated Tkv into the ILVs on the maturing endosome, prior to its transformation into the late endosome.

In summary, the study in this thesis shows that, unlike the previous indications that Rab5 is required for Dpp signaling to be initiated and, in its absence, the Dpp signaling range is reduced, could not be confirmed. Rather, Rab5 is required to shut down Dpp signaling, most likely through degradation of the activated receptor, and the absence of Rab5 leads to an accumulation of the extracellular Dpp along the Dpp-producing cells.

5.2 Role of endocytic trafficking in extracellular Dpp gradient formation

Different studies investigating the role of cellular trafficking on Dpp distribution and gradient formation have been conducted. In one model, trafficking factors have been proposed to expand the long-range Dpp gradient. One study illustrated that Dpp in the wing imaginal discs is internalized through clathrin-mediated endocytosis, and upon aberrant function of clathrin heavy chain and its adaptor protein α-Adaptin, the range of Dpp signaling activity is reduced (González-Gaitán & Jäckle, 1999). Another study proposed a receptor-mediated transcytosis model for formation of the long-range Dpp gradient in *Drosophila* wings (Entchev et al., 2000). In the receptor-mediated transcytosis model, the ligand is bound to the receptor, internalized inside the receiving cells, is trafficked intracellularly and released to signal the next cells, which in turn also internalizes and releases it as well. In the study by Entchev et al. (2000), the endocytosis-defective *shi*^{ts1} cells impaired Dpp progression, Rab5 dominant-negative cells

showed a reduced Dpp signaling range, and overexpression of Rab7 leading to an increased rate of lysosomal degradation led to a shortened Dpp signaling range, supporting their receptor-mediated transcytosis model (Entchev et al., 2000).

However, other studies have refuted the receptor-mediated transcytosis model (Belenkaya et al., 2004; Lander et al., 2002), and proposed the restricted extracellular diffusion mechanism for formation of the Dpp gradient. In the latter case, Dpp is proposed to bind to the its receptors on the cell surface for internalization and subsequent degradation. One study illustrated that Dpp movement is not hindered in absence of dynamin, and that dynamin is required for initiation of Dpp signaling activity (Belenkaya et al., 2004). They rather suggested that Dpp movement is regulated via the heparan sulfate proteoglycan (HSPG) Dally and Dlp, and proposed the restricted extracellular diffusion model, in which Dpp movement requires its interaction with HSPGs (Belenkaya et al., 2004). Later, by observing Dpp and its signaling activity behind clones of cells that were mutant for Tkv, Schwank et al. (2011) also argued against the receptor-mediated transcytosis model. They favored the restricted diffusion model, and suggested that the receptor-independent transcytosis has not yet been studied and could be a possible mechanism for Dpp transport.

Recently, the transcytosis model has re-emerged, this time independently of the receptor (Romanova-Michaelides et al., 2022). In this study, by utilizing the nanobody binding assay, the authors proposed that Dpp is endocytosed without its receptor Tkv, but through Dally and Pentagone. They also suggested that Dpp is recycled and re-exocytosed via the function of Rab4 and Rab11, and that this recycling is required for scaling of the Dpp gradient (Romanova-Michaelides et al., 2022).

In this study, we re-evaluated the role of different trafficking factors on formation of the extracellular Dpp gradient by utilizing the endogenously tagged alleles of *dpp*, *mGL-dpp* and *mSC-dpp*. We show that dynamin is a major regulator in shaping the extracellular Dpp gradient, and consistent with Belenkaya et al. (2004), in absence of dynamin, Dpp distribution is increased in the whole disc (Chapter 3-Fig.4 & Chapter 3-Fig.S1). In the absence of dynamin, Dpp no longer forms a conventional morphogen gradient, with the ligand concentrations being highest close to the source, and decreasing further away from the producing cells. In the absence of dynamin, Dpp concentration is rather higher in the lateral side of the disc that is further away from the source, and a lower concentration is observed closer to the producing

cells. This could be due to the expression pattern of the receptor. BMP receptors have been thought to be constitutively internalized and in absence of dynamin-mediated endocytosis, receptors have been found to be accumulated on the surface of the receiving cells (Hartung et al., 2006). As Tkv has a high binding affinity to Dpp, and is also accumulated in the absence of dynamin (Fig4.4, A-B), it can strongly bind Dpp and form such a gradient.

We also show that in the absence of Rab5, the extracellular Dpp accumulated, especially in the basolateral side of the cells close to the source (Chapter 3-Fig.4, C-E). This pattern of Dpp accumulation may also be due to the expression pattern of Tkv, as in absence of Rab5, Tkv also accumulated extracellularly in the apical and basolateral side (Fig.4.4). Extracellular Dpp may also be accumulating to a lower extent in the apical side, however, due to the difficulty of the quantification, this cannot be validated. These observations support the importance of the early endocytic factors in formation of the morphogen gradient. However, our observation was contradictory to that of Entchev et al. (2000), as they reported that Rab5 is required for formation of the long-range Dpp gradient. We show that in absence of Rab5, Dpp levels are not reduced, but rather expanded and Dpp still forms its long-range gradient. Based on our findings from dynamin and Rab5-defective discs, the receptor-mediated transcytosis model is unlikely to be the underlying mode of transport for Dpp. Our findings rather support the restricted extracellular diffusion model in which, the early endocytic factors are helping to shape the extracellular Dpp morphogen gradient by internalizing the bound Dpp to Tkv into the receiving cells. Indeed, disrupting the early endocytic factors leads to an accumulation of Tkv on the cell surface, leading to a disruption of the extracellular Dpp gradient.

Dynamin and Rab5 have also been shown to play a role in trafficking of other morphogens. For example, Hh also goes through dynamin- and Rab5-mediated endocytosis, and is accumulated apically when these factors are disrupted (Callejo et al., 2011). The function of Dynamin and Rab5 are also required for internalization of Wg, and in their absence, distribution of the extracellular Wg is expanded (Seto & Bellen, 2006).

On the other hand, we showed that the late endocytic factors play a minor role in shaping the extracellular Dpp gradient. Our findings indicated that knocking down the ESCRT components TSG101, Shrub and Vps4, as well as Rab7 did not affect the extracellular gradient (Chapter 3-Fig.6 & Fig.7). It has also been shown that knocking down ESCRT components and Rab7 also does not alter the extracellular Wg gradient (Marois et al., 2006; Rives et al., 2006).

We also observed that knocking down Rab11 and interfering with the function of slow recycling did not alter the extracellular Dpp gradient. While, knocking down Rab4, the marker for fast recycling minimally affected the extracellular gradient and led to a slight reduction in the extracellular gradient in the basal side of the discs (Chapter 3-Fig.8). According to the recent study by Romanova-Michaelides et al. (2022), suggesting that Dpp is recycled and re-exocytosed via Dally through the function of Rab4 and Rab11, we would have expected to observe a much lower extracellular Dpp gradient and defects in Dpp signaling activity in our experiments. However, Romanova-Michaelides et al. (2022) did not investigate the role of endocytic factors in the extracellular Dpp gradient, and mainly observed the reduction in the intracellular GFP-Dpp. It is possible that the endogenous levels of mGL-Dpp are not altered upon knocking down recycling factors, while the overexpressed GFP-Dpp in their experimental setup could show an aberrant phenotype, as the overexpression of GFP-Dpp is estimated to produce 400 times higher levels than the physiological level (Romanova-Michaelides et al., 2022). Nevertheless, to be able to make a concrete statement about the role of recycling in Dpp gradient formation, we need to knockdown Rab4 and Rab11 simultaneously. Knocking down only one of the factors does not necessarily terminate recycling all-together, as compensatory mechanisms can ensure that recycling still occurs through the other factor.

5.3 Role of endocytic trafficking in intracellular Dpp gradient formation

With the generation of the endogenously tagged *mGL-dpp* and *mSC-dpp*, we were able to follow the intracellular Dpp localization in endogenous conditions (Chapter 3-Fig.1). As intracellular mSC-dpp was observed to be colocalized with different endosomal markers, including Rab5, Rab7, Rab4 and Rab11 (Chapter 3-Fig.2), we decided to study the role of these endosomal compartments in regulating and shaping the Dpp gradient. We knocked down each of these endosomal markers via expression of RNAis against them in a temporally controlled manner, as expression of the RNAis for a prolonged period of time could have caused lethality.

We knocked down the early endosomal marker Rab5, which prevented the formation of the early endosomes and led to a reduction in the number of mGL-dpp positive puncta in the lateral side of the discs. However, there was an accumulation of early vesicles that were positive for mGL-Dpp in the most basal region of the wing pouch (Chapter 3-Fig.4, I-J), indicating that in the absence of Rab5, internalization is still taking place. mGL-Dpp is still able to be endocytosed, but in the absence of Rab5, the early endocytosed vesicles are unable to

fuse together with the early endosome and accumulate close to the cell surface. We ensured that the observed signal was only from the internalized mGL-Dpp by following the acid wash protocol to remove extracellular molecules prior to sample fixation (Romanova-Michaelides et al., 2022). Our observation demonstrated that the long-range Dpp gradient can still be shaped in absence of Rab5.

Knocking down the late endosomal marker Rab7 did not lead to any noticeable change in the intracellular mGL-Dpp gradient (Chapter 3-Fig.6), even though the majority of Dpp (observed through mSC-Dpp) was seen to be colocalized with Rab7 (Chapter 3-Fig.2, B-B’’’). It must be noted that Rab7 is not only the marker for the late endosome, but Rab7 is constantly replacing Rab5 on the maturing endosome. It is possible that the high degree of colocalization of mSC-Dpp with Rab7 could be on the maturing endosome. As knocking down Rab7 does not prevent the formation of the multi-vesicular bodies (MVBs) (Vanlandingham & Ceresa, 2009), it is possible that we do not observe an accumulation in mGL-Dpp because it is being sorted into and degraded in the MVBs via its receptors. Indeed, when disrupting the MVB formation by knocking down Vps4, we observed an accumulation of the intracellular mGL-Dpp (Chapter 3-Fig.7). In absence of Vps4, mGL-Dpp was accumulated in puncta in apical and basolateral regions in the discs, demonstrating that MVB formations may be required to degrade mGL-Dpp.

Lastly, we studied the role of the recycling endosomes in the intracellular mGL-Dpp distribution. The recycling endosomes have already been found to play a role in Wg and Hh distribution (Linnemannstöns et al., 2020; Pizette et al., 2021). In the case of mGL-Dpp, we observed that knocking down Rab4, the marker for fast recycling did not affect the intracellular mGL-Dpp gradient, while knocking down Rab11, the marker for slow recycling led to an accumulation mGL-Dpp in enlarged puncta (Chapter 3-Fig.8). The accumulated mGL-Dpp seen in the absence of Rab11 is possibly located in enlarged early endosomes, as preventing recycling leads to aberrant early endosomal structures (Fasano et al., 2018). It is also known that Rab11 plays a role in centrosome function during cytokinesis, and its absence can lead to inhibition of centrosome movement towards the cytokinetic bridge, resulting in daughter cells prone to being binucleated and/or having supernumerary centrosomes (Emery et al., 2005; Krishnan et al., 2022; Riggs et al., 2003). It has been reported that Sara endosomes associate with the spindle machinery to segregate a cell into two daughter cells (Bökel et al., 2006). The

Sara endosomes also contain Dpp and Tkv, to ensure the daughter cells inherit equal amount of signaling molecules and retain the Dpp signaling levels of the mother cell (Bökel et al., 2006). If cytokinesis in absence of Rab11 is disrupted, one reason why we see an accumulation of mGL-Dpp in enlarged puncta in the cells could be due to aberrations in Sara endosomes containing mGL-Dpp. Nevertheless, accumulation of mGL-Dpp in the absence of Rab11 indicates that the slow recycling endosome plays a role (either directly or indirectly) in regulating internalized Dpp, while not affecting the extracellular gradient nor Dpp signaling activity.

Both of our observations were contradictory to the reports by Romanova-Michaelides et al. (2022), which reported that Dpp is recycled via Rab4 and Rab11, and observed a drastic reduction in the intracellular GFP-Dpp in the absence of either Rab4 or Rab11. The discrepancy in the observations could either be due to the difference in experimental setups, or differences in observed locations in the wing discs. In the study by Romanova-Michaelides et al. (2022), the authors were over expressing GFP-Dpp in the Dpp-producing cells (*dppLG>LOP-eGFP-dpp*) while knocking down Rab4/Rab11 via RNAi only in the posterior compartment (via *enGal4* driver), and comparing the GFP-Dpp signal to the control (*dppLG>LOP-eGFP-dpp*). In our experimental setup, we studied the endogenous expression of *mGL-dpp*, and used the *apGal4* driver to knock down Rab4/Rab11 in the dorsal compartment, while comparing it to the ventral compartment as an internal control. Also, the majority of mGL-Dpp positive puncta are located in the basal side, and they may have been missed by Romanova-Michaelides et al. (2022) if the focus was only put on the lateral side of the wing discs.

5.4 Role of endocytic trafficking in Dpp signaling activity

Endocytic trafficking does not only influence the shape of morphogen gradients, but also regulates the activity of signaling pathways, meaning it can contribute to either activation and/or termination of signaling. It can also modulate receptor presentation at the cell surface, and provide a localized environment where signaling can take place (Piddini & Vincent, 2003). In this study, we also focused on studying the role of endocytosis on Dpp signaling activation and termination.

5.4.1 Role of early endocytic factors in Dpp signaling

It had been proposed that dynamin and clathrin-mediated internalization are required for Dpp signaling initiation (Belenkaya et al., 2004; González-Gaitán & Jäckle, 1999). We confirmed that the very early endocytic factors, including dynamin and clathrin, are indeed required for initiation of Dpp signaling activity (Chapter 3-Fig.3, A-C and Fig.4.10), indicating that Dpp needs to be internalized for its signaling activity to be initiated. However, Rab5, the marker of the early endosome that is required for fusing the early endocytosed vesicles together with the early endosome might not be essential for signal initiation.

Previous studies investigating the role of Rab5 in Dpp signaling range had speculated that in the absence of Rab5, endocytosis does not take place, and that Dpp signaling activity cannot be initiated in the absence of the early endosome (Moreno et al., 2002). In one study, the dominant negative form of Rab5 (blocked in the inactive GDP-bound state) was over-expressed in the posterior compartment of the wing imaginal discs, and an antibody staining against Spalt, a target gene of Dpp signaling pathway, showed a decrease in the range of Spalt (Entchev et al., 2000).

In another study investigating the mechanisms of cell competition, it was shown that inducing $Rab5^{DN}$ clones in the wing imaginal discs led to an increase in expression of the Dpp transcriptional repressor Brk. The authors argued that cells compete for Dpp to prevent apoptosis, which is triggered by Brk upregulation followed by JNK activation, and in the absence of a functional Rab5, Dpp cannot be endocytosed to initiate Dpp signaling (Moreno et al., 2002).

However, these statements were challenged by other reports. Several studies have reported that in absence of Rab5, internalization can still take place. Electron microscopy results from studying internalization of yolk proteins inside oocytes in *Drosophila* has shown that in the absence of Rab5, endocytosis still occurs; early endocytic vesicles can still be formed and are accumulated inside the cells, predominantly below the plasma membrane (Morrison et al., 2008). These vesicles can uncoat their clathrin coat, but nevertheless cannot fuse with other vesicles to form the later endocytic structures (Morrison et al., 2008). In Rab5S43N Drosophila synapses, an accumulation of early vesicles has also been observed (Wucherpfennig et al., 2003). Consistently, overexpressing rab5ile133, a Rab5 mutant protein defective in GTP

binding in cultured mammalian cells resulted in a 50% decrease in endocytosis rate as well as an accumulation of small vesicles at the periphery of the cells due to their inability to fuse efficiently with the early endosome (Bucci et al., 1992).

In our study, we observed an increase in pMad signal intensity and range in the absence of Rab5. To ensure the consistency of our results, we knocked down Rab5 using RNAis and the dominant negative form, and also analyzed *rab5*^{2} null mutant clones, and all these experimental approaches showed the same result (Chapter 3-Fig.3, D-K). The possible reasons why the previous studies were showing contradicting findings to ours could be that they knocked down Rab5 over a long period of time, leading to aberrant observations due to cell death. Rab5 is an important and a general factor in cellular trafficking, and when knocked out for too long, it can affect many cellular processes and be lethal. Therefore, in this study, we utilized tub-Gal80TS to temporally control the expression of Rab5 RNAis.

Our observations also indicated that in the absence of Rab5, mGL-Dpp cannot be observed in endosomes in the lateral side of the wing pouch, but rather in small vesicles in the most basal side of the disc (Chapter 3-Fig.4, I-J). The fact that both mGL-Dpp and Tkv-YFP were accumulated in early vesicles in the basal side of the discs suggest that the ligand and the receptor are able to be internalized, and in the absence of Rab5, both are accumulated in the early vesicles. This observation, together with our results demonstrating that knocking down Rab5 also leads to a decrease in the formation of the late endosomes (Fig.4.5), and that the ubiquitinated cargos destined to be degraded were also accumulated (Fig.4.6) could explain why Dpp signaling activity initiates and remains active in the absence of Rab5.

To evaluate if the increased Dpp signaling levels in the absence of Rab5 was due to the accumulation of the receptor in the early vesicles, we utilized deGradHA to temporally knockdown one copy of the receptor tagged with HA and eGFP. We were successfully able to rescue the increased Dpp signaling activity phenotype by knocking down Rab5 and one copy of the receptor simultaneously (Chapter 3-Fig.5). We used deGradHA instead of Tkv RNAi to knock down only one copy of the receptor, as using the RNAi would have removed all of the receptor, and already after 24 hours of RNAi expression, Dpp signaling would be completely terminated (Fig.4.3). Also, we were interested to decrease the protein levels of Tkv to test if Tkv was constantly activating Dpp signaling in Rab5-deficient cells.

We also ensured that the observed increase in Dpp signaling activity in absence of Rab5 is Dpp-dependent (Chapter 3-Fig.4, A), and that it is not due to an increase in Dpp expression (Chapter 3-Fig.4, B). Furthermore, as expected, knocking down Rab5 also led to an accumulation of the transmembrane HSPGs Dally and Dlp (Fig.4.8). However, the role of Dally accumulation in the increased Dpp signaling activity was ruled out, as knocking down simultaneously both Rab5 and Dally via RNAi, and knocking down Rab5 in *dally* mutant flies did not rescue the increased Dpp signaling activity phenotype in the medial region of the disc (Fig.4.9). However, in this experimental setup, the range of Dpp signaling activity was reduced in the lateral regions of the disc. This indicated that knocking down Rab5 in regions where Dpp is unable to reach does not lead to an increase in Dpp signaling activity.

5.4.2 Role of late endocytic factors in Dpp signaling

A previous study has investigated the role of lysosomal degradation in shaping the long-range Dpp gradient, and upon over-expression of a dominant gain of function *rab7* mutant, they observed a reduction in the range of Dpp target gene Spalt (Entchev et al., 2000). They proposed that enhancing lysosomal degradation reduces the Dpp signaling range. Furthermore, another study reported that the ESCRT-0 component Hrs plays a role in terminating a range of activated signaling receptors, including Tkv, and in absence of Hrs, ubiquitinated Tkv is accumulated in early endosomal compartments (Jékely & Rørth, 2003).

In our study, we revisited the role of late endocytic factors, and showed that the absence of Rab7 (both RNAi and mutant clones) did not affect Dpp signaling activity (Chapter 3-Fig.6). In contrast, knocking down different ESCRT components led to an increase in range and intensity of pMad (Chapter 3-Fig.7). Also, knocking down ESCRT components led to an accumulation of ubiquitinated Tkv in enlarged early endosomes (Chapter 3-Fig.7 & Fig.4.5), while knocking down Rab7 did not lead to any accumulation of ubiquitinated Tkv (Chapter 3-Fig.7). ESCRT components and MVBs have also been implicated in other signaling pathways. They are known to be required not only for degradation of Hh/Ptc ligand-receptor complex, but also to transfer Ptc from the apical to the basal region in the Hh receiving cells (González-Méndez et al., 2020).

The possibility that in the absence of lysosomal degradation other compensatory degradative mechanisms, such as proteasomal degradation could come into effect have been considered. Mutations in UBE3A, a critical enzyme involved in proteasomal degradation has been shown

to be involved in degradation of Tkv in *Drosophila* neuromuscular junctions (NMJs) (Zhao et al., 2015). However, mutations in this enzyme were found to have no role in regulating Tkv in Drosophila wing imaginal discs (Li et al., 2016). Nevertheless, the possibility for compensatory degradative pathways in absence of lysosomal degradation cannot be ruled out.

Our findings indicate that Dpp signaling is likely terminated through internalization of ubiquitinated Tkv into the MVBs, and not through its lysosomal degradation. Our observations were consistent and complementary to what has been reported by Jékely and Rørth (2003).

5.4.3 Role of recycling in Dpp signaling

With the recent publication from Romanova-Michaelides et al. (2022), the transcytosis model for Dpp has re-emerged, according to which Dpp is internalized via Dally in receiving cells and is recycled and re-exocytosed outside of the cells. They reported that in the absence of either Rab4 or Rab11, the intracellular GFP-Dpp gradient was drastically shrunk while the pMad gradient was not affected. Although we did not observe a similar reduction in the endogenous mGL-Dpp in our study, we can confirm that knocking down Rab4 or Rab11 leads to no changes in the pMad gradient (Chapter 3-Fig.9). It is interesting to note that when we knocked down Rab11, we observed an accumulation of enlarged mGL-Dpp positive puncta, but this accumulation did not have any effect on Dpp signaling activity. We can conclude from our observations that the recycling endosomes play no role in regulating the Dpp signaling activity.

5.4.4 Signaling endosomes

The endocytic vesicles called Sara endosomes are characterized by the presence of Sara (Smad Anchor for Receptor Activation) on their cell surface. Sara was initially discovered as an adaptor protein which mediated TGF-β signal transduction specifically in mammalian cells (Tsukazaki et al., 1998). However, Sara is not implicated in BMP signal transduction. Sara binds to unphosphorylated Smad2 and Smad3 of the TGF-β complex, but not to the BMP-specific Smad1, Smad5 and Smad8 (Tsukazaki et al., 1998). In *Drosophila*, Sara has been found to have a role in asymmetric division of the sensory organ precursor cells by partitioning Dpp signaling molecules among daughter cells during wing development (Bökel et al., 2006). However, in absence of Sara, both the pMad and Spalt patterns were found to be normal in disc cells in the interphase state (Bökel et al., 2006). Thus, although Sara is essential for recruiting

Smad2/3 to the receptor complex for phosphorylation in activin/TGF-β signaling (Panopoulou et al., 2002; Tsukazaki et al., 1998), it is not required in the same manner for Dpp/BMP signal transduction (Bökel et al., 2006). Consequently, we did not focus on the role of Sara endosomes in this thesis. Nevertheless, we can conclude that the endosomal compartments that contribute to activation of Dpp signaling include the early (clathrin-uncoated) vesicles, the early endosome, and the maturing endosome prior to formation of the late endosome.

5.5 Is Tkv the internalizing receptor of Dpp?

Romanova-Michaelides et al. (2022) had recently reported that Tkv is not the internalizing receptor of Dpp. Using the nanobody binding assay, they observed that, GFP-Dpp was able to be internalized in *tkv, brk* mutant clones. They proposed that Dpp and Tkv are internalized independently and Dpp signaling is activated when the two come in contact with each other inside the endosomes. Their statement has caused some controversy in the field, as until now, it was thought that Dpp is internalized via its receptors upon binding, to initiate signaling activity. However, this proposal has been challenged by Simon et al. (2023) who showed that Tkv is indeed internalizing Dpp, and Dally's function is to counteract this internalization. With the presence of the endogenous mGL-Dpp, I also investigated the effect of absence of Tkv on the levels of intracellular Dpp, and observed a reduction in number of mGL-Dpp positive puncta in Dpp-receiving cells upon knocking down Tkv (Fig.4.3). Also, by conducting a simultaneous extracellular staining for HA-Tkv and mGL-Dpp with α-HA and α-GFP antibodies, I showed that the receptor and the ligand colocalized together in the extracellular space, indicating that the two may be interacting with each other prior to internalization (Fig.4.2). These observations could further suggest that Dpp is being internalized via Tkv. Also, an interesting experiment to complement our findings would be to check the extent of colocalization of the receptor with the ligand upon knocking down the early endocytic factors. In absence of Dynamin and Rab5, we have already seen the two accumulating extracellularly, with mGL-Dpp accumulation patterns resembling that of the receptor (especially in shi^{ts1} flies). Upon disruption of the early endocytic factors, we would then expect to observe a higher degree of colocalization between the receptor and the ligand.

5.6 Utilization of protein binders to study protein functions in development

Our observations regarding the re-localization of GFP-Mad to the inner cell membrane indicated that forcing GFP-Mad to be localized to the cell membrane, possibly in a closer contact with Tkv, led to an increase in its phosphorylation (Fig.4.12, B). Furthermore, GrabFP (Intra) is a membranous construct containing the CD8 transmembrane protein which also goes through constant cellular trafficking. As endosomal structures are derived from the cell membrane, GrabFP (Intra) was also likely to be internalized and be present on the endosomal membranes. Therefore, it was also reasonable to find the pMad signal in puncta resembling the endosomal compartments upon its re-localization with GrabFP (Intra) in homozygous *mad-GFP* flies (Fig.4.12, D). In this experimental setup, no nuclear pMad signal was observed, and the smaller compartment size resembled a *dpp* mutant phenotype, indicating that nuclear localization of pMad is required for its function.

Consequently, we utilized this experimental setup to study on which endosomal compartments Mad-GFP was becoming phosphorylated. As expected from our previous findings (see Chapter 3), majority of the puncta pMad signal was localized on the early endosome. The pMad signal was also seen to be occasionally localized on the maturing/late endosome. This occasional colocalization of pMad with Rab7 could be occurring on the maturing endosome, as Rab5 is being replaced by Rab7, prior to the endolysosomal fusion. In this case, phosphorylation of Mad on the maturing endosome via Tkv can be explained. However, we have indicated in Chapter 3 that Dpp signaling activity is terminated via sorting of Tkv into ILVs prior to formation of the late endosome. Hence, phosphorylation of GFP-Mad on the late endosome would be unexpected. It may be likely that the colocalized pMad and Rab7 signal may be on the maturing endosome, and the non-colocalizing signal may be on the late endosome (Fig.4.13, E''). Nevertheless, we indicated that the majority of Mad-GFP is becoming phosphorylated on the early endosome. However, we could not draw any conclusion regarding the possibility that Mad can become phosphorylated from the cell membrane, as GrabFP (Intra) was seen to be not only membranous, but also present on the early and maturing/late endosomes.

6 Conclusion and outlook

In this study, I re-investigated the role of different trafficking factors in the formation of the extracellular and intracellular Dpp gradient, as well as their effect on Dpp signaling activity by utilizing the endogenously tagged *dpp* alleles. To address these long-standing biological questions, we utilized novel tools in the field. I showed that dynamin is a major regulator of the Dpp gradient and blocking dynamin-dependent endocytosis expanded the extracellular Dpp gradient and impaired Dpp signaling. I also illustrated that the function of Rab5 and the early endosome is required for regulation of the extracellular Dpp gradient and for termination of Dpp signaling activity through degrading Tkv. I also showed that sorting Tkv into ILVs, and not lysosomal degradation is required for termination of Dpp signaling activity without influencing the extracellular ligand gradient. Furthermore, by investigating the role of recycling endosomes, I found that they do not affect Dpp signaling activity, while the slow recycling endosomes are regulating localization of the intracellular Dpp, and the fast recycling endosomes play a minor role in the extracellular ligand gradient in the basal side of the disc cells. Taken together, our results suggest that extracellular Dpp morphogen gradient is shaped and interpreted by distinct endocytic trafficking pathways.

The endogenously tagged *dpp* alleles can now be used to further study the mechanisms of Dpp morphogen gradient formation at endogenous levels using live-imaging, fluorescence correlation spectroscopy (FCS) and fluorescence recovery after photobleaching (FRAP). With the availability of the endogenous tagging methods, variety of proteins of interest can now be tagged and studied under physiological conditions. Also, development of synthetic tools such as the protein binder toolset, together with the endogenously tagged proteins allow for visualization and manipulation of proteins at their endogenous levels *in vivo* in a controllable manner. These tools can help us further understand the role of different proteins and answer developmental questions.

7 References

Aberle, H., Haghighi, A. P., Fetter, R. D., McCabe, B. D., Magalhães, T. R., & Goodman, C. S. (2002). wishful thinking encodes a BMP type II receptor that regulates synaptic growth in Drosophila. *Neuron*, *33*(4), 545-558. https://doi.org/10.1016/s0896-6273(02)00589-5

Affolter, M., & Basler, K. (2007). The Decapentaplegic morphogen gradient: from pattern formation to growth regulation. *Nat Rev Genet*, *8*(9), 663-674. https://doi.org/10.1038/nrg2166

Affolter, M., Marty, T., Vigano, M. A., & Jaźwińska, A. (2001). Nuclear interpretation of Dpp signaling in Drosophila. *Embo j*, *20*(13), 3298-3305. https://doi.org/10.1093/emboj/20.13.3298

Aguilar, G., Matsuda, S., Vigano, M. A., & Affolter, M. (2019). Using Nanobodies to Study Protein Function in Developing Organisms. *Antibodies (Basel)*, *8*(1). https://doi.org/10.3390/antib8010016

Aguilar, G., Vigano, M. A., Affolter, M., & Matsuda, S. (2019). Reflections on the use of protein binders to study protein function in developmental biology. *Wiley Interdiscip Rev Dev Biol*, *8*(6), e356. https://doi.org/10.1002/wdev.356

Akiyama, T., Kamimura, K., Firkus, C., Takeo, S., Shimmi, O., & Nakato, H. (2008). Dally regulates Dpp morphogen gradient formation by stabilizing Dpp on the cell surface. *Dev Biol*, *313*(1), 408-419. https://doi.org/10.1016/j.ydbio.2007.10.035

Akiyama, T., User, S. D., & Gibson, M. C. (2018). Somatic clones heterozygous for recessive disease alleles of BMPR1A exhibit unexpected phenotypes in Drosophila. *Elife*, *7*, e35258. https://doi.org/10.7554/eLife.35258

Alborelli, I. (2016). *Characterization of the subcellular localization of the TGF-β receptors in the wing imaginal disc* [Doctoral Thesis, University of Basel].

Alonso, Y. A. M., Migliano, S. M., & Teis, D. (2016). ESCRT-III and Vps4: a dynamic multipurpose tool for membrane budding and scission. *Febs j*, *283*(18), 3288-3302. https://doi.org/10.1111/febs.13688

Amerik, A. Y., & Hochstrasser, M. (2004). Mechanism and function of deubiquitinating enzymes. *Biochim Biophys Acta*, *1695*(1-3), 189-207. https://doi.org/10.1016/j.bbamcr.2004.10.003

Anderson, E. N., & Wharton, K. A. (2017). Alternative cleavage of the bone morphogenetic protein (BMP), Gbb, produces ligands with distinct developmental functions and receptor preferences. *J Biol Chem*, *292*(47), 19160-19178. https://doi.org/10.1074/jbc.M117.793513

Aoyama, M., Sun-Wada, G. H., Yamamoto, A., Yamamoto, M., Hamada, H., & Wada, Y. (2012). Spatial restriction of bone morphogenetic protein signaling in mouse gastrula through the mVam2-dependent endocytic pathway. *Dev Cell*, *22*(6), 1163-1175. https://doi.org/10.1016/j.devcel.2012.05.009

Arora, K., Levine, M. S., & O'Connor, M. B. (1994). The screw gene encodes a ubiquitously expressed member of the TGF-beta family required for specification of dorsal cell fates in the Drosophila embryo. *Genes Dev*, *8*(21), 2588-2601. https://doi.org/10.1101/gad.8.21.2588

Ashe, H. L. (2005). BMP signalling: synergy and feedback create a step gradient. *Curr Biol*, *15*(10), R375-377. https://doi.org/10.1016/j.cub.2005.05.003

Ashique, A. M., Fu, K., & Richman, J. M. (2002). Signalling via type IA and type IB bone morphogenetic protein receptors (BMPR) regulates intramembranous bone formation, chondrogenesis and feather formation in the chicken embryo. *Int J Dev Biol*, *46*(2), 243-253. https://doi.org/10.1387/ijdb.011535

Attisano, L., Cárcamo, J., Ventura, F., Weis, F. M., Massagué, J., & Wrana, J. L. (1993). Identification of human activin and TGF beta type I receptors that form heteromeric kinase complexes with type II receptors. *Cell*, *75*(4), 671-680. https://doi.org/10.1016/0092-8674(93)90488-c

Babst, M., Katzmann, D. J., Snyder, W. B., Wendland, B., & Emr, S. D. (2002). Endosome-associated complex, ESCRT-II, recruits transport machinery for protein sorting at the multivesicular body. *Dev Cell*, *3*(2), 283-289. https://doi.org/10.1016/s1534-5807(02)00219-8

Bangi, E., & Wharton, K. (2006a). Dpp and Gbb exhibit different effective ranges in the establishment of the BMP activity gradient critical for Drosophila wing patterning. *Dev Biol*, *295*(1), 178-193. https://doi.org/10.1016/j.ydbio.2006.03.021

Bangi, E., & Wharton, K. (2006b). Dual function of the Drosophila Alk1/Alk2 ortholog Saxophone shapes the Bmp activity gradient in the wing imaginal disc. *Development*, *133*(17), 3295-3303. https://doi.org/10.1242/dev.02513

Basler, K., & Struhl, G. (1994). Compartment boundaries and the control of Drosophila limb pattern by hedgehog protein. *Nature*, *368*(6468), 208-214. https://doi.org/10.1038/368208a0

Bauer, M., Aguilar, G., Wharton, K. A., Matsuda, S., & Affolter, M. (2022). Heterodimerization-dependent secretion of BMPs in Drosophila. *bioRxiv*, 2022.2008.2004.502599. https://doi.org/10.1101/2022.08.04.502599

Beira, J. V., & Paro, R. (2016). The legacy of Drosophila imaginal discs. *Chromosoma*, *125*(4), 573-592. https://doi.org/10.1007/s00412-016-0595-4

Belenkaya, T. Y., Han, C., Yan, D., Opoka, R. J., Khodoun, M., Liu, H., & Lin, X. (2004). Drosophila Dpp morphogen movement is independent of dynamin-mediated endocytosis but regulated by the glypican members of heparan sulfate proteoglycans. *Cell*, *119*(2), 231-244. https://doi.org/10.1016/j.cell.2004.09.031

Bieli, D., Alborelli, I., Harmansa, S., Matsuda, S., Caussinus, E., & Affolter, M. (2016). Development and Application of Functionalized Protein Binders in Multicellular Organisms. *Int Rev Cell Mol Biol*, *325*, 181-213. https://doi.org/10.1016/bs.ircmb.2016.02.006

Bindels, D. S., Haarbosch, L., van Weeren, L., Postma, M., Wiese, K. E., Mastop, M., Aumonier, S., Gotthard, G., Royant, A., Hink, M. A., & Gadella, T. W., Jr. (2017). mScarlet: a bright monomeric red fluorescent protein for cellular imaging. *Nat Methods*, *14*(1), 53-56. https://doi.org/10.1038/nmeth.4074

Bischoff, M., Gradilla, A. C., Seijo, I., Andrés, G., Rodríguez-Navas, C., González-Méndez, L., & Guerrero, I. (2013). Cytonemes are required for the establishment of a normal Hedgehog morphogen gradient in Drosophila epithelia. *Nat Cell Biol*, *15*(11), 1269-1281. https://doi.org/10.1038/ncb2856

Blackman, R. K., Sanicola, M., Raftery, L. A., Gillevet, T., & Gelbart, W. M. (1991). An extensive 3' cis-regulatory region directs the imaginal disk expression of decapentaplegic, a member of the TGF-beta family in Drosophila. *Development*, *111*(3), 657-666. https://doi.org/10.1242/dev.111.3.657

Bökel, C., Schwabedissen, A., Entchev, E., Renaud, O., & González-Gaitán, M. (2006). Sara endosomes and the maintenance of Dpp signaling levels across mitosis. *Science*, *314*(5802), 1135-1139. https://doi.org/10.1126/science.1132524

Bosch, P. S., Ziukaite, R., Alexandre, C., Basler, K., & Vincent, J. P. (2017). Dpp controls growth and patterning in Drosophila wing precursors through distinct modes of action. *Elife*, *6*. https://doi.org/10.7554/eLife.22546

Boveri, T. (1901). uber die Polaritat des Seeigeleies. *Verh. D. phys. med. Ges. Wurzburg, NF*, *34*, 145-176.

Briscoe, J., Lawrence, P. A., & Vincent, J.-P. (2010). *Generation and Interpretation of Morphogen Gradients: a Subject Collection from Cold Spring Harbor Perspectives in Biology*. Cold Spring Harbor Perspective.

Bucci, C., Parton, R. G., Mather, I. H., Stunnenberg, H., Simons, K., Hoflack, B., & Zerial, M. (1992). The small GTPase rab5 functions as a regulatory factor in the early endocytic pathway. *Cell*, *70*(5), 715-728. https://doi.org/https://doi.org/10.1016/0092-8674(92)90306-W

Bucci, C., & Stasi, M. (2016). Endosome to Lysosome Transport. In R. A. Bradshaw & P. D. Stahl (Eds.), *Encyclopedia of Cell Biology* (pp. 408-417). Academic Press. https://doi.org/https://doi.org/10.1016/B978-0-12-394447-4.20041-2

Burke, R., & Basler, K. (1996). Dpp receptors are autonomously required for cell proliferation in the entire developing Drosophila wing. *Development*, *122*(7), 2261-2269. https://doi.org/10.1242/dev.122.7.2261

Callejo, A., Bilioni, A., Mollica, E., Gorfinkiel, N., Andrés, G., Ibáñez, C., Torroja, C., Doglio, L., Sierra, J., & Guerrero, I. (2011). Dispatched mediates Hedgehog basolateral release to form the long-range morphogenetic gradient in the Drosophila wing disk epithelium. *Proc Natl Acad Sci U S A*, *108*(31), 12591-12598. https://doi.org/10.1073/pnas.1106881108

Campbell, B. C., Nabel, E. M., Murdock, M. H., Lao-Peregrin, C., Tsoulfas, P., Blackmore, M. G., Lee, F. S., Liston, C., Morishita, H., & Petsko, G. A. (2020). mGreenLantern: a bright monomeric fluorescent protein with rapid expression and cell filling properties for neuronal imaging. *Proc Natl Acad Sci U S A*, *117*(48), 30710-30721. https://doi.org/10.1073/pnas.2000942117

Campbell, G., & Tomlinson, A. (1999). Transducing the Dpp morphogen gradient in the wing of Drosophila: regulation of Dpp targets by brinker. *Cell*, *96*(4), 553-562. https://doi.org/10.1016/s0092-8674(00)80659-5

Caussinus, E., Kanca, O., & Affolter, M. (2011). Fluorescent fusion protein knockout mediated by anti-GFP nanobody. *Nat Struct Mol Biol*, *19*(1), 117-121. https://doi.org/10.1038/nsmb.2180

Chadda, R., Howes, M. T., Plowman, S. J., Hancock, J. F., Parton, R. G., & Mayor, S. (2007). Cholesterol-sensitive Cdc42 activation regulates actin polymerization for endocytosis via the GEEC pathway. *Traffic*, *8*(6), 702-717. https://doi.org/10.1111/j.1600-0854.2007.00565.x

Chang, H. C., Newmyer, S. L., Hull, M. J., Ebersold, M., Schmid, S. L., & Mellman, I. (2002). Hsc70 is required for endocytosis and clathrin function in Drosophila. *J Cell Biol*, *159*(3), 477-487. https://doi.org/10.1083/jcb.200205086

Cherry, S., Jin, E. J., Ozel, M. N., Lu, Z., Agi, E., Wang, D., Jung, W. H., Epstein, D., Meinertzhagen, I. A., Chan, C. C., & Hiesinger, P. R. (2013). Charcot-Marie-Tooth 2B mutations in rab7 cause dosage-dependent neurodegeneration due to partial loss of function. *Elife*, *2*, e01064. https://doi.org/10.7554/eLife.01064

Christoforidis, S., McBride, H. M., Burgoyne, R. D., & Zerial, M. (1999). The Rab5 effector EEA1 is a core component of endosome docking. *Nature*, *397*(6720), 621-625. https://doi.org/10.1038/17618

Clague, M. J., & Urbé, S. (2003). Hrs function: viruses provide the clue. *Trends Cell Biol*, *13*(12), 603-606. https://doi.org/10.1016/j.tcb.2003.10.002

Cohen, B., Simcox, A. A., & Cohen, S. M. (1993). Allocation of the thoracic imaginal primordia in the Drosophila embryo. *Development*, *117*(2), 597-608. https://doi.org/10.1242/dev.117.2.597

Cook, O., Biehs, B., & Bier, E. (2004). brinker and optomotor-blind act coordinately to initiate development of the L5 wing vein primordium in Drosophila. *Development*, *131*(9), 2113-2124. https://doi.org/10.1242/dev.01100

Crick, F. (1970). Diffusion in Embryogenesis. *Nature*, *225*(5231), 420-422. https://doi.org/10.1038/225420a0

Dahmann, C., & Basler, K. (1999). Compartment boundaries: at the edge of development. *Trends Genet*, *15*(8), 320-326. https://doi.org/10.1016/s0168-9525(99)01774-6

de Celis, J. F., Garcia-Bellido, A., & Bray, S. J. (1996). Activation and function of Notch at the dorsal-ventral boundary of the wing imaginal disc. *Development*, *122*(1), 359-369.

De Robertis, E. M. (2006). Spemann's organizer and self-regulation in amphibian embryos. *Nature Reviews Molecular Cell Biology*, *7*(4), 296-302. https://doi.org/10.1038/nrm1855

Dey, N. S., Ramesh, P., Chugh, M., Mandal, S., & Mandal, L. (2016). Dpp dependent Hematopoietic stem cells give rise to Hh dependent blood progenitors in larval lymph gland of Drosophila. *Elife*, *5*. https://doi.org/10.7554/eLife.18295

Diaz-Benjumea, F. J., & Cohen, S. M. (1995). Serrate signals through Notch to establish a Wingless-dependent organizer at the dorsal/ventral compartment boundary of the Drosophila wing. *Development*, *121*(12), 4215-4225.

Doherty, D., Feger, G., Younger-Shepherd, S., Jan, L. Y., & Jan, Y. N. (1996). Delta is a ventral to dorsal signal complementary to Serrate, another Notch ligand, in Drosophila wing formation. *Genes & Development*, *10*(4), 421-434.

Doherty, G. J., & McMahon, H. T. (2009). Mechanisms of endocytosis. *Annu Rev Biochem*, *78*, 857-902. https://doi.org/10.1146/annurev.biochem.78.081307.110540

Driever, W., & Nüsslein-Volhard, C. (1988). A gradient of bicoid protein in Drosophila embryos. *Cell*, *54*(1), 83-93. https://doi.org/10.1016/0092-8674(88)90182-1

Dubois, L., Lecourtois, M., Alexandre, C., Hirst, E., & Vincent, J. P. (2001). Regulated endocytic routing modulates wingless signaling in Drosophila embryos. *Cell*, *105*(5), 613-624. https://doi.org/10.1016/s0092-8674(01)00375-0

Dunst, S., Kazimiers, T., von Zadow, F., Jambor, H., Sagner, A., Brankatschk, B., Mahmoud, A., Spannl, S., Tomancak, P., Eaton, S., & Brankatschk, M. (2015). Endogenously tagged rab proteins: a resource to study membrane trafficking in Drosophila. *Dev Cell*, *33*(3), 351-365. https://doi.org/10.1016/j.devcel.2015.03.022

Dupree, P., Parton, R. G., Raposo, G., Kurzchalia, T. V., & Simons, K. (1993). Caveolae and sorting in the trans-Golgi network of epithelial cells. *Embo j*, *12*(4), 1597-1605. https://doi.org/10.1002/j.1460-2075.1993.tb05804.x

Eaton, S., & Kornberg, T. B. (1990). Repression of ci-D in posterior compartments of Drosophila by engrailed. *Genes Dev*, *4*(6), 1068-1077. https://doi.org/10.1101/gad.4.6.1068

Ebisawa, T., Fukuchi, M., Murakami, G., Chiba, T., Tanaka, K., Imamura, T., & Miyazono, K. (2001). Smurf1 interacts with transforming growth factor-beta type I receptor through Smad7 and induces receptor degradation. *J Biol Chem*, *276*(16), 12477-12480. https://doi.org/10.1074/jbc.C100008200

Edeling, M. A., Smith, C., & Owen, D. (2006). Life of a clathrin coat: insights from clathrin and AP structures. *Nat Rev Mol Cell Biol*, *7*(1), 32-44. https://doi.org/10.1038/nrm1786

Emery, G., Hutterer, A., Berdnik, D., Mayer, B., Wirtz-Peitz, F., Gaitan, M. G., & Knoblich, J. A. (2005). Asymmetric Rab 11 endosomes regulate delta recycling and specify cell fate in the Drosophila nervous system. *Cell*, *122*(5), 763-773. https://doi.org/10.1016/j.cell.2005.08.017

Entchev, E. V., Schwabedissen, A., & González-Gaitán, M. (2000). Gradient formation of the TGF-beta homolog Dpp. *Cell*, *103*(6), 981-991. https://doi.org/10.1016/s0092-8674(00)00200-2

Eyster, C. A., Higginson, J. D., Huebner, R., Porat-Shliom, N., Weigert, R., Wu, W. W., Shen, R. F., & Donaldson, J. G. (2009). Discovery of new cargo proteins that enter cells through clathrin-independent endocytosis. *Traffic*, *10*(5), 590-599. https://doi.org/10.1111/j.1600-0854.2009.00894.x

Fasano, D., Parisi, S., Pierantoni, G. M., De Rosa, A., Picillo, M., Amodio, G., Pellecchia, M. T., Barone, P., Moltedo, O., Bonifati, V., De Michele, G., Nitsch, L., Remondelli, P., Criscuolo, C., & Paladino, S. (2018). Alteration of endosomal trafficking is associated with early-onset parkinsonism caused by SYNJ1 mutations. *Cell Death Dis*, *9*(3), 385. https://doi.org/10.1038/s41419-018-0410-7

Ferguson, E. L., & Anderson, K. V. (1992). Decapentaplegic acts as a morphogen to organize dorsal-ventral pattern in the Drosophila embryo. *Cell*, *71*(3), 451-461. https://doi.org/10.1016/0092-8674(92)90514-d

Fernández-Moreno, M. A., Farr, C. L., Kaguni, L. S., & Garesse, R. (2007). Drosophila melanogaster as a model system to study mitochondrial biology. *Methods Mol Biol*, *372*, 33-49. https://doi.org/10.1007/978-1-59745-365-3_3

Field, J., Nikawa, J., Broek, D., MacDonald, B., Rodgers, L., Wilson, I. A., Lerner, R. A., & Wigler, M. (1988). Purification of a RAS-responsive adenylyl cyclase complex from Saccharomyces cerevisiae by use of an epitope addition method. *Mol Cell Biol*, *8*(5), 2159-2165. https://doi.org/10.1128/mcb.8.5.2159-2165.1988

Franch-Marro, X., Marchand, O., Piddini, E., Ricardo, S., Alexandre, C., & Vincent, J. P. (2005). Glypicans shunt the Wingless signal between local signalling and further transport. *Development*, *132*(4), 659-666. https://doi.org/10.1242/dev.01639

Fuse, N., Hirose, S., & Hayashi, S. (1996). Determination of wing cell fate by the escargot and snail genes in Drosophila. *Development*, *122*(4), 1059-1067. https://doi.org/10.1242/dev.122.4.1059

Galbiati, F., Engelman, J. A., Volonte, D., Zhang, X. L., Minetti, C., Li, M., Hou, H., Jr., Kneitz, B., Edelmann, W., & Lisanti, M. P. (2001). Caveolin-3 null mice show a loss of caveolae, changes

in the microdomain distribution of the dystrophin-glycoprotein complex, and t-tubule abnormalities. *J Biol Chem*, *276*(24), 21425-21433. https://doi.org/10.1074/jbc.M100828200

Ghazi-Tabatabai, S., Saksena, S., Short, J. M., Pobbati, A. V., Veprintsev, D. B., Crowther, R. A., Emr, S. D., Egelman, E. H., & Williams, R. L. (2008). Structure and disassembly of filaments formed by the ESCRT-III subunit Vps24. *Structure*, *16*(9), 1345-1356. https://doi.org/10.1016/j.str.2008.06.010

Glebov, O. O., Bright, N. A., & Nichols, B. J. (2006). Flotillin-1 defines a clathrin-independent endocytic pathway in mammalian cells. *Nat Cell Biol*, *8*(1), 46-54. https://doi.org/10.1038/ncb1342

González-Gaitán, M., & Jäckle, H. (1999). The range of spalt-activating Dpp signalling is reduced in endocytosis-defective Drosophila wing discs. *Mech Dev*, *87*(1-2), 143-151. https://doi.org/10.1016/s0925-4773(99)00156-2

González-Méndez, L., Gradilla, A. C., Sánchez-Hernández, D., González, E., Aguirre-Tamaral, A., Jiménez-Jiménez, C., Guerra, M., Aguilar, G., Andrés, G., Falcón-Pérez, J. M., & Guerrero, I. (2020). Polarized sorting of Patched enables cytoneme-mediated Hedgehog reception in the Drosophila wing disc. *Embo j*, *39*(11), e103629. https://doi.org/10.15252/embj.2019103629

González-Méndez, L., Seijo-Barandiarán, I., & Guerrero, I. (2017). Cytoneme-mediated cell-cell contacts for Hedgehog reception. *Elife*, *6*. https://doi.org/10.7554/eLife.24045

Goody, R. S., Müller, M. P., & Wu, Y.-W. (2017). Mechanisms of action of Rab proteins, key regulators of intracellular vesicular transport. *Biological Chemistry*, *398*(5-6), 565-575. https://doi.org/doi:10.1515/hsz-2016-0274

Goold, C. P., & Davis, G. W. (2007). The BMP ligand Gbb gates the expression of synaptic homeostasis independent of synaptic growth control. *Neuron*, *56*(1), 109-123. https://doi.org/10.1016/j.neuron.2007.08.006

Gough, N. R., Xiang, X., & Mishra, L. (2021). TGF-β Signaling in Liver, Pancreas, and Gastrointestinal Diseases and Cancer. *Gastroenterology*, *161*(2), 434-452.e415. https://doi.org/10.1053/j.gastro.2021.04.064

Gradeci, D., Bove, A., Vallardi, G., Lowe, A. R., Banerjee, S., & Charras, G. (2021). Cell-scale biophysical determinants of cell competition in epithelia. *Elife*, *10*. https://doi.org/10.7554/eLife.61011

Gross, G. G., Junge, J. A., Mora, R. J., Kwon, H. B., Olson, C. A., Takahashi, T. T., Liman, E. R., Ellis-Davies, G. C., McGee, A. W., Sabatini, B. L., Roberts, R. W., & Arnold, D. B. (2013). Recombinant probes for visualizing endogenous synaptic proteins in living neurons. *Neuron*, *78*(6), 971-985. https://doi.org/10.1016/j.neuron.2013.04.017

Guerra, F., & Bucci, C. (2016). Multiple Roles of the Small GTPase Rab7. *Cells*, *5*(3). https://doi.org/10.3390/cells5030034

Haas, A. K., Fuchs, E., Kopajtich, R., & Barr, F. A. (2005). A GTPase-activating protein controls Rab5 function in endocytic trafficking. *Nat Cell Biol*, *7*(9), 887-893. https://doi.org/10.1038/ncb1290

Haerry, T. E. (2010). The interaction between two TGF-beta type I receptors plays important roles in ligand binding, SMAD activation, and gradient formation. *Mech Dev*, *127*(7-8), 358-370. https://doi.org/10.1016/j.mod.2010.04.001

Haerry, T. E., Khalsa, O., O'Connor, M. B., & Wharton, K. A. (1998). Synergistic signaling by two BMP ligands through the SAX and TKV receptors controls wing growth and patterning in Drosophila. *Development*, *125*(20), 3977-3987. https://doi.org/10.1242/dev.125.20.3977

Hamaratoglu, F., Affolter, M., & Pyrowolakis, G. (2014). Dpp/BMP signaling in flies: from molecules to biology. *Semin Cell Dev Biol*, *32*, 128-136. https://doi.org/10.1016/j.semcdb.2014.04.036

Hamaratoglu, F., de Lachapelle, A. M., Pyrowolakis, G., Bergmann, S., & Affolter, M. (2011). Dpp signaling activity requires Pentagone to scale with tissue size in the growing Drosophila wing imaginal disc. *PLoS Biol*, *9*(10), e1001182. https://doi.org/10.1371/journal.pbio.1001182

Han, C., Yan, D., Belenkaya, T. Y., & Lin, X. (2005). Drosophila glypicans Dally and Dally-like shape the extracellular Wingless morphogen gradient in the wing disc. *Development*, *132*(4), 667-679. https://doi.org/10.1242/dev.01636

Harmansa, S., & Affolter, M. (2018). Protein binders and their applications in developmental biology. *Development*, *145*(2). https://doi.org/10.1242/dev.148874

Harmansa, S., Alborelli, I., Bieli, D., Caussinus, E., & Affolter, M. (2017). A nanobody-based toolset to investigate the role of protein localization and dispersal in Drosophila. *Elife*, *6*. https://doi.org/10.7554/eLife.22549

Harmansa, S., Hamaratoglu, F., Affolter, M., & Caussinus, E. (2015). Dpp spreading is required for medial but not for lateral wing disc growth. *Nature*, *527*(7578), 317-322. https://doi.org/10.1038/nature15712

Hartung, A., Bitton-Worms, K., Rechtman, M. M., Wenzel, V., Boergermann, J. H., Hassel, S., Henis, Y. I., & Knaus, P. (2006). Different routes of bone morphogenic protein (BMP) receptor endocytosis influence BMP signaling. *Mol Cell Biol*, *26*(20), 7791-7805. https://doi.org/10.1128/mcb.00022-06

Haynie, J. L., & Bryant, P. J. (1986). Development of the eye-antenna imaginal disc and morphogenesis of the adult head in Drosophila melanogaster. *J Exp Zool*, *237*(3), 293-308. https://doi.org/10.1002/jez.1402370302

Heldin, C. H., Miyazono, K., & ten Dijke, P. (1997). TGF-beta signalling from cell membrane to nucleus through SMAD proteins. *Nature*, *390*(6659), 465-471. https://doi.org/10.1038/37284

Hemmati-Brivanlou, A., & Thomsen, G. H. (1995). Ventral mesodermal patterning in Xenopus embryos: expression patterns and activities of BMP-2 and BMP-4. *Dev Genet*, *17*(1), 78-89. https://doi.org/10.1002/dvg.1020170109

Hoffmann, F. M., & Goodman, W. (1987). Identification in transgenic animals of the Drosophila decapentaplegic sequences required for embryonic dorsal pattern formation. *Genes Dev*, *1*(6), 615-625. https://doi.org/10.1101/gad.1.6.615

Hsiung, F., Ramirez-Weber, F. A., Iwaki, D. D., & Kornberg, T. B. (2005). Dependence of Drosophila wing imaginal disc cytonemes on Decapentaplegic. *Nature*, *437*(7058), 560-563. https://doi.org/10.1038/nature03951

Huotari, J., & Helenius, A. (2011). Endosome maturation. *Embo j*, *30*(17), 3481-3500. https://doi.org/10.1038/emboj.2011.286

Hutagalung, A. H., & Novick, P. J. (2011). Role of Rab GTPases in membrane traffic and cell physiology. *Physiol Rev*, *91*(1), 119-149. https://doi.org/10.1152/physrev.00059.2009

Jaźwińska, A., Kirov, N., Wieschaus, E., Roth, S., & Rushlow, C. (1999). The Drosophila gene brinker reveals a novel mechanism of Dpp target gene regulation. *Cell*, *96*(4), 563-573. https://doi.org/10.1016/s0092-8674(00)80660-1

Jaźwińska, A., Rushlow, C., & Roth, S. (1999). The role of brinker in mediating the graded response to Dpp in early Drosophila embryos. *Development*, *126*(15), 3323-3334. https://doi.org/10.1242/dev.126.15.3323

Jékely, G., & Rørth, P. (2003). Hrs mediates downregulation of multiple signalling receptors in Drosophila. *EMBO Rep*, *4*(12), 1163-1168. https://doi.org/10.1038/sj.embor.7400019

Johnston, L. A., Prober, D. A., Edgar, B. A., Eisenman, R. N., & Gallant, P. (1999). Drosophila myc regulates cellular growth during development. *Cell*, *98*(6), 779-790. https://doi.org/10.1016/s0092-8674(00)81512-3

Katagiri, T., & Watabe, T. (2016). Bone Morphogenetic Proteins. *Cold Spring Harb Perspect Biol*, *8*(6). https://doi.org/10.1101/cshperspect.a021899

Kawabata, M., Imamura, T., & Miyazono, K. (1998). Signal transduction by bone morphogenetic proteins. *Cytokine Growth Factor Rev*, *9*(1), 49-61. https://doi.org/10.1016/s1359-6101(97)00036-1

Khalsa, O., Yoon, J. W., Torres-Schumann, S., & Wharton, K. A. (1998). TGF-beta/BMP superfamily members, Gbb-60A and Dpp, cooperate to provide pattern information and establish cell identity in the Drosophila wing. *Development*, *125*(14), 2723-2734. https://doi.org/10.1242/dev.125.14.2723

Kicheva, A., Pantazis, P., Bollenbach, T., Kalaidzidis, Y., Bittig, T., Jülicher, F., & González-Gaitán, M. (2007). Kinetics of morphogen gradient formation. *Science*, *315*(5811), 521-525. https://doi.org/10.1126/science.1135774

Kim, M., & Choe, S. (2011). BMPs and their clinical potentials. *BMB Rep*, *44*(10), 619-634. https://doi.org/10.5483/BMBRep.2011.44.10.619

Kirkham, M., Fujita, A., Chadda, R., Nixon, S. J., Kurzchalia, T. V., Sharma, D. K., Pagano, R. E., Hancock, J. F., Mayor, S., & Parton, R. G. (2005). Ultrastructural identification of uncoated caveolin-independent early endocytic vehicles. *J Cell Biol*, *168*(3), 465-476. https://doi.org/10.1083/jcb.200407078

Kobayashi, T., Lyons, K. M., McMahon, A. P., & Kronenberg, H. M. (2005). BMP signaling stimulates cellular differentiation at multiple steps during cartilage development. *Proc Natl Acad Sci U S A*, *102*(50), 18023-18027. https://doi.org/10.1073/pnas.0503617102

Kobayashi, T., Stang, E., Fang, K. S., de Moerloose, P., Parton, R. G., & Gruenberg, J. (1998). A lipid associated with the antiphospholipid syndrome regulates endosome structure and function. *Nature*, *392*(6672), 193-197. https://doi.org/10.1038/32440

Koenig, J. H., & Ikeda, K. (1989). Disappearance and reformation of synaptic vesicle membrane upon transmitter release observed under reversible blockage of membrane retrieval. *J Neurosci*, *9*(11), 3844-3860. https://doi.org/10.1523/jneurosci.09-11-03844.1989

Komada, M., & Soriano, P. (1999). Hrs, a FYVE finger protein localized to early endosomes, is implicated in vesicular traffic and required for ventral folding morphogenesis. *Genes Dev*, *13*(11), 1475-1485. https://doi.org/10.1101/gad.13.11.1475

Kornberg, T. (1981). Engrailed: a gene controlling compartment and segment formation in Drosophila. *Proc Natl Acad Sci U S A*, *78*(2), 1095-1099. https://doi.org/10.1073/pnas.78.2.1095

Krishnan, N., Swoger, M., Rathbun, L. I., Fioramonti, P. J., Freshour, J., Bates, M., Patteson, A. E., & Hehnly, H. (2022). Rab11 endosomes and Pericentrin coordinate centrosome movement during pre-abscission in vivo. *Life Sci Alliance*, *5*(7). https://doi.org/10.26508/lsa.202201362

Lakadamyali, M., Rust, M. J., & Zhuang, X. (2006). Ligands for clathrin-mediated endocytosis are differentially sorted into distinct populations of early endosomes. *Cell*, *124*(5), 997-1009. https://doi.org/10.1016/j.cell.2005.12.038

Lander, A. D., Nie, Q., & Wan, F. Y. (2002). Do morphogen gradients arise by diffusion? *Dev Cell*, *2*(6), 785-796. https://doi.org/10.1016/s1534-5807(02)00179-x

Langemeyer, L., Fröhlich, F., & Ungermann, C. (2018). Rab GTPase Function in Endosome and Lysosome Biogenesis. *Trends Cell Biol*, *28*(11), 957-970. https://doi.org/10.1016/j.tcb.2018.06.007

Lawe, D. C., Chawla, A., Merithew, E., Dumas, J., Carrington, W., Fogarty, K., Lifshitz, L., Tuft, R., Lambright, D., & Corvera, S. (2002). Sequential roles for phosphatidylinositol 3-phosphate and Rab5 in tethering and fusion of early endosomes via their interaction with EEA1. *J Biol Chem*, *277*(10), 8611-8617. https://doi.org/10.1074/jbc.M109239200

Lecuit, T., Brook, W. J., Ng, M., Calleja, M., Sun, H., & Cohen, S. M. (1996). Two distinct mechanisms for long-range patterning by Decapentaplegic in the Drosophila wing. *Nature*, *381*(6581), 387-393. https://doi.org/10.1038/381387a0

Lee, S., Tsai, Y. C., Mattera, R., Smith, W. J., Kostelansky, M. S., Weissman, A. M., Bonifacino, J. S., & Hurley, J. H. (2006). Structural basis for ubiquitin recognition and autoubiquitination by Rabex-5. *Nature structural & molecular biology*, *13*(3), 264-271.

Lepeta, K., Roubinet, C., Bauer, M., Vigano, M. A., Aguilar, G., Kanca, O., Ochoa-Espinosa, A., Bieli, D., Cabernard, C., Caussinus, E., & Affolter, M. (2022). Engineered kinases as a tool for phosphorylation of selected targets in vivo. *J Cell Biol*, *221*(10). https://doi.org/10.1083/jcb.202106179

Letsou, A., Arora, K., Wrana, J. L., Simin, K., Twombly, V., Jamal, J., Staehling-Hampton, K., Hoffmann, F. M., Gelbart, W. M., Massagué, J., & et al. (1995). Drosophila Dpp signaling is mediated by the punt gene product: a dual ligand-binding type II receptor of the TGF beta receptor family. *Cell*, *80*(6), 899-908. https://doi.org/10.1016/0092-8674(95)90293-7

Li, H., Qi, Y., & Jasper, H. (2013). Dpp signaling determines regional stem cell identity in the regenerating adult Drosophila gastrointestinal tract. *Cell Rep*, *4*(1), 10-18. https://doi.org/10.1016/j.celrep.2013.05.040

Li, W., Yao, A., Zhi, H., Kaur, K., Zhu, Y. C., Jia, M., Zhao, H., Wang, Q., Jin, S., Zhao, G., Xiong, Z. Q., & Zhang, Y. Q. (2016). Angelman Syndrome Protein Ube3a Regulates Synaptic Growth and

Endocytosis by Inhibiting BMP Signaling in Drosophila. *PLoS Genet*, *12*(5), e1006062. https://doi.org/10.1371/journal.pgen.1006062

Li, Z., Zhang, Y., Han, L., Shi, L., & Lin, X. (2013). Trachea-derived dpp controls adult midgut homeostasis in Drosophila. *Dev Cell*, *24*(2), 133-143. https://doi.org/10.1016/j.devcel.2012.12.010

Linnemannstöns, K., Witte, L., Karuna, M. P., Kittel, J. C., Danieli, A., Müller, D., Nitsch, L., Honemann-Capito, M., Grawe, F., Wodarz, A., & Gross, J. C. (2020). Ykt6-dependent endosomal recycling is required for Wnt secretion in the Drosophila wing epithelium. *Development*, *147*(15). https://doi.org/10.1242/dev.185421

Mandaravally Madhavan, M., & Schneiderman, H. A. (1977). Histological analysis of the dynamics of growth of imaginal discs and histoblast nests during the larval development ofDrosophila melanogaster. *Wilehm Roux Arch Dev Biol*, *183*(4), 269-305. https://doi.org/10.1007/bf00848459

Markstein, M. (2018). *Drosophila Workers Unite! A Laboratory Manual for Working with Drosophila*. University of Mass/Amherst. https://books.google.ch/books?id=rWt1vwEACAAJ

Marois, E., Mahmoud, A., & Eaton, S. (2006). The endocytic pathway and formation of the Wingless morphogen gradient. *Development*, *133*(2), 307-317. https://doi.org/10.1242/dev.02197

Marqués, G., Bao, H., Haerry, T. E., Shimell, M. J., Duchek, P., Zhang, B., & O'Connor, M. B. (2002). The Drosophila BMP type II receptor Wishful Thinking regulates neuromuscular synapse morphology and function. *Neuron*, *33*(4), 529-543. https://doi.org/10.1016/s0896-6273(02)00595-0

Marty, T., Müller, B., Basler, K., & Affolter, M. (2000). Schnurri mediates Dpp-dependent repression of brinker transcription. *Nat Cell Biol*, *2*(10), 745-749. https://doi.org/10.1038/35036383

Masucci, J. D., Miltenberger, R. J., & Hoffmann, F. M. (1990). Pattern-specific expression of the Drosophila decapentaplegic gene in imaginal disks is regulated by 3' cis-regulatory elements. *Genes Dev*, *4*(11), 2011-2023. https://doi.org/10.1101/gad.4.11.2011

Matsuda, S., Harmansa, S., & Affolter, M. (2016). BMP morphogen gradients in flies. *Cytokine Growth Factor Rev*, *27*, 119-127. https://doi.org/10.1016/j.cytogfr.2015.11.003

Matsuda, S., Schaefer, J. V., Mii, Y., Hori, Y., Bieli, D., Taira, M., Plückthun, A., & Affolter, M. (2021). Asymmetric requirement of Dpp/BMP morphogen dispersal in the Drosophila wing disc. *Nat Commun*, *12*(1), 6435. https://doi.org/10.1038/s41467-021-26726-6

Maxfield, F. R., & Yamashiro, D. J. (1987). Endosome acidification and the pathways of receptor-mediated endocytosis. *Adv Exp Med Biol*, *225*, 189-198. https://doi.org/10.1007/978-1-4684-5442-0_16

Mayor, S., Parton, R. G., & Donaldson, J. G. (2014). Clathrin-independent pathways of endocytosis. *Cold Spring Harb Perspect Biol*, *6*(6). https://doi.org/10.1101/cshperspect.a016758

McCabe, B. D., Marqués, G., Haghighi, A. P., Fetter, R. D., Crotty, M. L., Haerry, T. E., Goodman, C. S., & O'Connor, M. B. (2003). The BMP homolog Gbb provides a retrograde signal that regulates synaptic growth at the Drosophila neuromuscular junction. *Neuron*, *39*(2), 241-254. https://doi.org/10.1016/s0896-6273(03)00426-4

McMahon, H. T., & Boucrot, E. (2011). Molecular mechanism and physiological functions of clathrin-mediated endocytosis. *Nat Rev Mol Cell Biol*, *12*(8), 517-533. https://doi.org/10.1038/nrm3151

Mehlen, P., Mille, F., & Thibert, C. (2005). Morphogens and cell survival during development. *J Neurobiol*, *64*(4), 357-366. https://doi.org/10.1002/neu.20167

Meister, M., & Tikkanen, R. (2014). Endocytic trafficking of membrane-bound cargo: a flotillin point of view. *Membranes (Basel)*, *4*(3), 356-371. https://doi.org/10.3390/membranes4030356

Mettlen, M., Chen, P. H., Srinivasan, S., Danuser, G., & Schmid, S. L. (2018). Regulation of Clathrin-Mediated Endocytosis. *Annu Rev Biochem*, *87*, 871-896. https://doi.org/10.1146/annurev-biochem-062917-012644

Migliano, S. M., & Teis, D. (2018). ESCRT and Membrane Protein Ubiquitination. *Prog Mol Subcell Biol*, *57*, 107-135. https://doi.org/10.1007/978-3-319-96704-2_4

Milán, M., & Cohen, S. M. (2000). Temporal regulation of apterous activity during development of the Drosophila wing. *Development*, *127*(14), 3069-3078. https://doi.org/10.1242/dev.127.14.3069

Minami, M., Kinoshita, N., Kamoshida, Y., Tanimoto, H., & Tabata, T. (1999). brinker is a target of Dpp in Drosophila that negatively regulates Dpp-dependent genes. *Nature*, *398*(6724), 242-246. https://doi.org/10.1038/18451

Morata, G., & Lawrence, P. A. (1975). Control of compartment development by the engrailed gene in Drosophila. *Nature*, *255*(5510), 614-617. https://doi.org/10.1038/255614a0

Moreno, E., Basler, K., & Morata, G. (2002). Cells compete for decapentaplegic survival factor to prevent apoptosis in Drosophila wing development. *Nature*, *416*(6882), 755-759. https://doi.org/10.1038/416755a

Morgan, T. H. (1901). *Regeneration*. Macmillan.

Morrison, H. A., Dionne, H., Rusten, T. E., Brech, A., Fisher, W. W., Pfeiffer, B. D., Celniker, S. E., Stenmark, H., & Bilder, D. (2008). Regulation of early endosomal entry by the Drosophila tumor suppressors Rabenosyn and Vps45. *Mol Biol Cell*, *19*(10), 4167-4176. https://doi.org/10.1091/mbc.e08-07-0716

Mousavi, S. A., Malerød, L., Berg, T., & Kjeken, R. (2004). Clathrin-dependent endocytosis. *Biochem J*, *377*(Pt 1), 1-16. https://doi.org/10.1042/bj20031000

Müller, B., Hartmann, B., Pyrowolakis, G., Affolter, M., & Basler, K. (2003). Conversion of an extracellular Dpp/BMP morphogen gradient into an inverse transcriptional gradient. *Cell*, *113*(2), 221-233. https://doi.org/10.1016/s0092-8674(03)00241-1

Murakami, G., Watabe, T., Takaoka, K., Miyazono, K., & Imamura, T. (2003). Cooperative inhibition of bone morphogenetic protein signaling by Smurf1 and inhibitory Smads. *Mol Biol Cell*, *14*(7), 2809-2817. https://doi.org/10.1091/mbc.e02-07-0441

Nellen, D., Burke, R., Struhl, G., & Basler, K. (1996). Direct and long-range action of a DPP morphogen gradient. *Cell*, *85*(3), 357-368. https://doi.org/10.1016/s0092-8674(00)81114-9

Neul, J. L., & Ferguson, E. L. (1998). Spatially restricted activation of the SAX receptor by SCW modulates DPP/TKV signaling in Drosophila dorsal-ventral patterning. *Cell*, *95*(4), 483-494. https://doi.org/10.1016/s0092-8674(00)81616-5

Neumann, C. J., & Cohen, S. M. (1997). Long-range action of Wingless organizes the dorsal-ventral axis of the Drosophila wing. *Development*, *124*(4), 871-880.

Nguyen, M., Park, S., Marqués, G., & Arora, K. (1998). Interpretation of a BMP activity gradient in Drosophila embryos depends on synergistic signaling by two type I receptors, SAX and TKV. *Cell*, *95*(4), 495-506. https://doi.org/10.1016/s0092-8674(00)81617-7

Norman, M., Vuilleumier, R., Springhorn, A., Gawlik, J., & Pyrowolakis, G. (2016). Pentagone internalises glypicans to fine-tune multiple signalling pathways. *Elife*, *5*. https://doi.org/10.7554/eLife.13301

Nöthiger, R. (1972). The larval development of imaginal disks. In *The biology of imaginal disks* (pp. 1-34). Springer.

O'Connor, M. B., Umulis, D., Othmer, H. G., & Blair, S. S. (2006). Shaping BMP morphogen gradients in the Drosophila embryo and pupal wing. *Development*, *133*(2), 183-193. https://doi.org/10.1242/dev.02214

Oh, P., McIntosh, D. P., & Schnitzer, J. E. (1998). Dynamin at the neck of caveolae mediates their budding to form transport vesicles by GTP-driven fission from the plasma membrane of endothelium. *J Cell Biol*, *141*(1), 101-114. https://doi.org/10.1083/jcb.141.1.101

Ong, C., Yung, L. Y., Cai, Y., Bay, B. H., & Baeg, G. H. (2015). Drosophila melanogaster as a model organism to study nanotoxicity. *Nanotoxicology*, *9*(3), 396-403. https://doi.org/10.3109/17435390.2014.940405

Padgett, R. W., St Johnston, R. D., & Gelbart, W. M. (1987). A transcript from a Drosophila pattern gene predicts a protein homologous to the transforming growth factor-beta family. *Nature*, *325*(6099), 81-84. https://doi.org/10.1038/325081a0

Padgett, R. W., Wozney, J. M., & Gelbart, W. M. (1993). Human BMP sequences can confer normal dorsal-ventral patterning in the Drosophila embryo. *Proc Natl Acad Sci U S A*, *90*(7), 2905-2909. https://doi.org/10.1073/pnas.90.7.2905

Panopoulou, E., Gillooly, D. J., Wrana, J. L., Zerial, M., Stenmark, H., Murphy, C., & Fotsis, T. (2002). Early endosomal regulation of Smad-dependent signaling in endothelial cells. *J Biol Chem*, *277*(20), 18046-18052. https://doi.org/10.1074/jbc.M107983200

Pelkmans, L., Püntener, D., & Helenius, A. (2002). Local actin polymerization and dynamin recruitment in SV40-induced internalization of caveolae. *Science*, *296*(5567), 535-539. https://doi.org/10.1126/science.1069784

Penton, A., Chen, Y., Staehling-Hampton, K., Wrana, J. L., Attisano, L., Szidonya, J., Cassill, J. A., Massagué, J., & Hoffmann, F. M. (1994). Identification of two bone morphogenetic protein type I receptors in Drosophila and evidence that Brk25D is a decapentaplegic receptor. *Cell*, *78*(2), 239-250. https://doi.org/10.1016/0092-8674(94)90294-1

Piccolo, S., Sasai, Y., Lu, B., & De Robertis, E. M. (1996). Dorsoventral patterning in Xenopus: inhibition of ventral signals by direct binding of chordin to BMP-4. *Cell*, *86*(4), 589-598. https://doi.org/10.1016/s0092-8674(00)80132-4

Piddini, E., & Vincent, J. P. (2003). Modulation of developmental signals by endocytosis: different means and many ends. *Curr Opin Cell Biol*, *15*(4), 474-481. https://doi.org/10.1016/s0955-0674(03)00072-3

Pizette, S., Matusek, T., Herpers, B., Thérond, P. P., & Rabouille, C. (2021). Hherisomes, Hedgehog specialized recycling endosomes, are required for high level Hedgehog signaling and tissue growth. *J Cell Sci*, *134*(10). https://doi.org/10.1242/jcs.258603

Podinovskaia, M., & Spang, A. (2018). The Endosomal Network: Mediators and Regulators of Endosome Maturation. *Prog Mol Subcell Biol*, *57*, 1-38. https://doi.org/10.1007/978-3-319-96704-2_1

Poteryaev, D., Datta, S., Ackema, K., Zerial, M., & Spang, A. (2010). Identification of the switch in early-to-late endosome transition. *Cell*, *141*(3), 497-508. https://doi.org/10.1016/j.cell.2010.03.011

Pyrowolakis, G., Hartmann, B., Müller, B., Basler, K., & Affolter, M. (2004). A simple molecular complex mediates widespread BMP-induced repression during Drosophila development. *Dev Cell*, *7*(2), 229-240. https://doi.org/10.1016/j.devcel.2004.07.008

Raftery, L. A., & Umulis, D. M. (2012). Regulation of BMP activity and range in Drosophila wing development. *Curr Opin Cell Biol*, *24*(2), 158-165. https://doi.org/10.1016/j.ceb.2011.11.004

Raiborg, C., Malerød, L., Pedersen, N. M., & Stenmark, H. (2008). Differential functions of Hrs and ESCRT proteins in endocytic membrane trafficking. *Exp Cell Res*, *314*(4), 801-813. https://doi.org/10.1016/j.yexcr.2007.10.014

Ramel, M. C., & Hill, C. S. (2012). Spatial regulation of BMP activity. *FEBS Lett*, *586*(14), 1929-1941. https://doi.org/10.1016/j.febslet.2012.02.035

Raymond, C. K., Howald-Stevenson, I., Vater, C. A., & Stevens, T. H. (1992). Morphological classification of the yeast vacuolar protein sorting mutants: evidence for a prevacuolar compartment in class E vps mutants. *Mol Biol Cell*, *3*(12), 1389-1402. https://doi.org/10.1091/mbc.3.12.1389

Restrepo, S., Zartman, J. J., & Basler, K. (2014). Coordination of patterning and growth by the morphogen DPP. *Curr Biol*, *24*(6), R245-255. https://doi.org/10.1016/j.cub.2014.01.055

Rieder, S. E., Banta, L. M., Köhrer, K., McCaffery, J. M., & Emr, S. D. (1996). Multilamellar endosome-like compartment accumulates in the yeast vps28 vacuolar protein sorting mutant. *Mol Biol Cell*, *7*(6), 985-999. https://doi.org/10.1091/mbc.7.6.985

Riento, K., Frick, M., Schafer, I., & Nichols, B. J. (2009). Endocytosis of flotillin-1 and flotillin-2 is regulated by Fyn kinase. *J Cell Sci*, *122*(Pt 7), 912-918. https://doi.org/10.1242/jcs.039024

Riggs, B., Rothwell, W., Mische, S., Hickson, G. R., Matheson, J., Hays, T. S., Gould, G. W., & Sullivan, W. (2003). Actin cytoskeleton remodeling during early Drosophila furrow formation requires recycling endosomal components Nuclear-fallout and Rab11. *J Cell Biol*, *163*(1), 143-154. https://doi.org/10.1083/jcb.200305115

Rives, A. F., Rochlin, K. M., Wehrli, M., Schwartz, S. L., & DiNardo, S. (2006). Endocytic trafficking of Wingless and its receptors, Arrow and DFrizzled-2, in the Drosophila wing. *Dev Biol*, *293*(1), 268-283. https://doi.org/10.1016/j.ydbio.2006.02.006

Rogers, K. W., & Schier, A. F. (2011). Morphogen Gradients: From Generation to Interpretation. *Annual Review of Cell and Developmental Biology*, *27*(1), 377-407. https://doi.org/10.1146/annurev-cellbio-092910-154148

Romanova-Michaelides, M., Hadjivasiliou, Z., Aguilar-Hidalgo, D., Basagiannis, D., Seum, C., Dubois, M., Jülicher, F., & Gonzalez-Gaitan, M. (2022). Morphogen gradient scaling by recycling of intracellular Dpp. *Nature*, *602*(7896), 287-293. https://doi.org/10.1038/s41586-021-04346-w

Rosales, C., & Uribe-Querol, E. (2017). Phagocytosis: A Fundamental Process in Immunity. *Biomed Res Int*, *2017*, 9042851. https://doi.org/10.1155/2017/9042851

Roth, S., Stein, D., & Nüsslein-Volhard, C. (1989). A gradient of nuclear localization of the dorsal protein determines dorsoventral pattern in the Drosophila embryo. *Cell*, *59*(6), 1189-1202. https://doi.org/10.1016/0092-8674(89)90774-5

Rothbauer, U., Zolghadr, K., Tillib, S., Nowak, D., Schermelleh, L., Gahl, A., Backmann, N., Conrath, K., Muyldermans, S., Cardoso, M. C., & Leonhardt, H. (2006). Targeting and tracing antigens in live cells with fluorescent nanobodies. *Nat Methods*, *3*(11), 887-889. https://doi.org/10.1038/nmeth953

Rothberg, K. G., Ying, Y. S., Kamen, B. A., & Anderson, R. G. (1990). Cholesterol controls the clustering of the glycophospholipid-anchored membrane receptor for 5-methyltetrahydrofolate. *J Cell Biol*, *111*(6 Pt 2), 2931-2938. https://doi.org/10.1083/jcb.111.6.2931

Roubinet, C., Tsankova, A., Pham, T. T., Monnard, A., Caussinus, E., Affolter, M., & Cabernard, C. (2017). Spatio-temporally separated cortical flows and spindle geometry establish physical asymmetry in fly neural stem cells. *Nat Commun*, *8*(1), 1383. https://doi.org/10.1038/s41467-017-01391-w

Roy, S., Huang, H., Liu, S., & Kornberg, T. B. (2014). Cytoneme-mediated contact-dependent transport of the Drosophila decapentaplegic signaling protein. *Science*, *343*(6173), 1244624. https://doi.org/10.1126/science.1244624

Ruberte, E., Marty, T., Nellen, D., Affolter, M., & Basler, K. (1995). An absolute requirement for both the type II and type I receptors, punt and thick veins, for dpp signaling in vivo. *Cell*, *80*(6), 889-897. https://doi.org/10.1016/0092-8674(95)90292-9

Rushlow, C. A., Han, K., Manley, J. L., & Levine, M. (1989). The graded distribution of the dorsal morphogen is initiated by selective nuclear transport in Drosophila. *Cell*, *59*(6), 1165-1177. https://doi.org/10.1016/0092-8674(89)90772-1

Sabharanjak, S., Sharma, P., Parton, R. G., & Mayor, S. (2002). GPI-anchored proteins are delivered to recycling endosomes via a distinct cdc42-regulated, clathrin-independent pinocytic pathway. *Dev Cell*, *2*(4), 411-423. https://doi.org/10.1016/s1534-5807(02)00145-4

Sampath, T. K., Rashka, K. E., Doctor, J. S., Tucker, R. F., & Hoffmann, F. M. (1993). Drosophila transforming growth factor beta superfamily proteins induce endochondral bone formation in mammals. *Proc Natl Acad Sci U S A*, *90*(13), 6004-6008. https://doi.org/10.1073/pnas.90.13.6004

Saslowsky, D. E., Cho, J. A., Chinnapen, H., Massol, R. H., Chinnapen, D. J., Wagner, J. S., De Luca, H. E., Kam, W., Paw, B. H., & Lencer, W. I. (2010). Intoxication of zebrafish and mammalian cells by cholera toxin depends on the flotillin/reggie proteins but not Derlin-1 or -2. *J Clin Invest*, *120*(12), 4399-4409. https://doi.org/10.1172/jci42958

Schlossman, D. M., Schmid, S. L., Braell, W. A., & Rothman, J. E. (1984). An enzyme that removes clathrin coats: purification of an uncoating ATPase. *J Cell Biol*, *99*(2), 723-733. https://doi.org/10.1083/jcb.99.2.723

Schmid, E. M., & McMahon, H. T. (2007). Integrating molecular and network biology to decode endocytosis. *Nature*, *448*(7156), 883-888. https://doi.org/10.1038/nature06031

Scholpp, S., & Brand, M. (2004). Endocytosis controls spreading and effective signaling range of Fgf8 protein. *Curr Biol*, *14*(20), 1834-1841. https://doi.org/10.1016/j.cub.2004.09.084

Schuh, A. L., & Audhya, A. (2014). The ESCRT machinery: from the plasma membrane to endosomes and back again. *Crit Rev Biochem Mol Biol*, *49*(3), 242-261. https://doi.org/10.3109/10409238.2014.881777

Schwank, G., Dalessi, S., Yang, S. F., Yagi, R., de Lachapelle, A. M., Affolter, M., Bergmann, S., & Basler, K. (2011). Formation of the long range Dpp morphogen gradient. *PLoS Biol*, *9*(7), e1001111. https://doi.org/10.1371/journal.pbio.1001111

Scott, A., Chung, H. Y., Gonciarz-Swiatek, M., Hill, G. C., Whitby, F. G., Gaspar, J., Holton, J. M., Viswanathan, R., Ghaffarian, S., Hill, C. P., & Sundquist, W. I. (2005). Structural and mechanistic studies of VPS4 proteins. *Embo j*, *24*(20), 3658-3669. https://doi.org/10.1038/sj.emboj.7600818

Seto, E. S., & Bellen, H. J. (2006). Internalization is required for proper Wingless signaling in Drosophila melanogaster. *J Cell Biol*, *173*(1), 95-106. https://doi.org/10.1083/jcb.200510123

Seto, E. S., Bellen, H. J., & Lloyd, T. E. (2002). When cell biology meets development: endocytic regulation of signaling pathways. *Genes Dev*, *16*(11), 1314-1336. https://doi.org/10.1101/gad.989602

Shimmi, O., Umulis, D., Othmer, H., & O'Connor, M. B. (2005). Facilitated transport of a Dpp/Scw heterodimer by Sog/Tsg leads to robust patterning of the Drosophila blastoderm embryo. *Cell*, *120*(6), 873-886. https://doi.org/10.1016/j.cell.2005.02.009

Sieber, C., Kopf, J., Hiepen, C., & Knaus, P. (2009). Recent advances in BMP receptor signaling. *Cytokine Growth Factor Rev*, *20*(5-6), 343-355. https://doi.org/10.1016/j.cytogfr.2009.10.007

Simin, K., Bates, E. A., Horner, M. A., & Letsou, A. (1998). Genetic analysis of punt, a type II Dpp receptor that functions throughout the Drosophila melanogaster life cycle. *Genetics*, *148*(2), 801-813. https://doi.org/10.1093/genetics/148.2.801

Simon, N., Safyan, A., Pyrowolakis, G., & Matsuda, S. (2023). Dally is not essential for Dpp spreading or internalization but for Dpp stability by antagonizing Tkv-mediated Dpp internalization. *bioRxiv*, 2023.2001.2015.524087. https://doi.org/10.1101/2023.01.15.524087

Sivasankaran, R., Vigano, M. A., Müller, B., Affolter, M., & Basler, K. (2000). Direct transcriptional control of the Dpp target omb by the DNA binding protein Brinker. *Embo j*, *19*(22), 6162-6172. https://doi.org/10.1093/emboj/19.22.6162

Solinger, J. A., & Spang, A. (2013). Tethering complexes in the endocytic pathway: CORVET and HOPS. *Febs j*, *280*(12), 2743-2757. https://doi.org/10.1111/febs.12151

Sonnenfeld, M. J. (2009). GAL4/UAS Expression System. In M. D. Binder, N. Hirokawa, & U. Windhorst (Eds.), *Encyclopedia of Neuroscience* (pp. 1662-1666). Springer Berlin Heidelberg. https://doi.org/10.1007/978-3-540-29678-2_1904

Spemann, H., & Mangold, H. (1924). über Induktion von Embryonalanlagen durch Implantation artfremder Organisatoren. *Archiv für mikroskopische Anatomie und Entwicklungsmechanik*, *100*(3), 599-638.

Spencer, F. A., Hoffmann, F. M., & Gelbart, W. M. (1982). Decapentaplegic: a gene complex affecting morphogenesis in Drosophila melanogaster. *Cell*, *28*(3), 451-461. https://doi.org/10.1016/0092-8674(82)90199-4

Stapornwongkul, K. S., de Gennes, M., Cocconi, L., Salbreux, G., & Vincent, J. P. (2020). Patterning and growth control in vivo by an engineered GFP gradient. *Science*, *370*(6514), 321-327. https://doi.org/10.1126/science.abb8205

Steward, R. (1989). Relocalization of the dorsal protein from the cytoplasm to the nucleus correlates with its function. *Cell*, *59*(6), 1179-1188. https://doi.org/10.1016/0092-8674(89)90773-3

Stewart, A., Guan, H., & Yang, K. (2010). BMP-3 promotes mesenchymal stem cell proliferation through the TGF-beta/activin signaling pathway. *J Cell Physiol*, *223*(3), 658-666. https://doi.org/10.1002/jcp.22064

Strigini, M., & Cohen, S. M. (2000). Wingless gradient formation in the Drosophila wing. *Curr Biol*, *10*(6), 293-300. https://doi.org/10.1016/s0960-9822(00)00378-x

Struhl, G., Struhl, K., & Macdonald, P. M. (1989). The gradient morphogen bicoid is a concentration-dependent transcriptional activator. *Cell*, *57*(7), 1259-1273. https://doi.org/10.1016/0092-8674(89)90062-7

Tanimoto, H., Itoh, S., ten Dijke, P., & Tabata, T. (2000). Hedgehog creates a gradient of DPP activity in Drosophila wing imaginal discs. *Mol Cell*, *5*(1), 59-71. https://doi.org/10.1016/s1097-2765(00)80403-7

Teleman, A. A., & Cohen, S. M. (2000). Dpp gradient formation in the Drosophila wing imaginal disc. *Cell*, *103*(6), 971-980. https://doi.org/10.1016/s0092-8674(00)00199-9

Thompson, B. J., Mathieu, J., Sung, H. H., Loeser, E., Rørth, P., & Cohen, S. M. (2005). Tumor suppressor properties of the ESCRT-II complex component Vps25 in Drosophila. *Dev Cell*, *9*(5), 711-720. https://doi.org/10.1016/j.devcel.2005.09.020

Torroja, C., Gorfinkiel, N., & Guerrero, I. (2004). Patched controls the Hedgehog gradient by endocytosis in a dynamin-dependent manner, but this internalization does not play a major role in signal transduction. *Development*, *131*(10), 2395-2408. https://doi.org/10.1242/dev.01102

Trainor, P. A. (2016). Developmental Biology: We Are All Walking Mutants. *Curr Top Dev Biol*, *117*, 523-538. https://doi.org/10.1016/bs.ctdb.2015.11.029

Tripathi, B. K., & Irvine, K. D. (2022). The wing imaginal disc. *Genetics*, *220*(4). https://doi.org/10.1093/genetics/iyac020

Tsukazaki, T., Chiang, T. A., Davison, A. F., Attisano, L., & Wrana, J. L. (1998). SARA, a FYVE domain protein that recruits Smad2 to the TGFbeta receptor. *Cell*, *95*(6), 779-791. https://doi.org/10.1016/s0092-8674(00)81701-8

Tsuneizumi, K., Nakayama, T., Kamoshida, Y., Kornberg, T. B., Christian, J. L., & Tabata, T. (1997). Daughters against dpp modulates dpp organizing activity in Drosophila wing development. *Nature*, *389*(6651), 627-631. https://doi.org/10.1038/39362

Turing, A. M. (1952). The chemical basis of morphogenesis. *Philosophical Transactions of the Royal Society of London. Series B, Biological Sciences*, *237*(641), 37-72.

Turing, A. M. (1990). The chemical basis of morphogenesis. *Bulletin of Mathematical Biology*, *52*(1), 153-197. https://doi.org/10.1007/BF02459572

Ugur, B., Chen, K., & Bellen, H. J. (2016). Drosophila tools and assays for the study of human diseases. *Dis Model Mech*, *9*(3), 235-244. https://doi.org/10.1242/dmm.023762

Urbé, S., Sachse, M., Row, P. E., Preisinger, C., Barr, F. A., Strous, G., Klumperman, J., & Clague, M. J. (2003). The UIM domain of Hrs couples receptor sorting to vesicle formation. *J Cell Sci*, *116*(Pt 20), 4169-4179. https://doi.org/10.1242/jcs.00723

Urist, M. R. (1965). Bone: formation by autoinduction. *Science*, *150*(3698), 893-899. https://doi.org/10.1126/science.150.3698.893

Vanlandingham, P. A., & Ceresa, B. P. (2009). Rab7 regulates late endocytic trafficking downstream of multivesicular body biogenesis and cargo sequestration. *J Biol Chem*, *284*(18), 12110-12124. https://doi.org/10.1074/jbc.M809277200

Vigano, M. A., Ell, C. M., Kustermann, M. M. M., Aguilar, G., Matsuda, S., Zhao, N., Stasevich, T. J., Affolter, M., & Pyrowolakis, G. (2021). Protein manipulation using single copies of short peptide tags in cultured cells and in Drosophila melanogaster. *Development*, *148*(6). https://doi.org/10.1242/dev.191700

Wandinger-Ness, A., & Zerial, M. (2014). Rab proteins and the compartmentalization of the endosomal system. *Cold Spring Harbor perspectives in biology*, *6*(11), a022616.

Wang, R. N., Green, J., Wang, Z., Deng, Y., Qiao, M., Peabody, M., Zhang, Q., Ye, J., Yan, Z., Denduluri, S., Idowu, O., Li, M., Shen, C., Hu, A., Haydon, R. C., Kang, R., Mok, J., Lee, M. J., Luu, H. L., & Shi, L. L. (2014). Bone Morphogenetic Protein (BMP) signaling in development and human diseases. *Genes Dis*, *1*(1), 87-105. https://doi.org/10.1016/j.gendis.2014.07.005

Wang, S., Tang, N. H., Lara-Gonzalez, P., Zhao, Z., Cheerambathur, D. K., Prevo, B., Chisholm, A. D., Desai, A., & Oegema, K. (2017). A toolkit for GFP-mediated tissue-specific protein degradation in C. elegans. *Development*, *144*(14), 2694-2701. https://doi.org/10.1242/dev.150094

Wartlick, O., Kicheva, A., & González-Gaitán, M. (2009). Morphogen gradient formation. *Cold Spring Harb Perspect Biol*, *1*(3), a001255. https://doi.org/10.1101/cshperspect.a001255

Weiss, A., & Attisano, L. (2013). The TGFbeta superfamily signaling pathway. *Wiley Interdiscip Rev Dev Biol*, *2*(1), 47-63. https://doi.org/10.1002/wdev.86

Weiss, A., Charbonnier, E., Ellertsdóttir, E., Tsirigos, A., Wolf, C., Schuh, R., Pyrowolakis, G., & Affolter, M. (2010). A conserved activation element in BMP signaling during Drosophila development. *Nat Struct Mol Biol*, *17*(1), 69-76. https://doi.org/10.1038/nsmb.1715

Wharton, K. A., Cook, J. M., Torres-Schumann, S., de Castro, K., Borod, E., & Phillips, D. A. (1999). Genetic analysis of the bone morphogenetic protein-related gene, gbb, identifies multiple requirements during Drosophila development. *Genetics*, *152*(2), 629-640. https://doi.org/10.1093/genetics/152.2.629

Wharton, K. A., Thomsen, G. H., & Gelbart, W. M. (1991). Drosophila 60A gene, another transforming growth factor beta family member, is closely related to human bone morphogenetic proteins. *Proc Natl Acad Sci U S A*, *88*(20), 9214-9218. https://doi.org/10.1073/pnas.88.20.9214

Williams, J. A., Bell, J. B., & Carroll, S. B. (1991). Control of Drosophila wing and haltere development by the nuclear vestigial gene product. *Genes Dev*, *5*(12b), 2481-2495. https://doi.org/10.1101/gad.5.12b.2481

Williams, R. L., & Urbé, S. (2007). The emerging shape of the ESCRT machinery. *Nat Rev Mol Cell Biol*, *8*(5), 355-368. https://doi.org/10.1038/nrm2162

Wilson, I. A., Niman, H. L., Houghten, R. A., Cherenson, A. R., Connolly, M. L., & Lerner, R. A. (1984). The structure of an antigenic determinant in a protein. *Cell*, *37*(3), 767-778. https://doi.org/10.1016/0092-8674(84)90412-4

Wollert, T., & Hurley, J. H. (2010). Molecular mechanism of multivesicular body biogenesis by ESCRT complexes. *Nature*, *464*(7290), 864-869. https://doi.org/10.1038/nature08849

Wolpert, L. (1969). Positional information and the spatial pattern of cellular differentiation. *J Theor Biol*, *25*(1), 1-47. https://doi.org/10.1016/s0022-5193(69)80016-0

Wucherpfennig, T., Wilsch-Bräuninger, M., & González-Gaitán, M. (2003). Role of Drosophila Rab5 during endosomal trafficking at the synapse and evoked neurotransmitter release. *J Cell Biol*, *161*(3), 609-624. https://doi.org/10.1083/jcb.200211087

Xiao, Y. T., Xiang, L. X., & Shao, J. Z. (2007). Bone morphogenetic protein. *Biochem Biophys Res Commun*, *362*(3), 550-553. https://doi.org/10.1016/j.bbrc.2007.08.045

Xie, T., & Spradling, A. C. (1998). decapentaplegic is essential for the maintenance and division of germline stem cells in the Drosophila ovary. *Cell*, *94*(2), 251-260. https://doi.org/10.1016/s0092-8674(00)81424-5

Yamaguchi, N., Colak-Champollion, T., & Knaut, H. (2019). zGrad is a nanobody-based degron system that inactivates proteins in zebrafish. *Elife*, *8*. https://doi.org/10.7554/eLife.43125

Yamazaki, Y., Palmer, L., Alexandre, C., Kakugawa, S., Beckett, K., Gaugue, I., Palmer, R. H., & Vincent, J. P. (2016). Godzilla-dependent transcytosis promotes Wingless signalling in Drosophila wing imaginal discs. *Nat Cell Biol*, *18*(4), 451-457. https://doi.org/10.1038/ncb3325

Yu, S. R., Burkhardt, M., Nowak, M., Ries, J., Petrásek, Z., Scholpp, S., Schwille, P., & Brand, M. (2009). Fgf8 morphogen gradient forms by a source-sink mechanism with freely diffusing molecules. *Nature*, *461*(7263), 533-536. https://doi.org/10.1038/nature08391

Zecca, M., Basler, K., & Struhl, G. (1995). Sequential organizing activities of engrailed, hedgehog and decapentaplegic in the Drosophila wing. *Development*, *121*(8), 2265-2278. https://doi.org/10.1242/dev.121.8.2265

Zecca, M., & Struhl, G. (2007). Recruitment of cells into the Drosophila wing primordium by a feed-forward circuit of vestigial autoregulation. *Development*, *134*(16), 3001-3010. https://doi.org/10.1242/dev.006411

Zhang, H., Levine, M., & Ashe, H. L. (2001). Brinker is a sequence-specific transcriptional repressor in the Drosophila embryo. *Genes Dev*, *15*(3), 261-266. https://doi.org/10.1101/gad.861201

Zhao, G., Wu, Y., Du, L., Li, W., Xiong, Y., Yao, A., Wang, Q., & Zhang, Y. Q. (2015). Drosophila S6 Kinase like inhibits neuromuscular junction growth by downregulating the BMP receptor thickveins. *PLoS Genet*, *11*(3), e1004984. https://doi.org/10.1371/journal.pgen.1004984

Zhou, S., Lo, W. C., Suhalim, J. L., Digman, M. A., Gratton, E., Nie, Q., & Lander, A. D. (2012). Free extracellular diffusion creates the Dpp morphogen gradient of the Drosophila wing disc. *Curr Biol*, *22*(8), 668-675. https://doi.org/10.1016/j.cub.2012.02.065

Zhu, H., Kavsak, P., Abdollah, S., Wrana, J. L., & Thomsen, G. H. (1999). A SMAD ubiquitin ligase targets the BMP pathway and affects embryonic pattern formation. *Nature*, *400*(6745), 687-693. https://doi.org/10.1038/23293

Zimmerman, L. B., De Jesús-Escobar, J. M., & Harland, R. M. (1996). The Spemann organizer signal noggin binds and inactivates bone morphogenetic protein 4. *Cell*, *86*(4), 599-606. https://doi.org/10.1016/s0092-8674(00)80133-6

Zou, H., & Niswander, L. (1996). Requirement for BMP signaling in interdigital apoptosis and scale formation. *Science*, *272*(5262), 738-741. https://doi.org/10.1126/science.272.5262.738